May 26, 1999

Final Report

for work performed under
Cooperative Agreement No. DE-FC02-96CH10861

entitled
'Fibrous Monoliths: Economic Ceramic Matrix Composites from Powders'

Reporting Period 11/1/98 – 03/25/99

Submitted to

Bill Coblenz, DARPA – Defense Sciences Offices
Jill Jonkouski, DOE – Chicago Operations Office
Barb Lewandowski, DOE – Chicago Operations Office

From
Advanced Ceramics Research, Inc.
3292 East Hemisphere Loop
Tucson, AZ 85706-5013

Written by
Mark Rigali, Principal Investigator
Manish Sutaria
Anthony Mulligan
Peter Creegan
Ron Cipriani

DISCLAIMER

DISCLAIMER

Portions of this document may be illegible in electronic image products. Images are produced from the best available original document.

TABLE OF CONTENTS

I. Program Overview

This report describes the research efforts of Advanced Ceramics Research Inc. (ACR), Smith Tool Inc., the University of Michigan, and the Air Force Materials Directorate, Wright Laboratory (WL/MLLN) to develop and perform pilot-scale production of fibrous monolith composites. The principal focus of the program was to develop damage-tolerant, wear-resistant tooling for petroleum drilling applications and generate a basic mechanical properties database on fibrous monolith composites.

After investigating several different materials systems, ACR, Smith Tool, and the University of Michigan successfully developed a wear-resistant, damage-tolerant fibrous monolith coating (referred to as a "cap") for the inserts used in rock drill bits. This diamond and tungsten carbide based coating exhibited superior wear resistance and damage tolerance in laboratory and field testing as compared to the polycrystalline diamond coated inserts currently in use in the rock drilling industry. At the program's close, ACR has delivered nearly 1,000 fibrous monolith parts to Smith Tool for field testing and product qualification of inserts used on several different types of rock drill bits. ACR and Smith Tool have developed a strong partnership over the course of this program and will continue to work together to develop and commercialize the FM coated inserts. Future research projects for the team includes the development of material systems to improve wear and impact resistance in mining industry applications.

ACR provided FM materials to the Air Force Materials Directorate, Wright Laboratory for independent testing of the properties of fibrous monolith composites. WL/MLLN performed thermal and mechanical properties testing and using the data generated from testing, they created a detailed property database on fibrous monolith composites. In the future WL/MLLN will serve as a clearinghouse for the thermal and mechanical properties database generated on this program. The database will increase the exposure of the composites that were developed on this program as well as aid other potential users in determining the applicability of fibrous monolith systems for meeting their composite material needs.

II. Structure of the Program

For this Advanced Manufacturing Partnership program, Advanced Ceramics Research (ACR) formed a highly qualified team capable of developing and commercializing FM components for applications ranging from cutting tools to hot section components for gas turbines. The team members included ACR, Smith Tool Inc., the University of Michigan and Air Force Material Directorate, Wright Laboratory (WL/MLLN).

As the team leader, ACR served as the developer and supplier of fibrous monolith composite materials, test coupons, prototypes, and manufactured components. ACR has a considerable amount of expertise in the research, development, and fabrication of FM materials. The test billets and components produced by ACR were submitted to the other team members for evaluation and analysis. The Fibrous Monolith composite materials produced and evaluated under this program include Si_3N_4/BN, ZrB_2/BN, HfB_2/BN, Diamond/WC, and WC-Co/M FMs.

Smith Tool performed testing and evaluation of WC-Co/M and Diamond/WC FM drill bit inserts in its laboratories and at field test sites to determine suitability of FM materials for petroleum drilling applications. Smith Tool worked along with ACR to produce a new class of drill bits with higher fracture toughness and wear resistance.

University of Michigan (UM) provided research and development in a series of tasks to support ACR/Smith Tool efforts for developing WC-Co/M inserts. The UM also collaborated on the formulation of effective polymer binders for the coextrusion processing of WC-Co/M FMs, performed binder burnout studies, pressureless sintering studies, and microstructural characterization studies.

The Air Force Material Directorate, Wright Laboratory (WL/MLLN) received fibrous monolith materials from ACR under subcontractor to provide an independent evaluation of the mechanical behavior of the materials developed under the program. Some of the mechanical testing performed at WL/MLLN included tension, tensile creep rupture, tension-tension fatigue, and notch sensitivity. Also, WL/MLLN conducted microstructural characterization of as-received and post-test fracture specimens using optical and scanning electron microscopy.

III. Fibrous Monolith (FM) Background

Fibrous monoliths (FMs) are a new class of structural ceramics. They have mechanical properties similar to CFCCs, including very high fracture energies, damage tolerance, and graceful failure. Since they are monolithic ceramics, fibrous monoliths can be manufactured by conventional powder processing techniques using inexpensive raw materials. This combination of high performance and low cost is a breakthrough that could enable wider application of ceramics in energy and defense related applications.

FMs are sintered (or hot pressed) monolithic ceramics having a distinct fibrous texture. The two phases that make up the macroarchitecture of a FM are a primary phase in the form of elongated polycrystalline cells, or fibers, separated by a thin secondary phase in the form of cell boundaries. Typical volume fractions of the two phases are 80 to 95% for the primary (cell) phase and 5 to 20% for the interpenetrating (cell boundary) phase. The primary (cell) phase is typically a structural ceramic, such as Si_3N_4, SiC, ZrB_2, HfB_2, HfC, ZrO_2, or Al_2O_3, while the interpenetrating (cell boundary) phase is typically either a ductile metal, such as Ni, Ni-Cr, Nb, or a weakly bonded low shear strength material, such as graphite or hexagonal BN. The latter, weak interface FMs and several of the ductile interphase FMs, exhibit fracture behavior similar to CFCCs, such as C/C and SiC/SiC composites, including the ability to fail in a non-catastrophic manner.

Applications for fibrous monoliths are widespread and have recently included structures such as cutting tools, flat plates, solid hot gas containment tubes, radiant burner tubes, radiant burner panels, turbine vanes, hot gas filters, rocket nozzles, body armor panels, automotive engine components, and steering vanes for vectored thrust control all of which can all be readily formed from the green material. Advanced Ceramics Research, Inc. has mainly focused on the development of Si_3N_4/BN FMs for intermediate temperature turbine engine applications as well as ZrB_2-based/BN and HfB_2-based/BN FMs for both rocket and solar thermal propulsion applications. Tubes fabricated from ZrB_2/BN and HfB_2/BN FMs for solar thermal propulsion applications are designed to see use at temperatures approaching 3000 K. Our research has shown that the BN interlayer surrounding the diboride cells has rendered the material nearly insensitive to thermal shock.

IV. Production of 'Green' Fibrous Monolith Feedstock

The goal of this task was to scale up the fibrous monolith (FM) processing technology at ACR. ACR manufactured several different fibrous monolith materials on a pilot-scale level of production. Some of the FM systems included in this study were Si_3N_4/BN, WC/Co, WC/Co-Ni-Fe, Diamond/WC-Co, and Diamond/Co/Nb.

ACR is capable of producing several kg of fibrous monolith material in a typical 8-hour work day. This production capability was established during a four year Office of Navel Research (ONR) sponsored program entitled "Advanced Development of Fibrous Monolithic Ceramics". During this program, equipment was purchased in order to reach the pilot–scale production rate of 5 kg /day. Since the completion of the ONR program, ACR has purchased additional equipment including a Haake extruder/mixer and 3 additional ball mills. With this additional equipment ACR believes it is now capable of producing up to 10 kg/day of "green" Fibrous Monolith material.

A Fibrous Monolith "Green" Processing

The process of producing fibrous monolithic ceramics consists of several steps:

Step 1. In most cases, it is first necessary to produce mechanically activated and agglomerate-free ceramic powders with a particle size distribution in the range of a few tenths of microns to a few microns (μm) in size. ACR has two 3-tiered ball mill stations and several single tiered ball mills for milling operations (**Figure 1**).

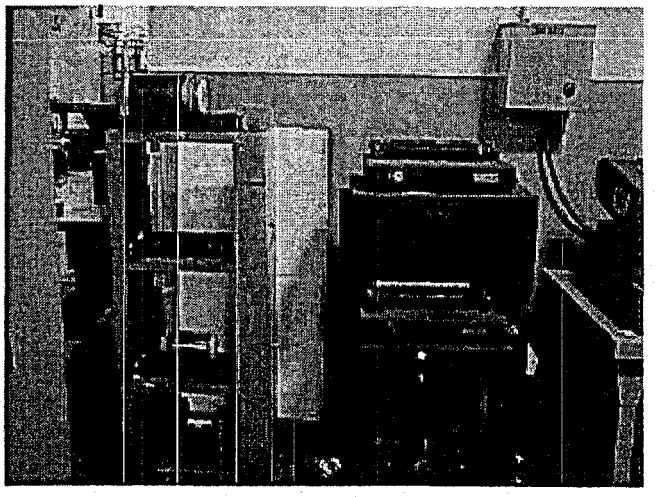

Figure 1. Ball Mill Stations.

Commercially obtained ceramic powders are ball milled in ethanol with Silicon Nitride (Si_3N_4) or Zirconium Oxide (ZrO_2) milling media. Sintering additives, when necessary, are added and milled together with the ceramic powders. Typical milling times are for periods of 24 to 120 hours, depending on the starting ceramic material. For example, Boron Nitride (BN) powder is milled for 24 to 48 hours, Silicon Nitride powder is milled for 48 hours, and Zirconium Carbide (ZrC), purchased as a fairly coarse refractory ceramic, is typically milled for a longer period, 72 to 120 hours. In some cases, the powders are processed as received. This is the case for the diamond and ceramic powders sent by Smith Tool to fabricate the fibrous monolith coated drill bit inserts produced during this program.

Step 2. Once the milling operation is completed, the ethanol/ceramic powder mixtures are separated and collected from the milling media using a perforated mill jar lid as a "strainer". The ethanol is then separated by distillation from the ceramic powder using a Buchi Rotovapor (**Figure 2**). The ceramic powders are then removed from the rotovapor jar and placed in labeled plastic jars. This process allows ACR to reclaim the ethanol solvent for reuse or proper disposal according to local, state, and federal waste disposal requirements.

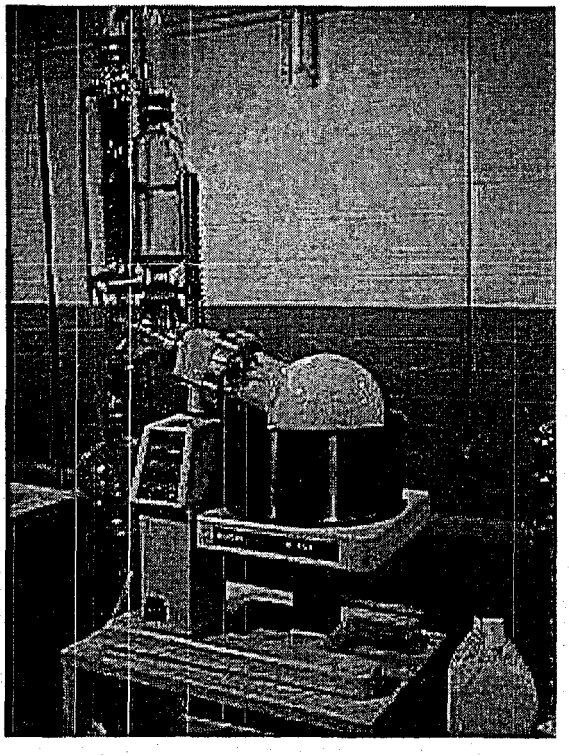

Figure 2. Buchi Rotovapor.

Step 3. The recovered ceramic powders are blended with thermoplastic melt-spinnable polymer binders and plasticizers, using the C.W. Brabender (**Figures 3 and 4**) or Haake high shear mixer, to form a smooth, uniformly suspended mixture called a "dope". For this program, ethylene ethylacrylate (EEA), ethylene vinylacetate (EVA), and Acryloid Copolymer Resin (B-67) were used as the thermoplastic binders. Heavy mineral oil (HMO) and methoxy polyethyleneglycol were used as plasticizers. A typical blend consists of 50 to 62 vol. % of the ceramic powder, 37 to 50 vol. % of the thermoplastics, and 0 to 12 vol. % of the plasticizers. Since the mixers have fixed volume reservoirs, the recipes devised to produce batches of the thermoplastic/ceramic blends are formulated on a volumetric, as opposed to a mass, basis. Thus the mass of a batch of ceramic/thermoplastic dope varies with the density of the ceramic powder. For example, a single batch of Si_3N_4 with a density of 3.44 g/cc produced approximately 1 kg 'green' compounded material.

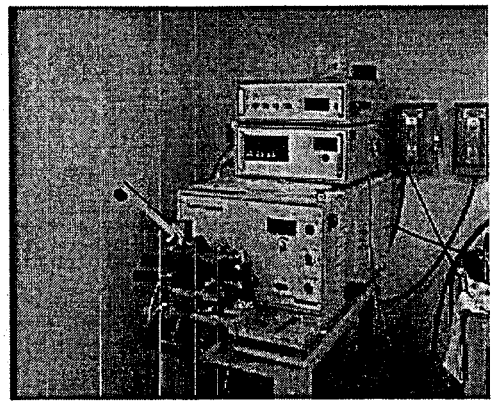

Figure 3. C.W. Brabender Plasticorder

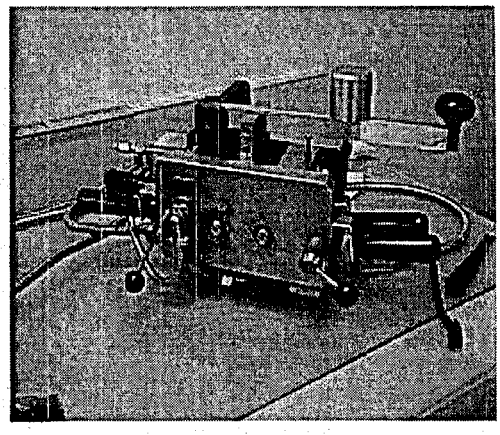

Figure 4. Close-up of Brabender Mixing Head

Step 4. After mixing, the dopes are warm pressed into green composite feedrods. A composite feedrod consists of a 'core' of a primary ceramic material enclosed by a cladding or 'shell' of a secondary ceramic material. 'Cores' are also referred to as 'cells' and 'shells' are also called 'boundaries'. ACR has purchased several sets of machine tooled core and shell dies so that the volume ratio of the core and shell of a composite feedrod can be systematically varied. We can produce 'green' composite feedrods (22 mm in diameter) with the following core/shell volume ratios: 90/10, 82.5/17.5, 69/31, and 50/50. The feedrod pressing station at ACR consists of four hydraulic vertical presses with heating stations, allowing ACR to press as up to four cores at a time (**Figure 5**). Two heated uniaxial platen presses are used to press the shells for the composite feedrods (**Figure 6**). Each of the platen presses will accommodate four shell die sets for a total of eight shells, enough to clad four cores and thus produce four composite feedrods at a time.

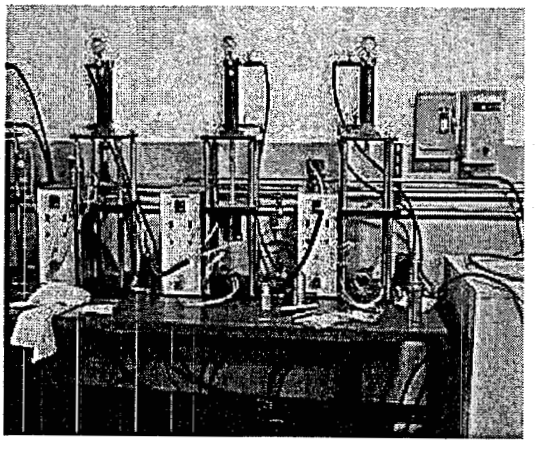

Figure 5. Hydraulic Vertical Rod Press Station.

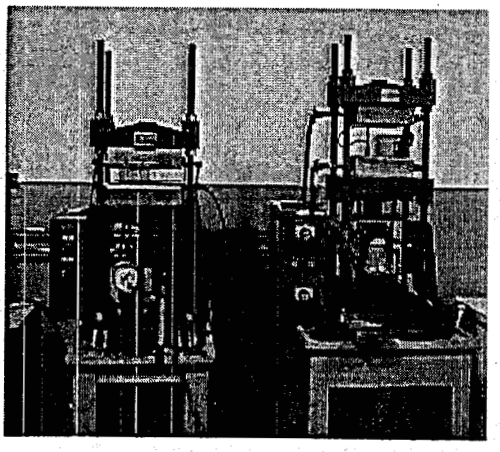

Figure 6. Platten Presses.

Step 5. The next step in 'green' processing is the extrusion of feedrods using ACR's computer numerically controlled (CNC) ball-screw extruder (**Figure 7**). Composite feedrods are extruded through a spinneret to produce a green 'filament'. This process is known as single filament co-extrusion (SFCX). By fabricating a spinneret with the appropriate orifice diameter ACR can easily produce any desired green 'filament' diameter between 0.25 and 6mm. The extruded filaments always maintain the volume ratio of the original feedrod. This is made possible by producing thermoplastic/ceramic blends of the cores and shells with carefully controlled rheological properties. The smallest filament or cell diameter that can be obtained by single filament co-extrusion is approximately 250 μm; smaller green filaments are too easily broken during the winding and extrusion process. To obtain cell sizes smaller than 250 μm, 1-2 mm green filaments are extruded and then bundled together to form a 22 mm multifilament feedrod. This multifilament feedrod is then extruded to through the same or a different diameter spinneret to produce a multifilament fiber or "filaments within filaments". In this manner, cell sizes approaching 20 to 30 microns can be produced by this multifilament coextrusion (MFCX) process. Co-extruding filaments with smaller cell sizes is difficult. This is because the cellular structure cannot be maintained as cell sizes of less than 20 μm begin to approach the ceramic powder's average particle size (typically 0.1 to 1μm).

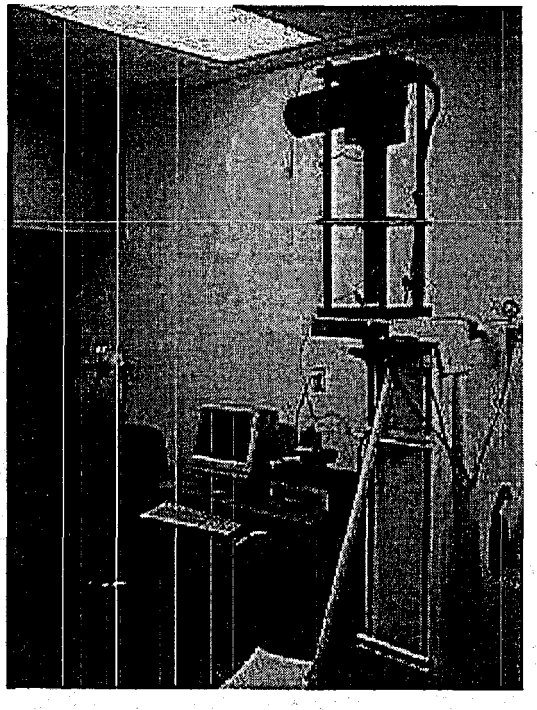

Figure 7. CNC High Pressure Extruder

Step 6. The flexible SDCX or MFCX 'green' filaments produced in the extrusion process can be woven, wound, braided, chopped (and pressed), or laid up to produce a near net shape preform. In a typical two dimensional (2D) lay-up, the green filament is wound on a drum (twelve inches in diameter), operated by computer control (**Figure 8**). Using this CNC drum winder, ACR can fabricate 2D parts with good fiber alignment. Once wound, green filament sheets can then be cut to the required shape and dimensions. The cut sheets can then be laid up in any standard 2D architecture (i.e. uniaxial, 0°/90°, quasi-isotropic, etc.). After the 2D preform is laid-up, a uniaxial platen press is used to warm laminate the part. This laminated preform is then placed in the binder burnout furnace (**Figure 9**) to remove the polymer binder.

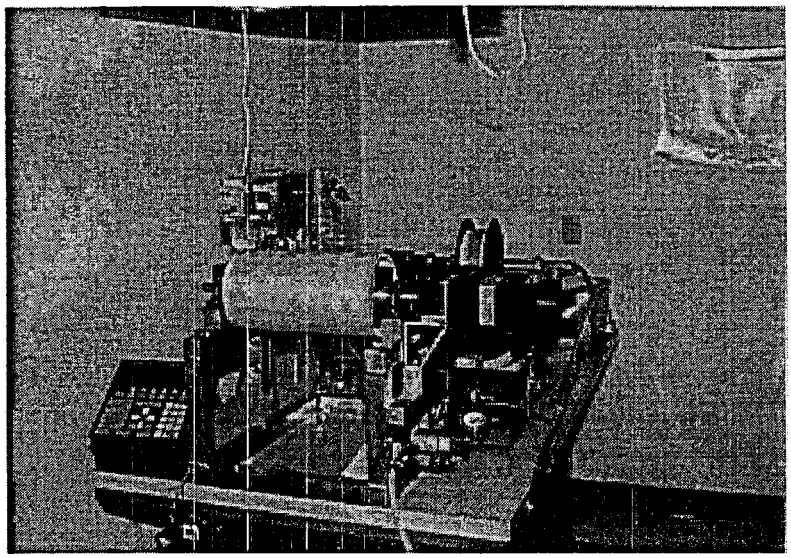

Figure 8. ACR's CNC Winder.

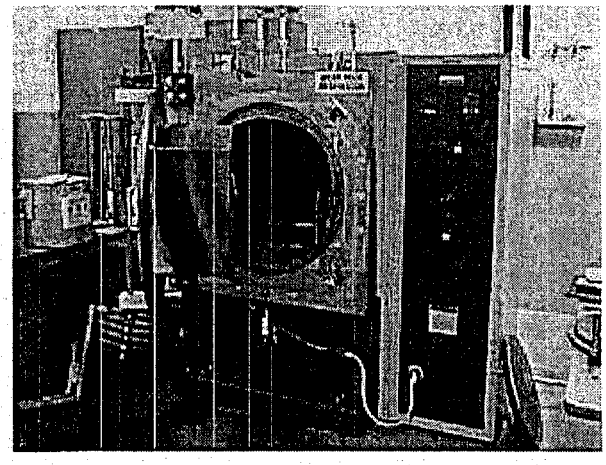

Figure 9. ACR's Binder Burnout Furnace

Step 7. Final consolidation and densification of the part is obtained by hot pressing. ACR's induction hot-press is capable of a maximum temperature of 2400 °C, and a maximum load of 100 tons (**Figure 10**). It can be operated in several different environments including vacuum, Argon, and Nitrogen atmospheres. It should be noted that some progress towards consolidation and densification of Si_3N_4/BN fibrous monolith test bars and billets by pressureless sintering was made towards the end of this program (as discussed in a later section of this report).

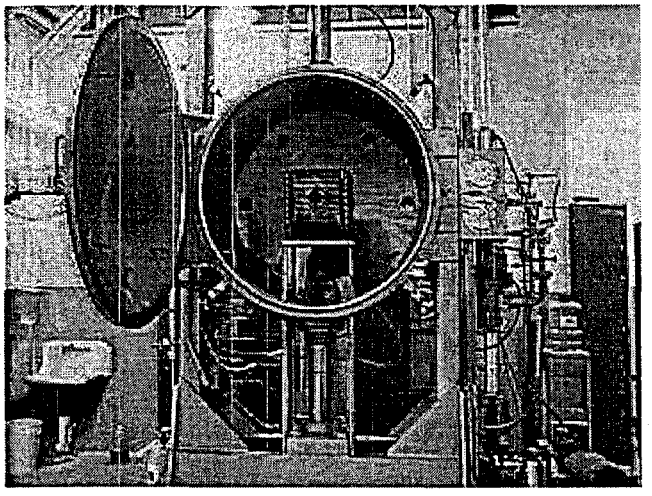

Figure 10. ACR's Hot Press.

As described above in processing steps, FM composites are truly monolithic composites and are processed by conventional powder processing technique using inexpensive raw ceramic powders. While somewhat labor-intensive, fibrous monolith composite processing is extremely versatile. FM composites can be produced from any set of thermodynamically compatible set of ceramic powders and/or metals. In addition, the flexible filaments produced during green processing are easily wound, braided or layed up to produce near net shape composite parts.

B. Fabrication of Si_3N_4/BN Billets for Independent Testing at WL/MLLN:

The purpose of this work was to establish an independent verification of the mechanical properties of fibrous monolith composites. ACR manufactured a number of Si_3N_4/BN FM billets for basic mechanical property evaluations that were subsequently performed at WL/MLLN. Verification of fibrous monolith performance by an independent DOD research group will generate a FM database without the presumed bias of an in-house study. WL/MLLN will also serve as a clearinghouse for this database, increasing the exposure of the materials developed on this program to other Air Force, DOD, and commercial applications.

ACR and the Materials Research Laboratory at Wright-Patterson Air force Base agreed on a test matrix for Si_3N_4/BN FM materials in early September of 1998. Based on this agreement, ACR fabricated 18 SFCX Si_3N_4/BN FM billets with several different lay-ups. The test matrix consisted of the following SFCX Si_3N_4/BN fibrous monolith billets with a cell to boundary volume ratio of 82.5/17.5:

1) Nine 6" x 6" x 1/8" billets with quasi-isotropic fiber lay-up,
2) Four 6" x 6" x 1/8" billets with symmetric 0/90 fiber lay-up,
3) Four 6" x 6"x 1/8" billets with random chopped fiber architecture, and
4) One 6" x 6" x 1/8" billet of uniaxial fiber lay-up.

In order to fabricate these billets, Si_3N_4 (with Y_2O_3 and Al_2O_3 sintering additives) and BN powders were individually ball milled for 48 hours. The milled Si_3N_4 and BN powders were recovered and then individually blended with thermoplastics and pressed into feedrods. These feedrods were extruded into 340 μm green filament. The extruded fiber was either wound on plastic sheets using computer controlled winding machine or in the case of the chopped fiber billets, cut into 1 cm lengths. Spray glue was used to facilitate adhering of green fiber to plastic sheets. The sheets were cut into 6.5" x 6.5" squares and stacked to desired orientations. A total of 40 'green' layers were stacked to obtain a final thickness of 0.125". The stacked layers or chopped fibers were placed in a steel die and compressed into a dense green billet using a heated Platten Press. The binder removal step followed the lamination step. The binder was removed by placing laminated billets in graphite die and heating graphite die in the binder burnout furnace. The graphite dies were then transferred to the hot-press, where the final consolidation of FM billets took place. The hot-pressing conditions for the consolidation of these billets were 1740 °C, 3.0 ksi pressure, and N_2 gas environment. The billets were post-machined to their final size (6" x 6" x 1/8") using a surface grinding machine prior to shipping to WL/MLLN. Nominal cell (Si_3N_4) dimensions of the billets were 150 μm and 250 μm in the hot pressing and normal to hot-pressing directions, respectively. The corresponding thickness of cell boundary (BN) was 15 μm and 20 μm, respectively.

ACR also supported Argonne National Laboratory's efforts on their program to develop oxide/oxide fibrous monolith entitled "Development of Advanced Fibrous Monoliths." ACR fabricated two Si_3N_4/BN FM with uniaxial and biaxial fiber orientations for ANL's independent testing of FM materials. These billets were processed in similar fashion as those supplied to WL/MLLN.

V. Independent Testing of Fibrous Monoliths at WL/MLLN

The independent testing of the 18 Si_3N_4/BN FM billets was conducted at WL/MLLN by Larry Zawada, Jim Stahler, and Jennifer Finch. The test matrix included tensile fast fracture tests at room temperature, 1150°C, and 1250°C; creep rupture tests at 1150°C; fatigue at 1150°C; fatigue with water fog exposure at 1150°C; and toughness testing at room temperature and 1150°C.

Progress reports have been provided periodically to ACR and DOE. The final report will be completed by Larry Zawada and submitted to DOE independent of this report.

VI. Carbide-based Fibrous Monoliths

Developmental work on the carbide- and diamond-based fibrous monolith coatings for drill bit inserts focused on the following material systems (cell/boundary):

1. WC (6%Co)/Co
2. WC (6%Co)/W-14%Ni-6%Fe
3. Diamond (WC-Co)/WC (11%Co)
4. Diamond (WC-Co)/WC (14%Co)
5. Diamond (WC-Co)/Nb
6. Diamond (WC-Co)/Co/Nb

Overall, the Diamond (WC-Co) with WC-Co cell boundaries were of the most interest to our commercial partner, Smith Tool. As a result, the majority of the research effort was focused on developing this material system. ACR's success in producing Diamond (WC-Co)/WC (11%Co) FM inserts with better wear resistance and impact tolerance then Smith Tool's state-of-the-art polycrystalline diamond coated insert led us to focus most of the research effort on developing a viable commercial product. The research on FM systems listed above are presented in the following sections in the chronological order of their development. Early work focused on the WC/Co systems followed by the development of the Diamond/WC systems. In the last several months of the program ACR worked on Diamond-cell FMs with ductile Nb and Co/Nb interfaces.

A. WC (6%Co)/ Co and WC (6%Co)/ W-14%Ni-6%Fe Fibrous Monoliths

Green FM Development

Developmental work on this program began with the WC (6%Co)/ Co and the WC (6%Co)/ W-14%Ni-6%Fe fibrous monolith systems.

ACR and Smith Tool began by studying the influence of the wax content on powder particle size of Smith's WC (6%Co) powder and ACR's ability to blend this powder with thermoplastics to obtain a viable fibrous monolith extrusion. The WC (6%Co) powder required a balling milling step with the inclusion of a small amount of a wax binder in order to achieve a particle size small enough (<5 μm) to use in ACR's blending and extrusion process. Smith Tool varied the wax content in the powder from 0.25 to 2 vol.% and ball milled the powders in their lab. This study was necessary in order for Smith Tool to be able to provide a consistent WC (6%Co) powder for the remainder of the program. It was determined that a wax content of 0.25% provided powder with a consistent average particle size of 4 μm.

At ACR, the powders were blended with various thermoplastics, plasticizers, and modifiers in a C.W. Brabender Plasticorder in order to obtain a formulation for each powder constituent. **Tables 1** through **3** provide the formulations for the Co, W-14%Ni-

6%Fe, and WC (6%Co) powders along with their respective polymers, plasticizers, and modifiers. These formulations provided the best extrusion/coextrusion behavior during the fibrous monolith 'green' fabrication process.

Table 1. Cobalt 'Shell' Material Formulation

Material	Density (g/cc)	Volume (cc)	Volume %	Weight (g)
Co	8.90	19.74	47.00	175.69
Graphite	2.25	1.18	2.80	2.65
EEA*	0.93	15.12	36.00	14.06
MPEG-550†	1.10	6.00	14.20	----

* EEA = Ethyleneethylacrylate

† MPEG-550 = 550 avg. MW of Methoxypolyethylene glycol

Table 2. Tungsten-Nickel-Iron 'Shell' Material Formulation

Material	Density (g/cc)	Volume (cc)	Volume %	Weight (g)
W-14%Ni-6% Fe	15.42	21.52	51.20	331.80
EEA	0.93	12.80	30.50	11.90
HMO#	0.88	1.70	4.10	----
Stearic Acid	0.85	0.89	2.10	0.75
MPEG-550	1.10	5.10	12.10	----

HMO = Heavy mineral oil

Table 3. Tungsten Carbide - 6% Cobalt 'Core' Material Formulation

Material	Density (g/cc)	Volume (cc)	Volume %	Weight (g)
WC(6%Co)	14.96	25.20	60.00	376.99
EEA	0.93	13.99	33.30	13.01
B-67@	1.06	1.55	3.70	1.65
HMO	0.88	1.30	3.00	----

@ B-67 = Acrylic copolymer resin

Utilizing the 'green' materials outlined above, 3" x 3" billets were then fabricated from both the WC (6%Co)/Co and WC (6%Co)/W-Ni-Fe fibrous monolith compositions. In preparation, the WC(6%Co)/thermoplastic was compressed into 90 vol.% fibrous monolith 'core' feedrods and Co/thermoplastic and W-Ni-Fe/thermoplastic materials were compressed into 10 vol.% fibrous monolith 'shells'. The 'shells' and 'cores' were assembled and extruded through a 2 mm spinnerette and the 2 mm extrudate was then sectioned into 5 inch long spaghetti. Approximately 86 spaghetti were rebundled and extruded a second time through a 1 mm spinnerette. The final 1 mm extrudate (containing ~86 WC/metal fibrous monolith cells) was sectioned to 3 inch lengths and layed up with uniaxial and 0°/90° fiber orientations and laminated into 0.5 inch thick 'green' billets. A total of twelve billets were fabricated (**Table 4**).

Table 4. Composition and Architecture of Green FM Billets

Sample #	FM Composition	Layup
ACRAMP001	WC(Co)/Co	[0°]
ACRAMP002	WC(Co)/Co	[0°]
ACRAMP003	WC(Co)/Co	[0°]
ACRAMP004	WC(Co)/Co	[0°]
ACRAMP005	WC(Co)/W-Ni-Fe	[0°]
ACRAMP006	WC(Co)/W-Ni-Fe	[0°]
ACRAMP007	WC(Co)/W-Ni-Fe	[0°/90°]
ACRAMP008	WC(Co)/W-Ni-Fe	[0°]
ACRAMP009	WC(Co)/W-Ni-Fe	[0°]
ACRAMP010	WC(Co)/W-Ni-Fe	[0°]
ACRAMP011	WC(Co)/W-Ni-Fe	[0°]
ACRAMP012	WC(Co)/W-Ni-Fe	[0°]

Several months into the program, ACR experienced problems with the viscosity (torque) of the WC (6%Co)/polymer batches. We believed that the manufacturer of the WC-based powder has altered the surface chemistry of their powder, possibly due to a change in surfactant.

In order to combat this problem, ACR began milling the powders in-house for a 5 day milling cycle in order to strip off the surfactant and reduce the particle size of the starting powder. This allowed for tighter control of the batch viscosity but it also required changing the powder/binder recipes. **Tables 5** and **6** outline the new formulations for the W-Ni-Fe and WC(6%Co) powders, respectively, along with their respective polymers, plasticizers, and modifiers.

Table 5. Modified Tungsten-Nickel-Iron 'Shell' Material Formulation

Material	Density (g/cc)	Volume (cc)	Volume %	Weight (g)
W-14%Ni-6% Fe	15.42	26.40	62.86	407.11
EEA*	0.93	13.59	32.36	12.64
B-67@	1.06	1.51	3.60	1.60
MPEG-550†	1.10	5 cc	11.91	----
HMO#	0.88	2 cc	4.80	----

* EEA = Ethyleneethylacrylate

@ B-67 = Acrylic copolymer resin

† MPEG-550 = 550 avg. MW of Methoxypolyethylene glycol

HMO = Heavy mineral oil

These formulations provided the best extrusion/coextrusion behavior during the fibrous monolith 'green' fabrication process. Note that the B-67 polymer was switched from the 'Core' material to the 'Shell' material. This was done in order to decrease the torque of the W-Ni-Fe/binder recipe while leaving the WC(6%Co)/binder as high as possible.

Table 6. Modified Tungsten Carbide (6% Cobalt) 'Core' Material Formulation

Material	Density (g/cc)	Volume (cc)	Volume %	Weight (g)
WC(6%Co)	14.96	26.46	63.00	395.84
EEA	0.93	15.54	37.00	14.45

Burnout Studies

As it turns out, much of the work performed in the first few months of the program focused on binder development and their burnout characteristics. Binder pyrolysis is a complicated, rate-controlled issue, and it can be affected by a number of factors including: polymer and plasticizer selection; ceramic or metal powder type, burnout atmosphere, and the lamination pressures being applied to the 'green' bodies.

ACR began modifying the burnout characteristics of its FM systems by replacing EVA, a binder traditionally used in ACR's FM green processing, with the acryloid resin, B-67. EVA has a tendency to breakdown too rapidly during binder burnout causing excessive cracking and bloating in the billets or fabricated parts. By replacing EVA with B-67, ACR expected to minimize cracking and bloating while running a short, 42.75 hour, binder burnout schedule.

Unfortunately, the first several billets (**Table 4** above) showed signs of bloating and cracking after final consolidation and hot pressing. This bloating and cracking likely occurred during binder burnout. The elimination of these features requires a change in our standard binder burnout schedule (shown in **Profile #1**). It has been observed in past research that fine metal powders can catalyze the decomposition reactions that occur during binder burnout. This can lead to bloating and cracking of FM components. To eliminate the bloating and cracking problems, a slower binder burnout profile was developed and applied to the pyrolysis of the remaining ten billets (**Profile #2**). The change to a 71.5 hour burnout schedule greatly reduced the bloating and cracking problem observed with the billets burned out using **Profile 1#**.

Profile #1 (Total time = 42.75 hours):

1) heat at 60°C/hour to 160°C and no hold time
2) heat at 6°C/hour to 300°C and no hold time
3) heat at 12°C/hour to 390°C and no hold time
4) heat at 18°C/hour to 500°C and no hold time
5) heat at 60°C/hour to 600°C and hold for 2 hours

Profile #2 (Total time = 71.5 hours):

1) heat at 12°C/hour to 160°C and hold for 2 hours
2) heat at 6°C/hour to 300°C and hold for 2 hours
3) heat at 6°C/hour to 400°C and hold for 2 hours
4) heat at 12°C/hour to 500°C and no hold time
5) heat at 18°C/hour to 600°C and hold for 1 hours

After implementing the new burnout schedule, ACR attempted to determine if lamination pressure was going to be a concern for our binder/powder formulations. To evaluate this ACR sent samples of the three different binder/powder systems that were being used in the program to the University of Michigan. Rodney Trice performed binder burnout tests on these systems. The following is a summary of his results taken from a report submitted in September of 1997 (**Appendix A**, attached to this final report, is a copy of The University of Michigan's report submitted to ACR on 9/31/97):

Material 1: EVA/EEA/HMO/WC(6%Co) powder ('Old' binder system for cells)
Material 2: EEA/B-67/HMO/WC(6%Co) powder ('New' binder system for cells)
Material 3: EEA/HMO/MPEG-550/W-Ni-Fe powder

Several pellets, 28 mm in diameter and 7 mm thick, were prepared by pressing chunks of compounded green material at approximately 150°C. (Note: temperature was monitored by attaching a thermocouple to the outer shell of the metal die. When the outer shell reached 100°C, the load was applied. The heated platens used for warm lamination were then turned off and a fan was used to further cool the platens and die.) Three different processing conditions were investigated for each of the three materials:

(1) 2000 psi molding pressure
(2) 2000 psi molding pressure followed by a 20 hour anneal at 140°C
(3) 500-600 psi molding pressure.

The samples were measured and weighed before burnout. Binder burnout experiments were conducted using the Profile # 2 (a 71.5 hrs burnout cycle). This cycle was carried out in flowing nitrogen. Following burnout, the samples were weighed and carefully measured. The results of these measurements are shown in **Table 7.** Percentage calculations were based on the original dimension or weight. The samples were examined visually. Materials 2 and 3 exhibited some bloating. Some minor bloating was observed in Material 1 prior to binder burnout when the samples were annealed for 20 hour at 140 °C (Processing condition # 2).

Additional bloating was observed in this material after binder burnout. Material 3 bloated and cracked during binder burnout for the 500-600 psi molding condition. Optical photomicrographs of these samples before and after burnout are shown in **Figure 12.** For all materials, weight loss was approximately 2.8-4.5%.

To summarize the binder burnout studies, ACR utilized the 72.5 hours binder burnout schedule for the production of test billets and the larger FM components produced during this program. This schedule minimized bloating especially in the thicker parts. Because of the observation that higher molding pressures tend to reduce the effects of bloating, cracking, and delamination we pressed green feedrods at the higher molding pressures. This became particularly important during the production of the FM drill bit coatings produced later in the program (see below) as it minimized and even eliminated delamination problems observed in the binder burnout of these parts. The addition of an annealing step, such as the 20 hours anneal at 140 °C, did not show a significant reduction in the problems associated with binder burnout. For this reason an annealing step was not implemented in the green processing of the fibrous monoliths developed on this program.

Table 7. Results of the Binder Burnout Experiments

Warm Pressing Conditions	Physical Parameters	Material 1	Material 2	Material 3
2000 psi	Thickness Increase, %	2.64	2.96	4.84
	Weight Loss, %	4.4	3.6	4.0
	Comments	OK	OK	OK
2000 psi + 140°C anneal for 20 hrs.	Thickness Increase, %	9.58	1.36	0.40
	Weight Loss, %	3.7	3.5	2.8
	Comments	Bloated	OK	OK
500-600 psi	Thickness Increase, %	4.23	3.13	2.52
	Weight Loss, %	4.4	3.8	4.5
	Comments	OK	OK	Bloated and Cracked

Material 1 – 2000 psi plus 20 hr anneal at 140°C
Before Burnout

Material 3 – 500 psi
Before Burnout

Material 1 – 2000 psi plus 20 hr anneal at 140°C
After Burnout

Material 3 – 500 psi
After Burnout

Figure 12. Photomicrograph of samples before and after binder rnout.

Characterization of WC(Co) Fibrous Monoliths

As described above, twelve sample billets were fabricated during the first several months of this program for microstructural analyses at The University of Michigan as well hardness and wear testing at Smith Tool. **Table 8** lists the twelve sample billets prepared along with their composition, lay-up, and the conditions for their consolidation by hot pressing.

Table 8. Hot Pressing of WC (Co)/Metal Fibrous Monolith Billets

Sample #	FM Composition	Layup	Hot Pressing Temp. (°C)	Hot Pressing Pressure (ksi)
ACRAMP001	WC(Co)/Co	[0°]	1330 °C	2 ksi
ACRAMP002	WC(Co)/Co	[0°]	1330 °C	2 ksi
ACRAMP003	WC(Co)/Co	[0°]	1250 °C	1 ksi
ACRAMP004	WC(Co)/Co	[0°]	1200 °C	1 ksi
ACRAMP005	WC(Co)/W-Ni-Fe	[0°]	1460 °C	1 ksi
ACRAMP006	WC(Co)/W-Ni-Fe	[0°]	1460 °C	1 ksi
ACRAMP007	WC(Co)/W-Ni-Fe	[0°/90°]	1460 °C	1 ksi
ACRAMP008	WC(Co)/W-Ni-Fe	[0°]	1390°C	1 ksi
ACRAMP009	WC(Co)/W-Ni-Fe	[0°]	1290°C	1 ksi
ACRAMP010	WC(Co)/W-Ni-Fe	[0°]	1250° C	1 ksi
ACRAMP011	WC(Co)/W-Ni-Fe	[0°]	1250° C	1 ksi
ACRAMP012	WC(Co)/W-Ni-Fe	[0°]	1250° C	1 ksi

The first few WC (Co)/W-Ni-Fe billets (samples ACRAMP005, ACRAMP006, and ACRAMP007) and WC (Co)/Co billets (samples ACRAMP001, ACRAMP002, and ACRAMP003) were hot pressed at temperatures too high for these systems. While the billets looked good on initial inspection, after sectioning and microstructural analysis at the University of Michigan it was found that the Co and W-Ni-Fe metals underwent significant flow during hot pressing and the fibrous monolith architecture was destroyed. Billets ACRAMP004, ACRAMP008, and ACRAMP009 were hot pressed at successively lower temperatures.

Figure 13 is a SEM photomicrograph of a WC (Co)/Co FM sample taken from billet ACRAMP003). Energy dispersive spectroscopy (EDS) showed that the 'cells' contained WC (Co) while the 'cell boundaries' contained only graphite (an additive to the cobalt 'cell boundary' powder). This type of microstructure is common for all of the WC

(Co)/Co billets. EDS showed that the cells contain much greater than their original 6% Co, indicating that it had been forced into the cells from the cell boundaries during hot pressing.

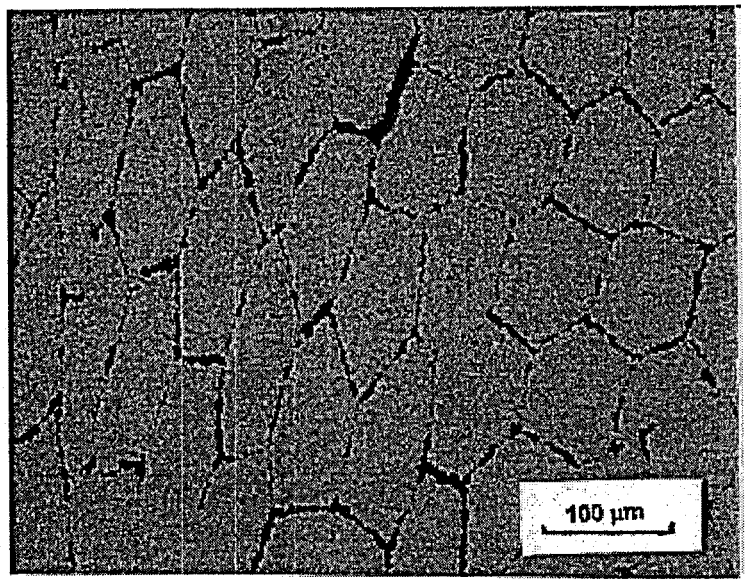

Figure 13. SEM photomicrograph of cross-section of a WC (Co)/Co fibrous monolith billet

Wear Resistance Studies

In addition to the scanning electron microscope analyses, Smith Tool subjected WC (6%Co)/ W-Ni-Fe (90 vol. %/10 vol. %) fibrous monolith composite samples to wear tests, ASTM G65 and ASTM B611, which are the low stress and high stress abrasion wear tests, respectively. In the ASTM G65 test, abrasive particles (semi-rounded 50/70 mesh (210/300 mm) silica sand) were fed between a test material and a rotating chlorobutyl rubber wheel. The test material was pressed against the rotating wheel at a specific force of 130 N (30 lbs). The speed of the rotating wheel was 200±10 rpm and the sand flow rate was 380 - 430 g/min. The weight loss of the material was measured by weighing each sample before and after a 6000 revolution test and then converting to a volume loss in cubic centimeters per 1000 revolutions. The stress exerted on the sample was low enough as not to crush the abrasives in the ASTM G65 test. On the contrary, in the ASTM B611 test the abrasive particles, 30 mesh (590mm) angular aluminum-titanium oxide, were fed and crushed between an annealed AISI 1020 steel wheel and a test material. Some degree of impact on the test material was encountered due to large particles. The abrasive in the slurry was fed between the test material and the wheel by the rotating wheel at 100±10 rpm. The test material was pressed against the rotating wheel with a 196 N (44 lbs) force for 1000 revolutions. The wear number was expressed as the reciprocal of the volume loss (in cubic centimeters) of the test material per 1000 revolutions. The larger the number in the ASTM B611 test, the better the wear resistance.

The test results compared to those of Smith Tool's standard 406 grade cemented carbide material are given **Table 9**. The substantial improvement in high stress abrasion resistance implies a higher toughness for the 90 WC (6%Co)/10 W-Ni-Fe fibrous monolith composite.

Table 9. Summary of Wear Resistance Data on WC-based Fibrous Monoliths

Material	Low stress wear resistance (10^{-3} cm^3/1000 revolutions)	High stress wear resistance (1000 revolutions/cm^3)
90 WC(6%Co)/10 W-Ni-Fe	1.60	**18.10**
406 grade WC-Co	**1.10**	11.40

B. Diamond-WC-Co/WC (Co) Fibrous Monoliths

Green FM Development

Approximately six months after this program began, ACR started work on powder binder formulations at the request of Smith Tool for the fabrication of diamond-carbide fibrous monoliths for drilling tool inserts. Smith Tool believed that fibrous monolith processing applied to their polycrystalline diamond compact (PCD) technology had tremendous potential for improving their hard rock drilling bits. Smith shipped a polycrystalline diamond powder with WC and Co additives (Diamond 817 powder) to ACR in of 1998. ACR and Smith chose WC - Co powders as the cell boundary materials.

A fully developed test matrix agreed upon by Smith Tool and ACR is shown in **Table 10**. This test matrix includes two different tungsten carbide compositions, three different cell sizes, and three different cell/cell boundary ratios. This will allow us to evaluate the effects of composition, cell size, and cell to boundary ratios on the wear and impact resistance of the Diamond /WC FM inserts.

The diamond and WC powders shipped by Smith Tool were blended with various thermoplastics, plasticizers, and modifiers in a C.W. Brabender Plasticorder in order to obtain a formulation for each powder constituent. **Tables 11 and 12** give the formulations for the WC 411 and DIA817 powders along with their respective polymers, plasticizers, and modifiers. These formulations provided the best extrusion/coextrusion behavior during the fibrous monolith 'green' fabrication process.

Table 10. Test Matrix of DIA817/WC-Co Fibrous Monoliths.

Sample	Vol. %	C:Cb	Composition	Cell Size
A	82.5/17.5	10	DIA817/WC411	100 μm
B	82.5/17.5	10	DIA817/WC411	200 μm
C	82.5/17.5	10	DIA817/WC614	100 μm
D	82.5/17.5	10	DIA817/WC614	200 μm
E	70/30	5	DIA817/WC411	100 μm
F	70/30	5	DIA817/WC411	200 μm
G	70/30	5	DIA817/WC614	100 μm
H	70/30	5	DIA817/WC614	200 μm
I	50/50	1	DIA817/WC411	50 μm
J	50/50	1	DIA817/WC614	50 μm

WC411 = WC powder with 11 wt % Co
WC614 = WC powder with 14 wt % Co

Table 11. Tungsten Carbide - 11% Cobalt 'Shell' Material Formulation

Material	Density (g/cc)	Volume (cc)	Volume %	Weight (g)
WC411	14.44	23.52	56.00	339.63
EEA*	0.93	16.38	39.00	15.23
B-67@	1.06	1.26	3.00	1.34
MPEG-550†	1.10	0.80	2.00	-----

* EEA = Ethyleneethylacrylate
@ B-67 = Acrylic copolymer resin
† MPEG-550 = 550 avg. MW of Methoxypolyethylene glycol

Table 12. Diamond/Tungsten Carbide/Cobalt 'Core' Material Formulation

Material	Density (g/cc)	Volume (cc)	Volume %	Weight (g)
DIA817	4.01	25.83	61.50	103.58
EEA	0.93	15.12	36.00	14.06
HMO#	0.88	1.00	2.50	-----

HMO = Heavy mineral oil

Utilizing these 'green' materials, 0.79" diameter x 3" long 'green' rods were then fabricated from the DIA817/WC411 fibrous monolith composition. **Figure 14** is a photograph of one of these rods. Three rods were prepared by the following procedure: DIA817/thermoplastic was compressed into 90 vol.% fibrous monolith 'core' feedrods; WC411/thermoplastic was compressed into 10 vol.% fibrous monolith 'shells'; the 'shells' and 'cores' were assembled and extruded through a 2 mm spinnerette; the 2 mm extrudate was sectioned at ~5 inch lengths, rebundled as ~86 cells, and extruded through a 1 mm spinnerette; and the final 1 mm extrudate (containing ~86 WC/metal fibrous monolith cells) was sectioned to 3.5 inch lengths, rebundled, and laminated in a 20 mm diameter die. This procedure provided 3" long feedrods with ~130 μm diameter cells in the fibrous monolith structure positioned down the long axis of the rods.

The 'green' rods were then sectioned radially into 0.030" thick x 20 mm diameter wafers. The wafers were sanded down to a thickness of 0.025", dried at 55°C, loaded into a niobium can, and laminated into a hemispherically shaped caps using a steel die and WC punch. **Figure 15** is a photograph showing several of the 'green' disks before lamination, as well as the tooling required to shape the caps. **Figure 16** shows the green discs before and after lamination into hemispheres whose outer surface fits the inside of Smith's Nb cans and inner surface fits on top of Smith's WC inserts. The 'green' DIA817/WC411 caps were bonded to the bottom of the niobium cans with a thin layer of adhesive and sent to Smith Tool for firing. At Smith, the Nb cans were loaded with two transition layers of diamond+WC+Co and a fully dense WC (Co) insert (see the schematic in **Figure 17**). The inserts were then cold pressed in a 40 ton press, loaded into a six-sided press, and pressed at ~800,000 psi at a temperature of 1300°C for 4 to 5 minutes. After firing, the niobium can was removed in a boiling caustic solution followed by sand blasting and a minimum of machining to produce a finished insert for one of Smith's production bits for petroleum drilling.

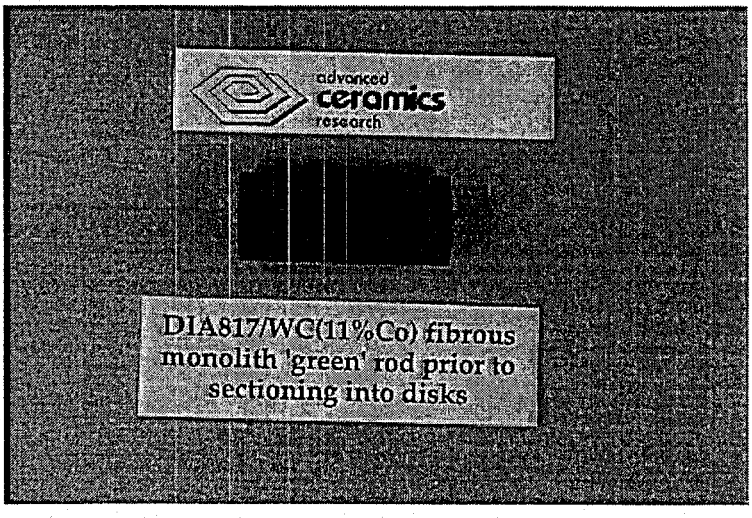

Figure 14. Photograph of a DIA817/WC(11%Co) fibrous monolith 'green' rod prior to sectioning into disks for drilling tool inserts.

Figure 15. Photograph of DIA817/WC(11% Co) fibrous monolith green discs and the lamination tooling used to press and shape the discs.

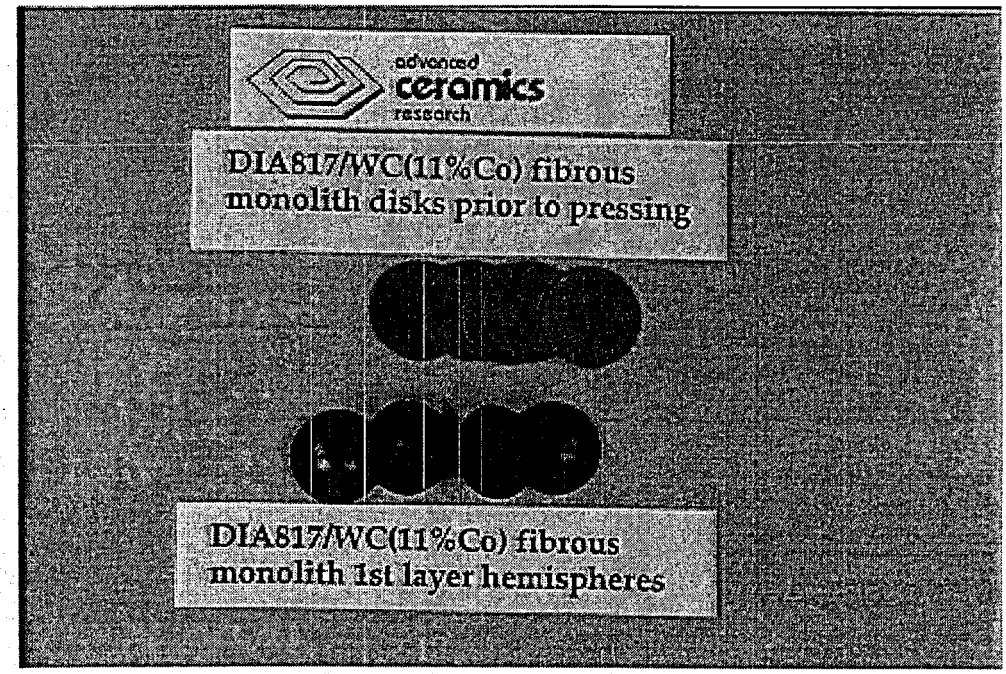

Figure 16. Photograph of a DIA817/WC(11%Co) fibrous monolith 'green' disks both before and after pressing into 1st layer hemispheres.

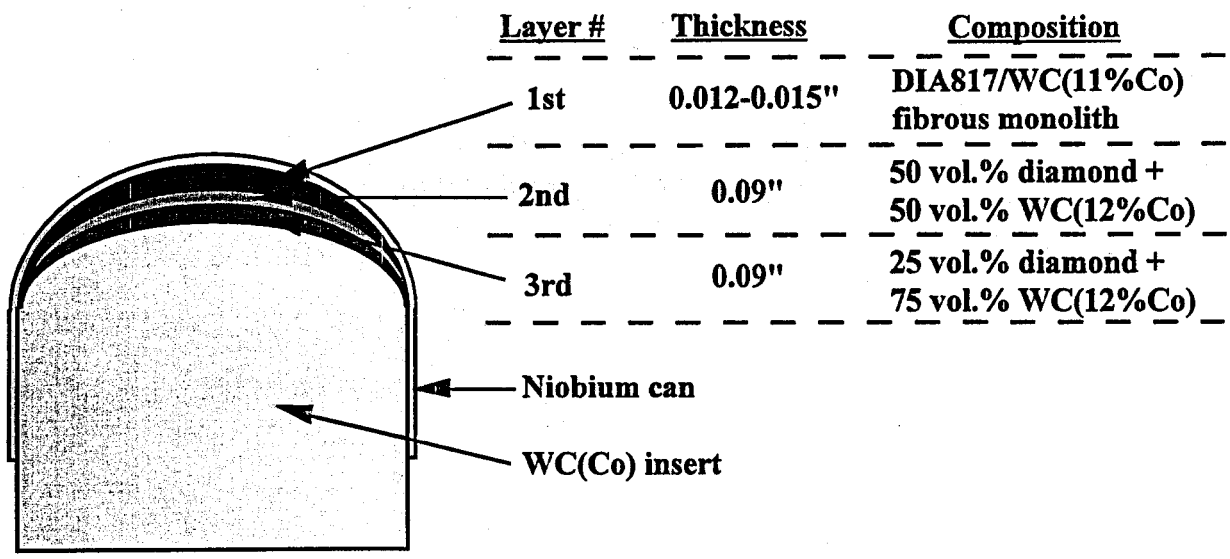

Figure 4. Schematic showing the layers required for fabricating WC tool bit inserts with DIA817/WC fibrous monolith as the surface layer.

Binder Burnout Studies

Smith Tool reported an occasional problem with the cracking and delamination of the DIA817/WC-Co hemispheres during the binder burnout of these parts at their Megadiamond facility in Provo, UT. This observation necessitated additional binder burnout studies to evaluate a cause and effect a solution. Megadiamond uses a 29 hour binder burnout schedule for their parts. To simplify the production of FM components at the Megadiamond facility and avoid disrupting their production by setting up a special binder burnout schedule ACR suggested we try preparing our parts using the 29 hour binder burnout schedule. Initially, the very thin FM parts produced by ACR appeared to be amenable to the shorter burnout schedule. However, after several runs Megadiamond observed wrinkled and cracked inserts after removal from the hot press. These textures are typically associated with binder burnout problems so ACR began a series of experiments to determine the cause.

The first experiment consisted of heating green FM flats to 160 °C at a rate of 21.0 °C/hr and holding for an hour. The FM samples showed no cracking during this step of Megadiamond's profile. ACR then heated the FM flats through the first two steps of Megadiamond's profile to 300 °C at a rate of 35.1 °C/hr to get to temperature in 7.83 hours, followed by a hold for an hour at 300 °C. Again, the samples showed no cracking during this binder burnout profile. Efforts to reproduce cracking in the 300-400 and 400–600 steps also failed to produce any observable cracking or delamination in ACR's furnace.

The cracking may be occurring during the cool down but ACR's inability to reproduce the cracking and delamination effects makes it difficult to ascertain the cause of the problem. Towards end of the program, delamination problems were again observed in parts ACR produced for Smith Tool. Smith Tool informed ACR that these problems are also observed on occasion in the standard polycrystalline diamond parts Megadiamond produces on a daily basis. At this time cause of the intermittent problems with binder burnout remains a mystery but Megadiamond continues to explore the cause at their Provo, UT facility.

Characterization of DIA817/WC (Co) Fibrous Monoliths

Several 0.030" thick x 20 mm diameter 'green' wafers were sent to the University of Michigan for structural characterization of their cell/cell boundary morphology. The University of Michigan prepared three reports that were submitted to ACR in January and February of 1998. The University of Michigan reports are appended to this report (see **Appendix B, Appendix C** and **Appendix D**). **Appendix B** and **C** focused on the green flats produced by ACR while **Appendix D** is an examination of a hot pressed insert of one of the original green discs.

A summary of these reports follows:

After receipt of the wafers from ACR, the samples were individually polished down to 1 μm surface finish and observed by scanning electron microscopy (SEM) in back–scattered mode. In this mode, the tungsten and cobalt present in the cell boundaries appears as the high contrast phase. **Figures 18** and **19** show SEM images of the 'green' DIA817/WC411 fibrous monoliths having a nominally 100 and 200 μm cell sizes, respectively. The diamond-carbide cells appear in low contrast while the cobalt binder and tungsten carbide grains appear in bright contrast.

As can be seen in **Figure 18**,and is typical for the FM parts produced by ACR, the diamond cell size and shapes remain fairly uniform from sample to sample. Occasionally, distorted cells can be observed like those seen in **Figure 19**. These distorted cells tend to be found adjacent to the bundle boundaries. This means that the these distorted cells are the filaments on the outer edge of the multifilament feedrod and are in contact with the steel extrusion die walls during the second pass extrusion. The distorted filaments are almost always observed in the first and last segments (12 inches or so in length) of filament extruded during the second pass. These distorted filaments are thus a consequence of the extrusion process. To minimize, or eliminate their presence, ACR now visually inspects the extruded second pass filaments to remove distorted or non-uniform filaments before producing the final green parts.

DIA817/WC(11%Co) - 82.5/17.5 Vol.%
Nominal Cell Size = 100 μm

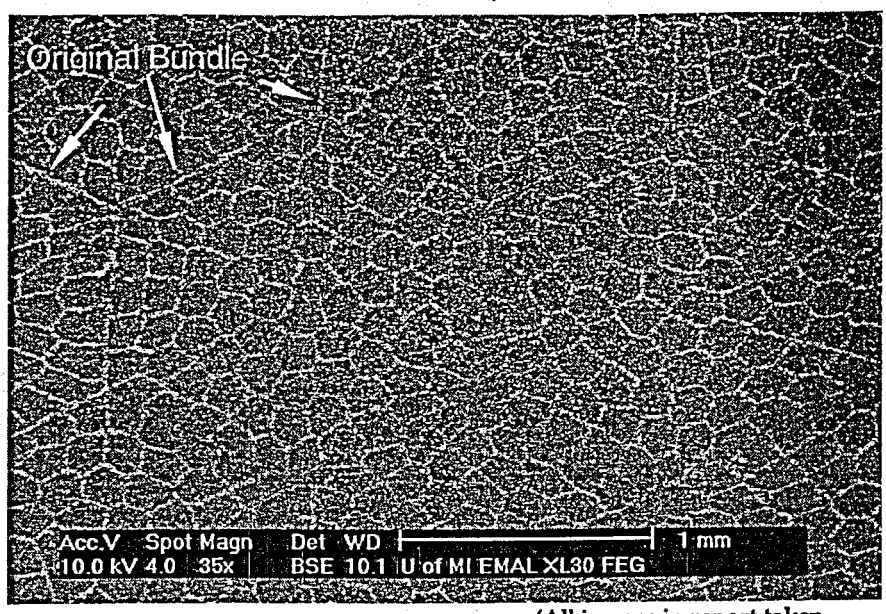

(All images in report taken
in back-scattered imaging mode.)

DIA817/WC(11%Co) - 82.5/17.5 Vol.%
Nominal Cell Size = 100 μm

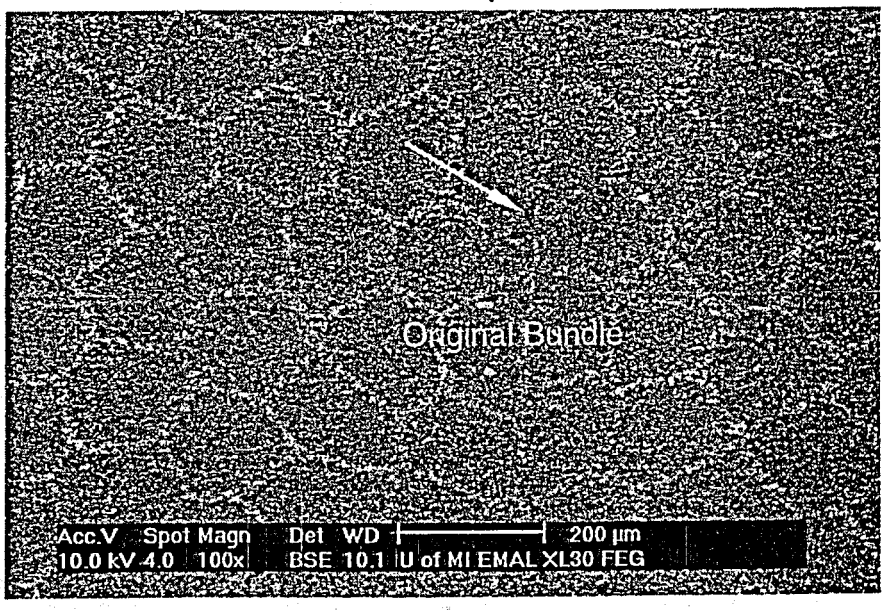

Measured Cell Size = 150 μm (includes cell and one cell boundary)
Measured Thickness of Cell Boundaries = 10–15 μm

Figure 18. Back-Scattered SEM images of the 'green' DIA(817)/WC(11%Co) FMs having a nominally 100 μm cell size. The diamond-carbide cells appear dark while the cobalt binder and tungsten carbide grains appear in bright contrast.

DIA817/WC(11%Co) - 82.5/17.5 Vol.%
Nominal Cell Size = 200 μm

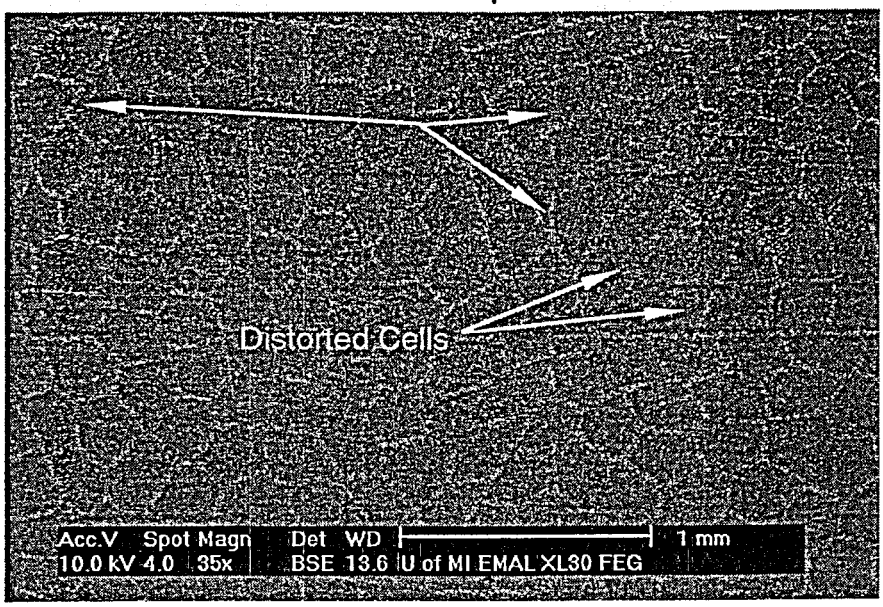

DIA817/WC(11%Co) - 82.5/17.5 Vol.%
Nominal Cell Size = 200 μm

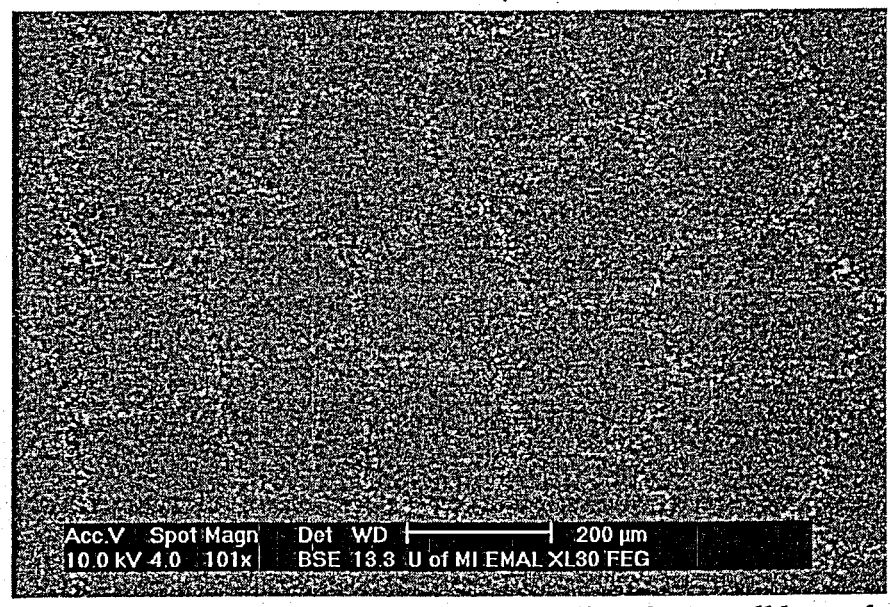

Measured Cell Size = 240 μm (includes cell and one cell boundary)
Measured Thickness of Cell Boundaries = 20 μm

Figure 19. Back-Scattered SEM images of the 'green' DIA(817)/WC(11%Co) fibrous monoliths having a nominally 200 μm cell size. The diamond-carbide cells appear dark while the cobalt binder and tungsten carbide grains appear in bright contrast.

Location: Near the Top of the Insert

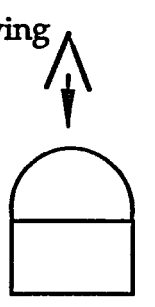

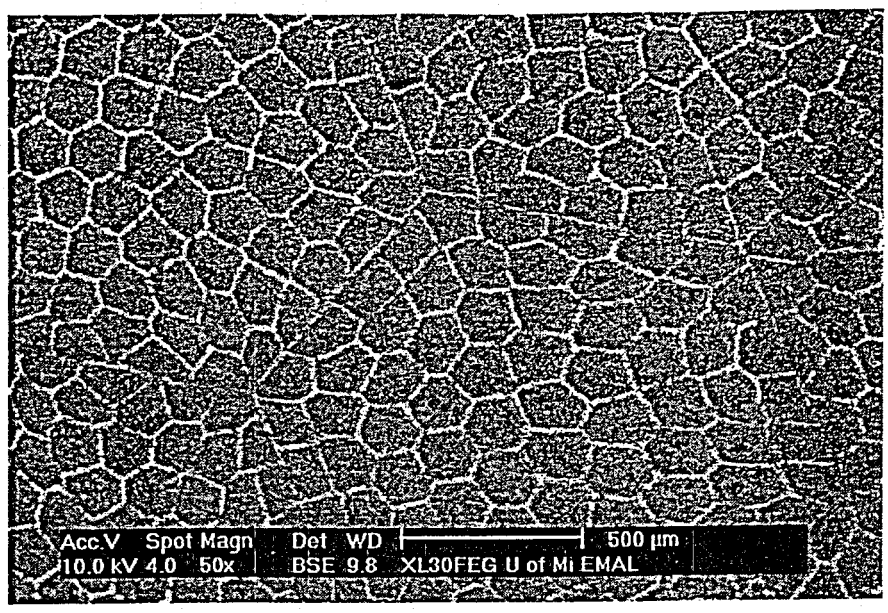

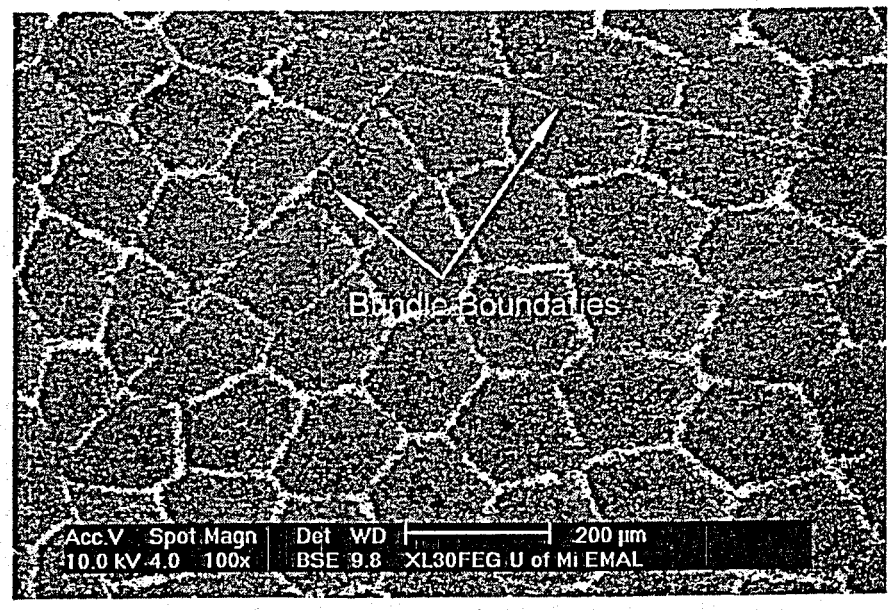

Figure 20. Back–scattered SEM images generated near the top of the tool bit insert. The cell boundaries and bundle boundaries are clearly defined in these images, and the cells are homogenous in size.

Location: Near the Top of the Insert

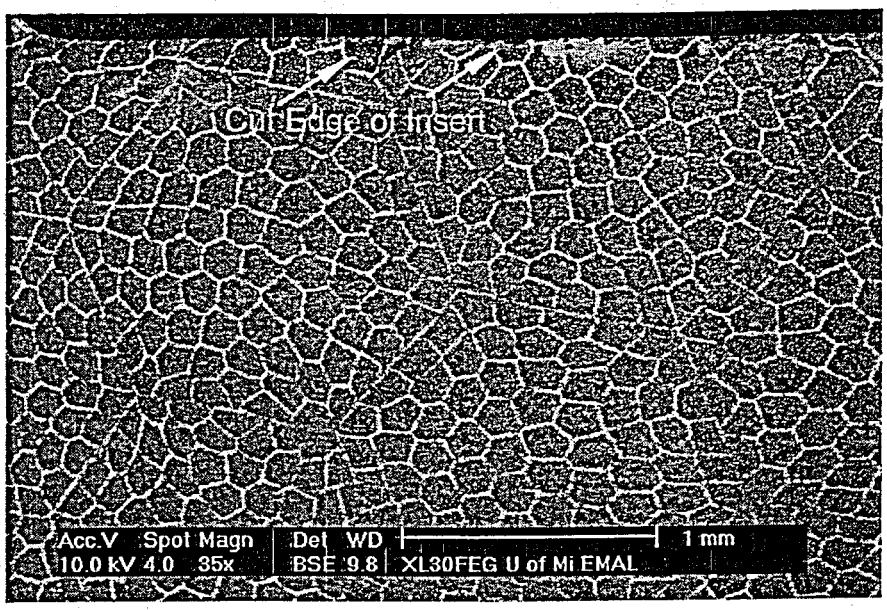

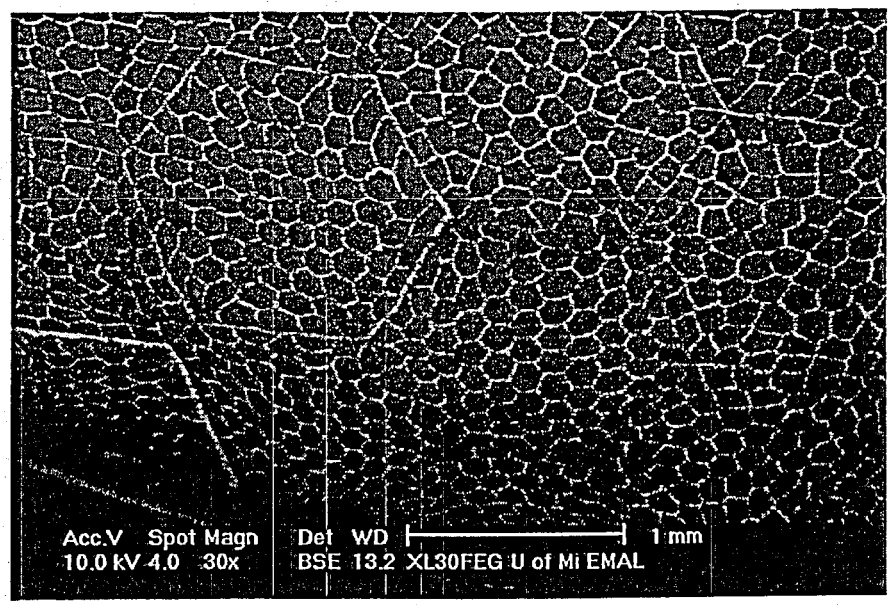

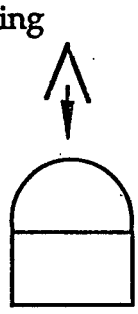

Figure 21. Low magnification SEM photomicrographs of the tool bit insert, looking down from the top. In the top image, the cut edge is apparent. The bottom image is looking down the side of the insert. Clearly shown in both images are homogenous cells.

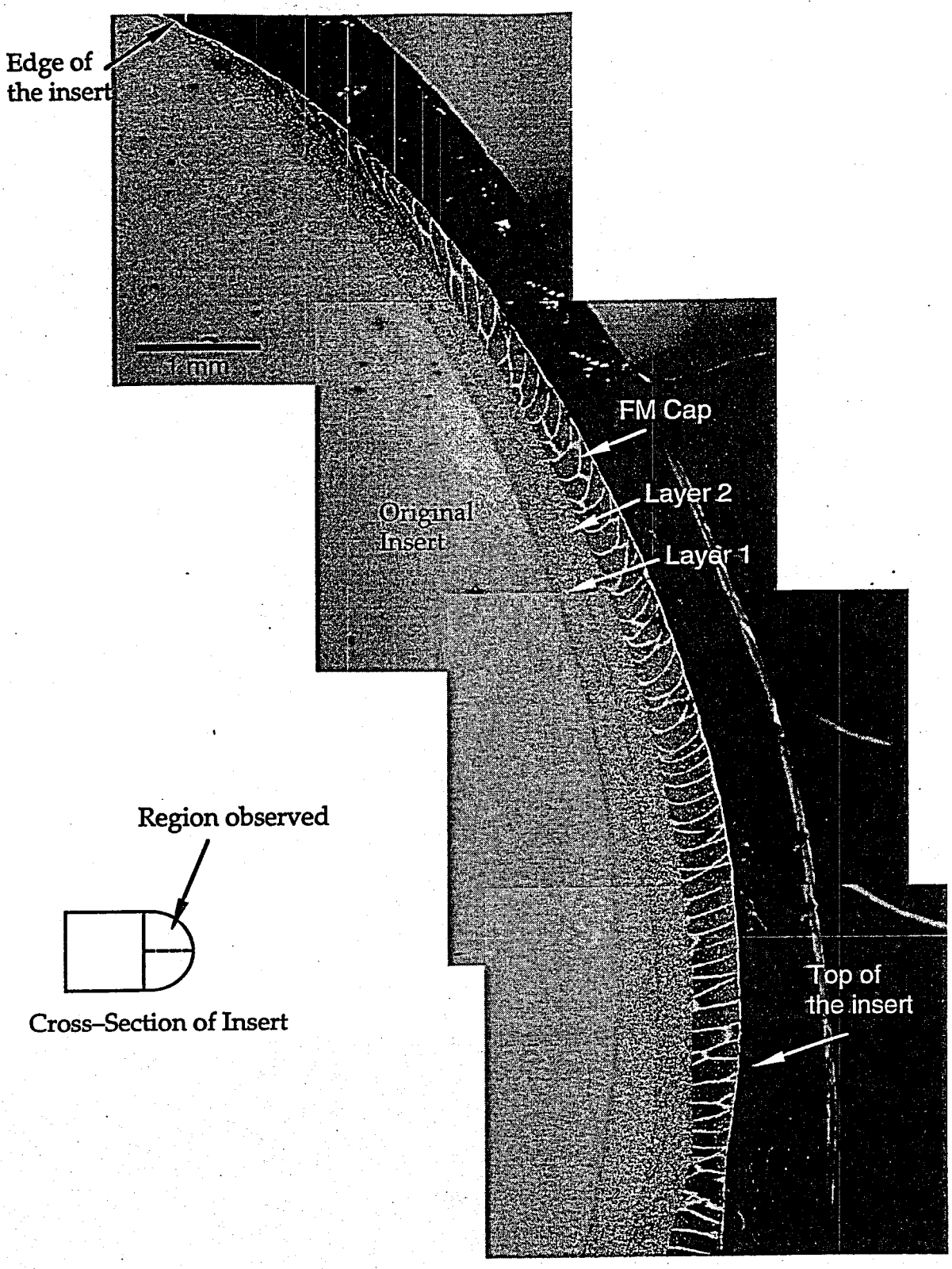

Figure 22. Composite image showing one–half of the FM cap. The thickness of the cap is greatest at the top of the insert.

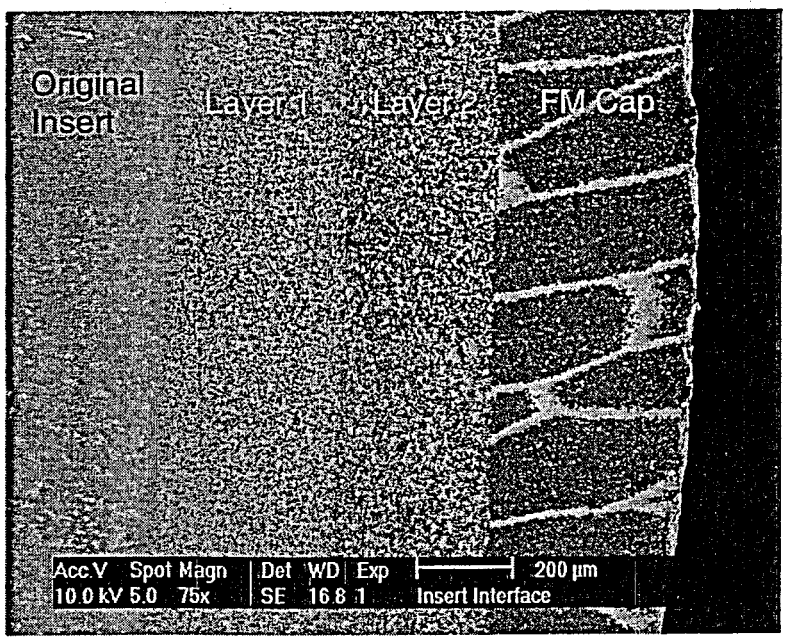

(a). Secondary electron image

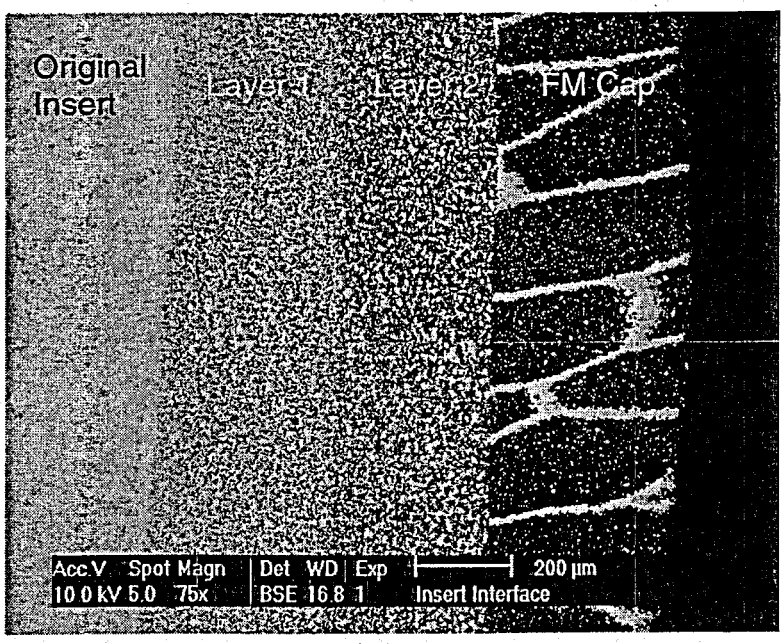

(b). Back–scattered electron image

Figure 23. Cross–sectional view of the interfaces in the insert. The top image was taken in a secondary electron imaging mode while the bottom micrograph was taken in a BSE imaging mode.

In addition to the SEM examination of the green caps and flats a hot pressed insert was also sent to the University of Michigan for microstructural characterization (**Appendix D**). SEM analyses were performed in both back–scattered (BSE) and secondary electron mode. In the BSE mode, the tungsten and cobalt present in the cell boundaries appeared as the high contrast phase. EDS was also performed. The drill bit was sectioned in half and its cross-section was surface ground with a 600 grit diamond wheel. Polishing of the cross-section was attempted with diamond polishing wheels with little success. The insert was then cleaned and a thin layer of Au/Pd coating was applied to its outer surface. Images were taken from three perspectives - looking down from the top and side of the insert at the as-fabricated fibrous monolith surface layer, as well as a cross-sectional perspective detailing all of the layers in the tool bit insert.

The SEM images in **Figures 20** and **21** show the macrostructure of the cells and cell boundaries. In general, the cells associated with the fibrous monolith cap were very homogeneous in size over the entire hemisphere. Cell distortion was only noted in the very small region where the cap "ran out" into the original WC drill bit (along the side of the insert). Note that distortions of the cells in this region are of little consequence because this area of the insert sees little wear or impact during drill bit operation. Low magnification SEM images of the cross-section reveal the 3 distinct layers and the original WC insert (**Figure 22**). The fibrous monolith cap is approximately 300 μm thick near the top of the drill (**Figure 23**). Higher magnification images reveal no cracking at any of the interfaces. In addition, limited energy dispersive spectroscopy (EDS) was performed on the bit revealing three distinct phases apparent in the cells. The dark or low contrast regions are predominantly C (diamond). A medium contrast phase is also apparent that is rich in Co (the metal which binds the diamond particles together). There are also a few regions having a higher contrast in the cells with an identical composition to the cell boundary phase – predominantly W (probably WC).

Impact Resistance

Smith Tool subjected several Diamond817/WC411 coated inserts to impact resistance testing. The test involved measuring the drop height to failure (in inches) of a component as a fixed weight is dropped from increasing heights until the part fails. The FM inserts were tested and then compared to Smith's standard polycrystalline diamond coated inserts. Preliminary results indicated that the FM coated inserts exhibited only 70% of the impact resistance observed for the standard insert. An examination of the drop tested FM inserts indicated the presence of uneven surface and an irregular cell structure. To improve the impact resistance of the FM inserts, ACR produced a second set of inserts with a uniform FM cell structure and even surface finish. The results showed a considerable improvement with impact resistance values equivalent to and in some tests slightly higher then the values obtained for Smith Tool's standard inserts. Smith Tool was pleased with these results in conjunction with the wear resistance testing results described below.

Wear Testing

In addition to the SEM work performed at the University of Michigan, Smith Tool performed wear testing of the Diamond 817/WC FM inserts with the various cell to boundary ratios detailed in **Table 10** (above). The testing involved making multiple linear cuts with square fibrous monolith inserts across a slab of Sierra Granite until a cutting distance of 500 meters was achieved. A total of seventeen FM inserts (several of each of the different types) were tested at several different cutting depths which ranged from ~0.5 to 1 mm deep into the granite surface. For comparison, Smith also tested their standard diamond insert under identical conditions. Before and after cutting the granite slab, the inserts were weighed to determine material loss from the insert during the cutting operation. They were then studied by scanning electron microscopy (SEM). The weight loss measurements enabled Smith to quantify material loss as a result of wear and chipping. The SEM observations were made to distinguish if the measured material loss was a result of wear or chipping or both. Weight loss measurements and SEM observations indicated that our FM inserts outperformed Smith's standard inserts. Sixteen out of 17 of our FM inserts exhibited less weight loss, wear, and damage as compared to Smith's standard diamond insert.

Earlier testing that Smith had performed using a slab of the Nugget Sandstone instead of the Sierra Granite did not show a distinct difference between our FMs and their standard diamond inserts. The observations that the FM inserts exhibited less wear then Smith Tool's standard inserts was very significant because the Sierra Granite represents a much harder drilling medium then the Nugget Sandstone. The FM inserts maybe particularly useful for drilling in formations with strengths and hardness similar to the Sierra Granite. Drill bits with FM inserts will be able to achieve greater drilling depths when the rock formation hardness becomes too high for their conventional bits. Smith could develop a new line of drill bits using FM inserts for drilling in hard formations and for drilling deep oil wells. This will give Smith a big advantage over their competitors since the FM inserts offer a significant improvement in performance when drilling hard rock formations.

C. Field Testing / Product Qualification / Pilot Production

Based upon the results of the laboratory wear and impact testing, Smith Tool ordered several hundred FM green parts from ACR. These caps were hot pressed onto WC inserts and then pressed into rock drill bits for a number of down-hole drilling tests. The field drilling tests were performed to determine if the enhanced wear resistance of the diamond/WC FM insert coatings offered any performance advantages in an actual rock drilling application.

Hammer Bit Testing and Product Qualification

The first field test was performed with using a Smith Tool 'Hammer Bit' featuring 15 DIA/WC inserts on the face of the bit. The testing took place in mid-March of 1998. ACR research scientist Greg Hilmas and ACR president Anthony Mulligan traveled to Eastern-Kentucky on March 9 and 10 and observed a drill rig that was in the process of

drilling for natural gas using several of Smith Tool's hammer bits. At the site, about an hour southwest of Prestonsburg, KY, a hammer bit containing 15 DIA/WC fibrous monolith inserts was being readied for insertion into the drill rig (**Figure 24**).

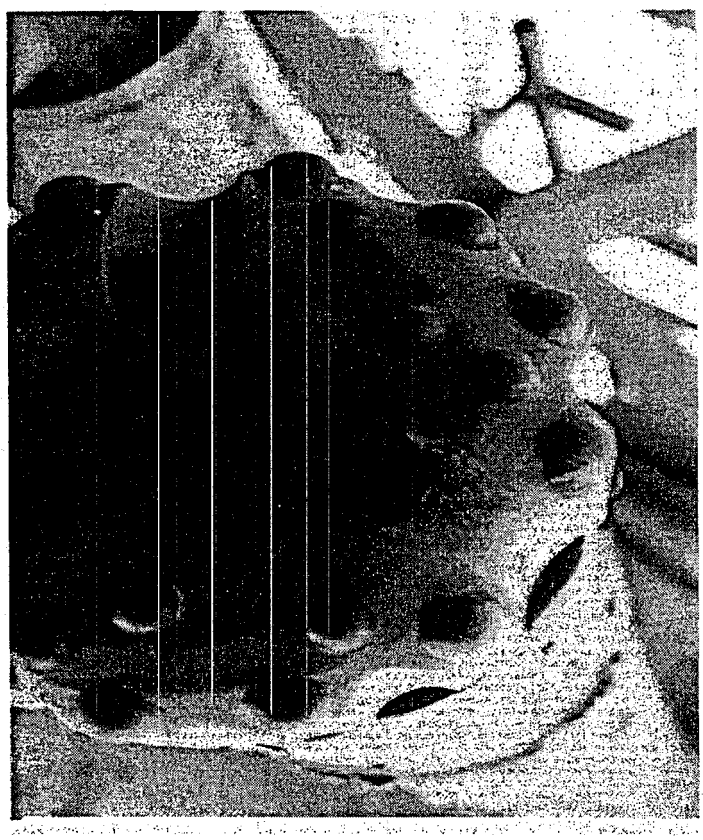

Figure 24. End-on view of the 8.5 inch in Diameter 'Hammer Bit' with the DIA817/WC (11% Co) inserts before its Insertion Down Hole.

On Tuesday, March 10, the rig was drilling at ~1850 feet and was expected to go to 3800 to 4000 feet before striking natural gas. The initial plan was that the hammer bit with fibrous monolith inserts would not be utilized until the last ~1000 feet of drilling. However, this plan was changed by Smith Tool. Instead of finishing the first hole, a new hole was started at a site very close to the one described above using the Hammer bit with the 15 FM inserts. The drilling conditions reported in the driller's log were "severe" in a hard, silicified sedimentary rock formation called the Maxton Sandstone. The FM Hammer Bit drilled an interval from 30 feet to 1,551 feet when it was pulled from the hole for inspection. The inspection revealed that the FM inserts were undamaged and showed little evidence of wear. The decision was made to place the bit back in the hole and continue drilling. At 2,527 feet "the bit had stopped penetrating the formation and was tripped out of hole for inspection" according to the drilling log. The bit was damaged beyond use and a tri-cone bit was used to complete the interval. Based on drilling logs obtained from this area, Hammer bits with the standard polycrystalline

diamond inserts drill to an average depth of 2,690 feet. The Hammer bit with the FM inserts drilled a total of 2,497 feet leaving it ~190 feet short of average. The drilling report concluded by noting that " this was a very good first attempt and the (FM Hammer) bit did a very good job although coming up short on footage"

The results of this first field test were considered very encouraging. Based on these results, Smith Tool decided to expand the field testing and requested 390 additional 8mm tool bit insert caps and 275 9mm flat disks for use in their tri-cone roller cone bits. These additional inserts were delivered to Smith Tool on May 14th, 1998.

Tri-cone Roller Bit Testing and Product Qualification

After delivery to Smith Tool in mid-May of 1998, the caps and discs were sent to Smith's subsidiary Megadiamond where they were hot pressed onto WC inserts. The 8 mm caps were hot pressed onto 5/16 inch gauge-row inserts for field testing in fifteen tri-cone roller bits. The gauge row is the outer most row of inserts on the cones of the tri-cone bit (**Figure 25**). These inserts are responsible for precisely maintaining the gauge (diameter) of the hole during drilling. It is described as a high-wear, low-impact drilling environment. The FM diamond WC inserts were alternated with Smith Tool's standard polycrystalline diamond inserts on the gauge row of the fifteen tri-cone roller bits. This placement allowed ACR and Smith Tool to make side by side comparison of the two insert types under identical drilling conditions.

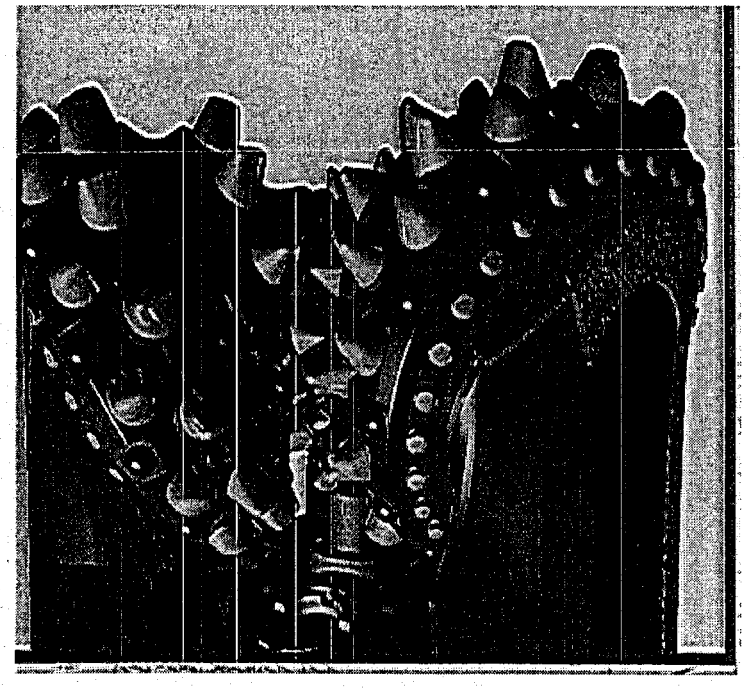

Figure 25. Smith Tool's Tri-cone Roller Bit. The Gauge Inserts are the Outermost Row of Inserts on each of the Three Cones.

The bits were completed in July of 1998 and sold as engineering requests (ERs). Unfortunately, Smith Tool's sales were slow as a result of exceptionally low oil and gas prices in the Summer and Fall of 1998. Four of the fifteen bits were sold, however, and Smith Tool was able to obtain field test results on these bits in September and Early October of 1998. The results of the field testing of three of the bits were summarized in a report compiled and presented to ACR by Engineer Brian White during a visit to ACR by Smith Tool in mid October 1998. Brian White's report (see **Appendix E**) indicated that the FM gauge row inserts performed extremely well in the three field tests. In two of the three cases the tri-bits successfully drilled the required intervals and were capable of being used again. The third tri-cone bit had six broken gauge row inserts and was unable to drill its designated interval. When ACR learned of the failure of the third bit in September, it was unclear whether any of the broken inserts were FM inserts. After a careful examination of the bit and individual inserts, Smith Tool revealed in October that the six failed inserts were their own standard polycrystalline diamond coated inserts. While the ACR's FM inserts showed small, micron sized chip damage to a few individual cells, none of the FM inserts had failed and were actually capable of reuse.

Based on the field testing results Smith Tool sent ACR three purchase orders totaling 750 insert caps to be delivered in January of 1999. These PO's comprised a request for 300 7/16 and 250 9/16 inch semi-round top (SRT) diamond/WC fibrous monolith inserts and 200 5/16 inch gauge row inserts. The SRT inserts comprise the next row of inserts on the tri-cone bits. These bits are involved with cutting the rock during drilling and receive higher impact loading then the gauge row inserts. Successful qualification and comparable field testing results of the SRT inserts is extremely important Smith Tool because the improved performance of these inserts will lead to a competitive advantage in the hard rock drilling market. Production of the 7/16 and 9/16 SRT caps began in late November and was completed in January of 1999. Brian White, Zak Fang (Materials Research Manager), and several production engineers from Smith Tool visited ACR a number of times in November, December, (of 1998) and January of 1999 during this period to observe the production of inserts on the three purchase orders. ACR completed all the purchase orders smoothly after Smith and ACR designed custom pressing dies for shaping green FM flat discs into the dome shaped SRT caps. These caps were hot pressed by Megadiamond onto inserts and pressed into 20 drill bits that were put up for sale as ER's in April of 1999. Smith Tool also ordered an additional 200 of the 5/16 FM insert caps at the request of their marketing and sales departments who wanted to market and sell additional drill bits with FM inserts the Spring of 1999.

At the time of the writing of this report (mid-May, 1999) five tri-cone roller bits with the 9/16 inch FM inserts have been completed and are for sale as Engineering Requests. The 7/16 inserts and 5/16 inch inserts will be pressed into drill bits at Smith Tool's Ponca City, OK in the next several weeks.

D. Diamond-WC-Co /Nb and Diamond-WC-Co /Co/Nb Fibrous Monoliths

Green FM Development

Following the field testing of the Smith 'Hammer Bit' (described above), micro-hardness tests performed by Smith Tool on several DIA817/WC(11%Co) fibrous monolith inserts revealed that the WC(11%Co) cell boundaries did not appear to be exhibiting sufficient crack deflection for the Hammer Bit application. These preliminary results suggested that the WC(11%Co) cell boundary material may be too brittle for effective crack deflection in aggressive drilling environments. In order to improve the observed crack deflection, Smith Tool and ACR began developmental work on a third generation of FM cellular inserts that utilize ductile Niobium (Nb) metal as a cell boundary material. The Nb metal was expected to improve crack deflection in the FM inserts being used in bits for aggressive drilling environments.

The first type of cell boundary material fabricated was pure ductile Niobium (Nb) metal. ACR and Smith Tool also decided to investigate a second cell boundary composed of Co and Nb metals. The second cell boundary material was a "double shell" composed of an inner Cobalt (Co) shell surrounded by a outer Nb shell. In this FM architecture, the green Co shell was placed in direct contact with the green Diamond 817 or WC feedrod to prevent possible chemical reactions between the Nb and the diamond or WC cell material during hot pressing (e.g. the formation of NbC). These two cell boundary materials were expected provide energy dissipation of fractures and microcracks through crack blunting mechanisms

After several weeks of discussion, ACR and Smith tool decided on a test matrix in August of 1998 for a preliminary evaluation of Diamond and WC FMs with Nb and Co/Nb ductile cell boundaries. The proposed test matrix is summarized in **Table 13.**

Table 13. Diamond and WC FMs with Nb and Co/Nb Cell Boundaries

Sample	Volume %	C/C_b	Composition	Cell Size, μm
A	70/30	3.33	Dia817/Nb	100
B	70/15/15	3.33	Dia817/Co/Nb	100
C	70/30	3.33	WC406/Nb	100
D	70/15/15	3.33	WC406/Co/Nb	100
E	70/30	3.33	Dia (20μm)/Nb	100
F	70/15/15	3.33	Dia (20 μm)/Co/Nb	100

Note: C/C_b is a ratio of the thickness of the cell as compared to the cell boundary.

Samples E and F in **Table 13** were composed of a pure diamond powder with an average grain size of 20 μm. Smith Tool believed that the Co and Nb metals in the shells of these samples would migrate into the pure diamond cores during hot pressing and cement the individual cores. It was hoped that this would be a simple way of creating a Nb or Co/Nb cermet in these FMs.

Before beginning work on the new test matrix, Smith and ACR fabricated a test feedrod using Smith's Diamond 817 powder as the cellular material and Nb metal as the cell boundary material. This allowed us to verify the production of an extrudable feedrod with a Nb metal shell. The Nb metal were blended with thermoplastics, plasticizers, and modifiers in the C.W. Brabender Plasticorder using the recipes shown in **Tables 14** and **15**. These recipes were based on a nickel metal recipe formulated for on previous ACR R&D project. The Nb recipe blended well on the first attempt producing an extrudable material.

Table 14. Niobium Metal 'Shell' Material Formulation

Material	Density (g/cc)	Volume (cc)	Volume %	Mass (g)
Nb metal	**8.57**	**54.00**	**22.68**	**194.37**
EEA*	**0.93**	**45.00**	**18.90**	**17.58**
MPEG-550†	**1.10**	**1.00**	**0.42**	**0.46**

*EEA = Ethyleneethylacrylate.

†MPEG-550 = 550g average molecular weight Methoxypropylene glycol.

Table 15. Co Metal 'Shell' Formulation

Material	Density (g/cc)	Volume %	Volume (cc)
Co Metal	**8.90**	**52.00**	**21.84**
EEA*	**0.93**	**37.00**	**15.54**
Steric Acid	**0.85**	**5.00**	**7.50**
B-67@	**1.06**	**4.00**	**6.00**
MPEG-550†	**1.10**	**2.00**	**0.84**

* EEA = Ethyleneethylacrylate.

@ B-67 = Acryloid Resin

† MPEG-550 = 550g average molecular weight Methoxypropylene glycol.

The Nb shell and Diamond 817 formulations were pressed into shells and cores respectively and then coextruded to produce a single 19 mm fibrous monolith feedrod. The extrusion of the feedrod worked very well.

Next, ACR attempted to produce feedrods with Nb and Co metal shells with cores composed of the Diamond/WC/Co (Diamond 817 powder), WC-Co and the 20 μm pure diamond powder. After several attempts, the Co metal was successfully blended with thermoplastics, plasticizers, and modifiers allowing ACR successfully produce Co shells.

Using previously developed formulas for core and shell, Diamond 817 feedrod with Co and Nb shells were fabricated successfully. This feedrod was extruded twice to produce a final cell to boundary ratio of 3.33 with a cell size of ≈100 μm. The 'green' flats were cut to size and were delivered to Smith. Unfortunately, these same recipes for Nb and Co shells were incompatible with the WC 406 core material. This is because the viscosity of Nb and Co shell materials were higher than that of core material making it impossible to extrude a useable feedrod. Numerous attempts to increase the viscosity of WC 406 to match that of the Nb and Co shells were unsuccessful.

Despite the problems with the WC(406), ACR successfully blended the 20 μm diamond powder with thermoplastics using the formulation given in **Table 16.** The formulation produced an extrudable blend of thermoplastics with the 20 μm Diamond powder. ACR fabricated Nb and Co shell materials to produce 20 μm Diamond/ Nb and 40 μm Diamond/Co/Nb flats for Smith. These flats were hot pressed onto flat WC inserts for wear testing.

Table 16. Diamond (20 μm) 'Core' Material Formulation

Material	Density (g/cc)	Volume %	Volume (cc)	Mass(g)
Diamond (20 μm)	**3.51**	**61.60**	**25.87**	**90.81**
EEA*	**0.93**	**36.00**	**15.12**	**14.06**
HMO#	**0.88**	**2.40**	**1.00**	**0.88**

* EEA = Ethyleneethylacrylate.
# Heavy Mineral Oil

Feed rods were produced out of the Diamond 817 and 20 μm diamond powders using both Nb and Co/Nb as cell boundaries. Several flats from each feed rod were sent to Smith Tool. The flats were hot pressed onto flat WC discs at Megadiamond and then sent back to Smith Tool for study. Analyses performed by Smith Tool in October and November of 1998 on the flat inserts included Vicker's hardness testing and scanning electron microscope (SEM) analyses.

The cell boundaries of three cellular materials were tested using the Vickers hardness method. The 3 grades were the diamond 817 with a WC-Co boundary, Nb boundary (sample A in **Table 13** above, and Co/Nb boundary (sample B in **Table 13** above). Each of the three samples was tested at a 500 g load and the results are summarized in **Table 17** below:

Table 17. Summary of Vicker's Hardness Testing

MATERIAL	VHN_{500g}
WC-Co (411)	1832 ± 29
Nb	1617 ± 44
Co/Nb	1287 ± 32

These results show a clear decrease in hardness as the boundary material has been changed. The difference between the Nb and Co/Nb is significant and suggested that the Nb boundary may have reacted to form NbC. Preliminary SEM analyses performed by Brian White confirm this hypothesis. EDS analyses show the presence of Nb and C in what appears to be a singe phase in the boundaries of the Diamond 817/Nb samples. This is not the case for the Co/Nb sample. The individual Co and Nb phases can be distinguished and there does not appear to be any carbon present with the Nb

After obtaining these preliminary results, Smith revealed the successful results of the field testing on the Diamond 817/WC-Co gauge row inserts. Based on these results, Smith and ACR decided to focus on scaling up and beginning production of the Diamond 817/WC-Co inserts for the remainder of the AMP program.

VII. ACR Research Closely Related to the AMP Program

The goal of this research is to develop alternative processing methods in FM processing that will lower the overall production cost of the composites making them more attractive to potential users of the technology who are cost conscious. This goal can be achieved in two ways: (1) alternative methods that lower processing costs, and (2) alternative methods that lower labor costs. ACR began to address both issues over the coarse of this program.

A. Pressureless Sintering of Si_3N_4/BN Fibrous Monoliths

A research effort to consolidate Si_3N_4/BN FMs by pressureless sintering, as opposed to the traditional method of hot pressing, was undertaken in the fall of 1998. This majority of this work was done by ACR research scientist Manish Sutaria. The hot-pressing process is costly and time intensive in comparison to pressureless sintering. Hence, a less expensive and faster process to fabricate FM components is significant and is likely to lead to an increased number of applications for these structural composite ceramics.

ACR has conducted a number of pressureless sintering experiments to consolidate Si_3N_4/BN FMs on the past programs with limited success (DFM). This is because it is extremely difficult to pressureless sinter fully dense hexagonal boron nitride (BN) cell boundaries without the addition of sintering aids. It has been observed during Si_3N_4/BN FM processing via hot-pressing that BN cell boundary contained glassy phases as a result

of the migration of sintering aids from the Si_3N_4 into the BN. This migration of glass appeared to aid the consolidation of the FM. The addition of sintering aids directly to the BN phase may also aid in the consolidation of FMs by pressureless sintering. Based on estimates of the amount of glass present in a dense hot pressed Si_3N_4/BN FM sample, ACR added an equivalent amount of sintering aids to the BN. This was done during green processing when the BN was blended with thermoplastics. The sintering aid additions to BN for pressureless sintering of Si_3N_4/BN FMs are listed in **Table 18.** In each case standard sintering aids (6 wt% Y_2O_3 and 4 wt% Al_2O_3) were added to the Si_3N_4.

Table 18. Glass Additions to Boron Nitride for Pressureless Sintering Experiments

System	Weight Percentages					
	BN	Al_2O_3	Y_2O_3	SiO_2	Borosilicate	Si_3N_4
BN/YAS Glass	86.08	2.72	8.14	3.05	-	-
BN/YAS Glass + Si_3N_4	81.78	2.58	7.73	2.90	-	5.00
BN/Borosilicate Glass	75.00	-	-	-	25.00	-

YAS Glass = Ytttria Alumina Silica Glass

Si_3N_4/BN FM test bars with BN containing the glass sintering aids (**Table 18**) were fabricated by rapid prototyping. When observed under microscope in cross section, several of these green bars showed some porosity. In order to close this porosity these bars were warm isostatically pressed prior to pressureless sintering. The test bars were placed in ACR's binder burnout furnace to remove polymer binders and then sintered at 1750 °C and 3 psi N_2.

Samples of the Si_3N_4/BN FM containing BN with YAS Glass (System 1) shattered during sintering and were recovered as individual Si_3N_4 filaments. These Si_3N_4 filaments were strong suggesting a good densification. However, the FM did not sinter properly resulting in the shattered filaments. In System 2, a small amount of Si_3N_4 (5 wt. %) was added with the sintering aids to improve the sinterablity of the BN. Since Si_3N_4 is easily sintered, its presence together with the sintering aids in the BN may enhance the sintering of the BN in the FM system. The sintered test bars of this system held together. Unfortunately, the test bars were not very strong as the individual Si_3N_4 filaments could be separated from the matrix by hand as the BN interface was weak and poorly consolidated. Similar to System 2, test bars from System 3 (BN with borosilicate glass) were also weak. It is likely that the flaking and delamination of Si_3N_4/BN FMs of the latter two systems is the result of the volume increase of BN during sintering. If this is the case then an increase in pressure (i.e. over-pressure sintering) should improve the

sintering of Si_3N_4/BN FMs. Test bars from all three systems have been sent to Argonne National Laboratory for microscopic evaluation to determine the distribution of the glassy phases.

B. Solid Freeform Fabrication of FM

The FM green filaments and spaghetti are often manually wound on a drum or a mandril during the green processing of FM components. This step in FM green processing is labor intensive. By producing FM green parts to near net shape using ACR's solid freeform capabilities, we can reduce our labor costs and improve the reproducibility of fabricated FM parts. An estimate of the cost savings resulting from the free form fabrication of FM parts indicates that ACR can reduce its labor cost for fabricating green parts by 50%.

In the last quarter of 1998, ACR fabricated several test bars and test billets using its extrusion freeform fabrication (EFF). EFF machine consists of a high-pressure extrusion head (designed by ACR) and a X-Y-Z motion table. A motion architect computer program controls the X-Y-Z motion table. Using our standard binder system (EEA and EVA), ACR fabricated and hot-pressed Si_3N_4/BN billets with two different fiber orientations (uniaxial and 0°/90°). Figure 26 shows a 'green' Si_3N_4/BN billet made by this process. These billets were sent to ANL for mechanical testing. Preliminary results indicate that they have similar or better strengths than the traditional hand layed-up billets with an improvement in reliability. The improved in reliability is believed to be due to good fiber alignment. Figure 27 shows the cross-section of a Si_3N_4/BN FM test bar fabricated by EFF machine.

Although EFF machine can make Si_3N_4/BN FM billets, the software is currently not capable of making complex shaped parts. Thus, ACR's intentions were to transfer the process to its Stratasys Fused Deposition Modeler (FDM) with a retrofitted high-pressure extrusion head. The difference between the ACR's EFF machine and the FDM modeler is that the deposition codes for complex parts can easily be generated from a computer model on the FDM machine. The disadvantage of the FDM modeler is that its load capacity is limited to the extent that Si_3N_4/BN FMs can not be extruded with the current binder system. A low temperature and low viscosity binder system is necessary to extrude FM filament on the FDM machine. The obvious solution was for ACR to modify our standard binder system by adding a small amount of wax. The wax addition reduced the viscosity by half and lowered the extrusion temperature by 50 °C. With this modified binder system, ACR was able to make Si_3N_4/BN FM test bars on the FDM machine. ACR also supplied several of these wax based Si_3N_4/BN FM feedrods to ANL for extrusion experiments on their FDM machine. Microscopic observations indicate uniform BN coating on Si_3N_4 cells.

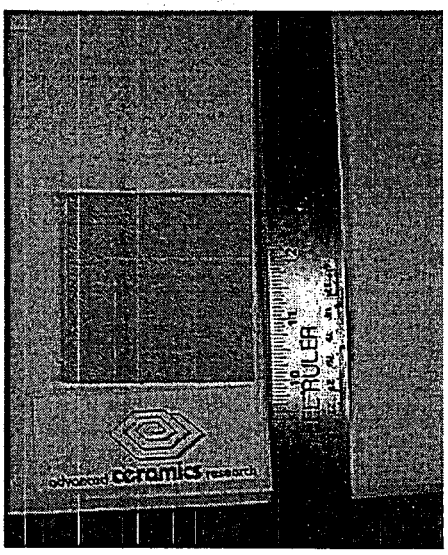

Figure 26. 'Green' 3" x 3" x 0.25" Si_3N_4/BN FM billet fabricated using EFF machine.

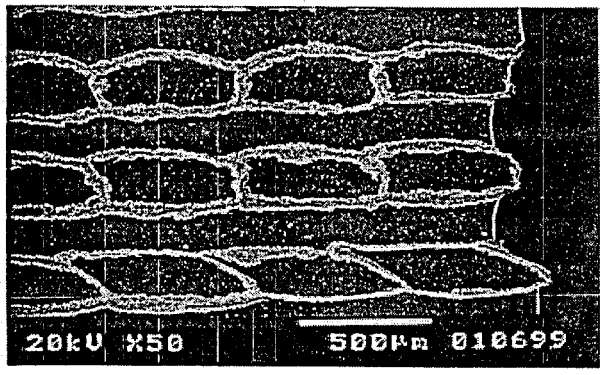

Figure 27. Cross-section of Si_3N_4/BN FM billet fabricated by EFF machine

C. FM Samples for Solar Turbines for FOD Evaluation

Solar Turbines, a Caterpillar Company based in San Diego CA, expressed interest in the potential of FM composites in helping to minimize or eliminate the foreign object damage (FOD) to its Si_3N_4 in turbine engine components. ACR has conducted several discussions over the past year with Solar Turbine engineers regarding incorporation of Si_3N_4/BN FMs as a replacement for Si_3N_4 turbine vanes in their turbine engines. Monolithic Si_3N_4 is a good candidate for this application but it is, as most brittle ceramics, susceptible to foreign object damage. The coating technology developed for drill bits during the AMP program may be applicable to improving the FOD resistance of the Si_3N_4 turbine vanes.

To test the FM coating capability in minimizing FOD, ACR fabricated Si_3N_4/BN FM coatings and hot pressed them three different Si_3N_4 based substrates. Solar Turbines agreed to test the billets in order to evaluate the composite's ability to reduce foreign object damage. ACR fabricated three different sets of FMs and sent them to Solar Turbines for testing. The three billets fabricated were: 1) a Si_3N_4/BN FM coating on a monolithic Si_3N_4 substrate, 2) a Si_3N_4/BN FM coating on a unidirectional Si_3N_4/BN FM substrate, and 3) a Si_3N_4/BN FM coating on a quasiisotropic Si_3N_4/BN FM substrate. A two step process was used to fabricate these samples. First, a unidirectional Si_3N_4/BN billet (3" x 4.5" x 0.5") was laminated using multiple extruded Si_3N_4/BN filaments. The individual cell size was ≈ 200 μm. The billet was sectioned into thin slices (0.12") along its width to expose the cells. Next, substrate materials were processed. For monolithic Si_3N_4 substrate, Si_3N_4 powder was compounded with thermoplastics and pressed into a 3" x 3" x 0.125" billet. For FM substrates (uniaxial and quasiisotropic), Si_3N_4/BN 'green' fiber was extruded to 340 μm filaments and manually layed-up to the desired architectures. The layed-up billets were then warm laminated. The final dimensions of the billets were 3" x 3" x 0.125". Following the green lamination of the substrates, the 0.12" FM slices were placed on the three substrates such that the orientation of the cells in the slices were normal to the surface of the substrates. The three coated substrates were then warm laminated to join the coating to the each substrate's surface. The overall thickness of the FM coating was ~25% of the overall thickness of the billet. The billets were placed in binder burnout for four days and then hot-pressed at 1750 °C and 3.1 Ksi. **Figure 28** shows the cross-sections illustrating the architectures of the consolidated billets. Four test bars (0.118" x 0.157" x 1.97") were sectioned from each billet and sent to Solar Turbines in early May of 1999 for threshold impact resistance testing at elevated temperatures.

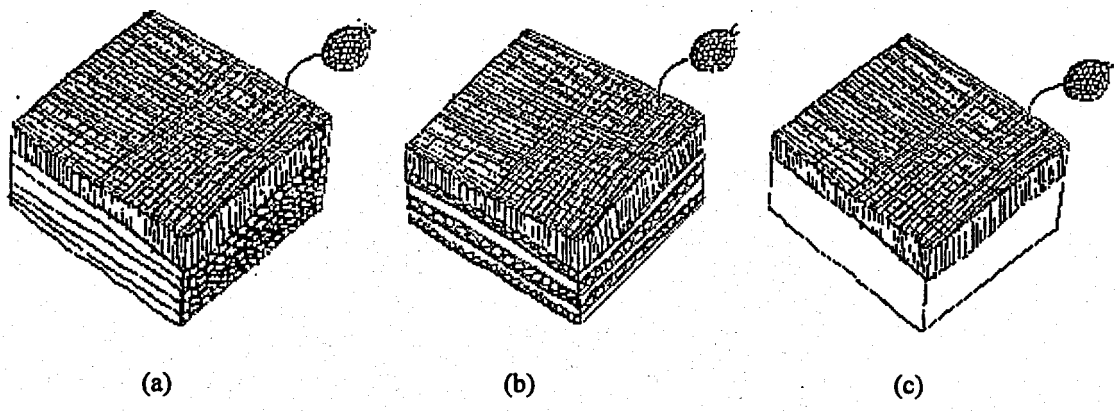

Figure 28. Sketches of the Si_3N_4/BN FM samples sent to Solar Turbines, illustrating the orientation of the FM coating and fiber orientations of the substrates. a) FM coated multifilament FM billet with a uniaxial substrate. b) FM coated multifilament FM billet with a quasi-isotropic substrate. c) FM coated billet with a monolithic Si_3N_4 substrate.

Appendix A. Binder Burnout and Microscopy Studies for the AMP Program

By

Rodney Trice

9/31/97
Rodney Trice

Binder Burnout and Microscopy Studies for the WC Program
Report #1

I. Binder Burnout Experiments

Three different green materials were tested. They were designated as follows:

Material 1: EVA/EEA/HMO/WC (6 wt.% Co)
Material 2: EEA/B–67/HMO/WC (6 wt.% Co)
Material 3: EEA/HMO/MPEG–550/W–Ni–Fe

Pellets, 28 mm in diameter and 7 mm thick, were prepared by pressing chunks of green material at temperatures of approximately 150°C. (Note: temperature was monitored by attaching a thermocouple to the outer shell of the metal die. When the outer shell reached 100°C, load was applied. The heated platens were turned off and a fan was used to further cool the platens and die.) Three different processing conditions were investigated for each of the 3 materials. These included (1) 2000 psi molding pressure (2) 2000 psi molding pressure followed by a 20 hour anneal at 140°C and (3) 500–600 psi molding pressure. Samples were measured and weighed before binder burnout.

Binder burnout experiments were conducted using the standard burnout cycle as of 9/97. The cycle, run in flowing nitrogen, is as follows:

Rate (°C/hr)	Temperature (°C)	Hold Time (Hrs)
12	160	2
6	300	2
6	400	2
12	500	0
18	600	1

Following burnout, samples were weighed and carefully measured. The results of these measurements are shown in Table 1. Percentage calculations were based on the original dimension or weight. Overall, only materials 1 and 3 exhibited bloating. Some bloating was observed in material 1 after the 20 hour, 140°C anneal. Additional bloating was observed in this material after binder burnout. Material 3 bloated and cracked during binder burnout for the low molding pressure condition. Optical micrographs of these samples before and after burnout are shown in Figures 1. For all materials, weight loss was approximately 2.8–4.5%.

II. Microscopy of Hot-Pressed WC (6 wt. % Co)/W-Ni-Fe Fibrous Monoliths

Cells of WC (6 wt. % Co) with cell boundaries of W-Ni-Fe comprised the fibrous monolith architecture. The volume ratio of cells to cell boundaries was 9:1. Hot pressed samples of WC (6 wt. % Co)/W-Ni-Fe were mounted, polished and observed in a SEM. Two hot-pressing temperatures were investigated, 1290°C and 1390°C. Two different orientations were investigated, designated "A" and "B". The physical meaning of these orientations was not described in the original paperwork received with the samples. The following figures describe the results.

Figure 2 shows low- and high-magnification images for the sample hot-pressed at 1390°C and in the "B" orientation. A predominant "white" phase is apparent, surrounded by regions of "dark" phase. The dark phase was not necessarily continuous. Porosity is also evident at low magnifications. Figure 3a shows a 1390°C sample in the B orientation after a 60 second nital etch. The dark phase seems to have been removed. Figure 3b shows a 1390°C sample in the A orientation. No difference in microstructure was observed as compared to the 1390°C sample oriented in the B orientation.

Figure 4 shows low- and high- magnification images for the sample hot-pressed at 1290°C. No orientation was designated. The observed microstructure was similar to the specimens processed at 1390°C. There may have been more porosity in the 1290°C hot-pressed sample.

EDS was used determine the elements in each of the observed phases. The results are shown in Figure 5. The white phase is predominantly tungsten. Carbon was also observed. However, the sample was coated with a thin layer of carbon before the experiment due to specimen charging. The black microstructure contained Fe, Ni, Co, W and carbon. A greater number of counts were observed for Fe, Ni, and Co than for W or carbon. A elemental map was attempted but the results were not as conclusive as the spectrum data shown in Figure 5. As a result, the elemental map is not included in this report.

It is unclear if the sub-millimeter architecture remains following hot-pressing. A low magnification image of a sample processed at 1290°C is shown in Figure 6. There are several fine, white boundaries present near the top of the micrograph that may be the cell boundary material. This is not observed in the lower half of the micrograph.

Table 1. Results of the binder burnout experiments.

Warm Pressing Condtions	Physical Parameters	Material 1	Material 2	Material 3
2000 Psi	Thickness Increase, % Weight Loss, % Comments	2.64 4.4 OK	2.96 3.6 OK	4.84 4.0 OK
2000 Psi + 140 °C Anneal for 20 Hours	Thickness Increase, % Weight Loss, % Comments	9.58 3.7 Bloated	1.36 3.5 OK	0.40 2.8 OK
500–600 Psi	Thickness Increase, % Weight Loss, % Comments	4.23 4.4 OK	3.13 3.8 OK	12.52 4.5 Bloated and Cracked

Material 1 contains EVA/EEA/HMO/WC (6 wt. % Co)
Material 2 contains EEA/B-67/HMO/WC (6 wt. % Co)
Material 3 contains EEA/HMO/MPEG-550/W-Ni-Fe

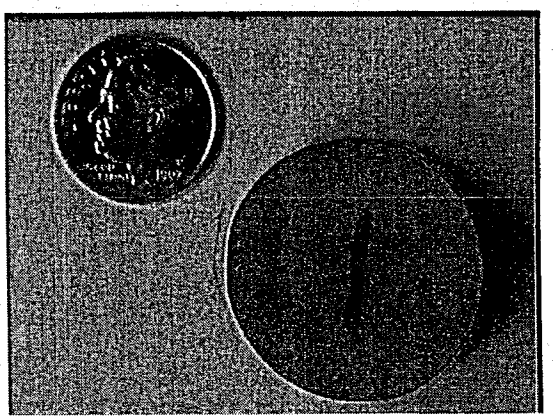

Material 1 – 2000 psi plus 20 hr anneal at 140°C
Before Burnout

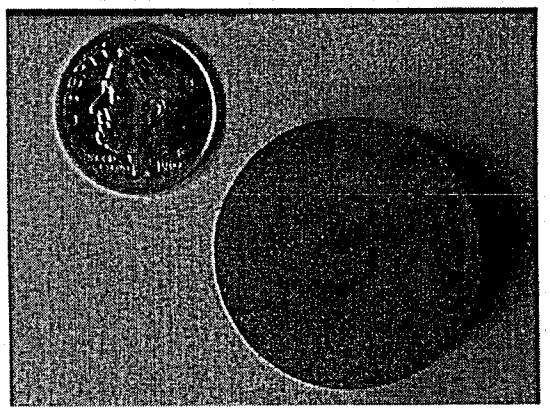

Material 3 – 500 psi
Before Burnout

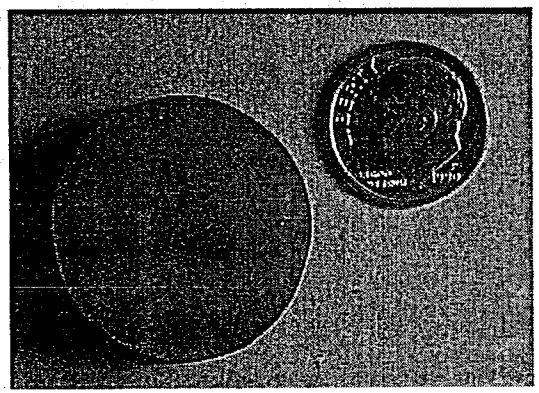

Material 1 – 2000 psi plus 20 hr anneal at 140°C
After Burnout

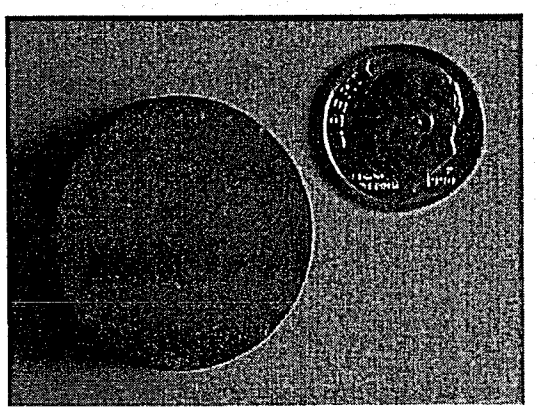

Material 3 – 500 psi
After Burnout

Figure 1: Images before and after burnout for the two bloating conditions.

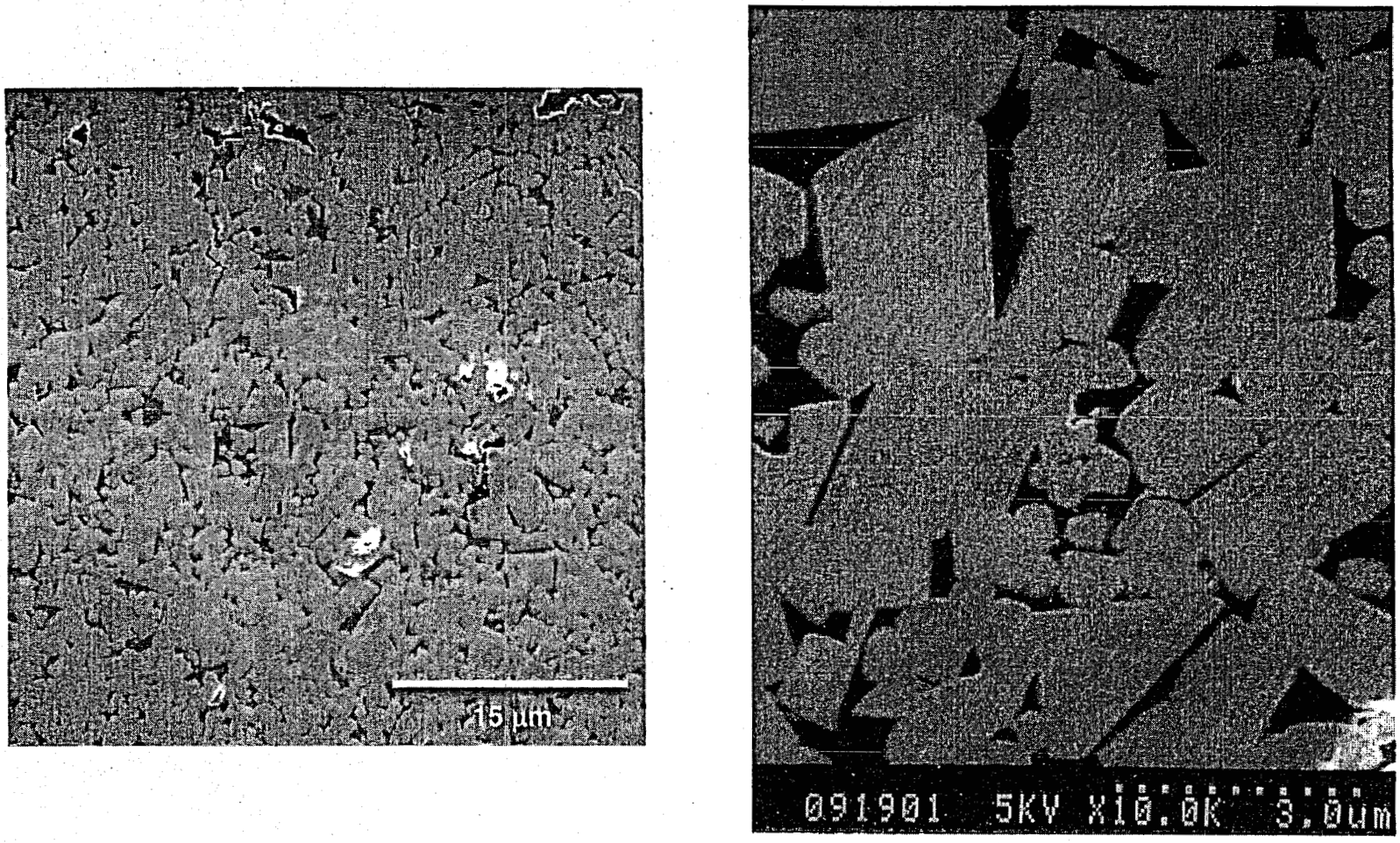

Figure 2. SEM micrographs of the 1390°C hot–pressed sample in the B orientation.

Figure 3a. Nital etched specimen hot–pressed at 1390°C in the B orientation.

Figure 3b. SEM micrograph of specimen hot–pressed at 1390°C in the A orientation.

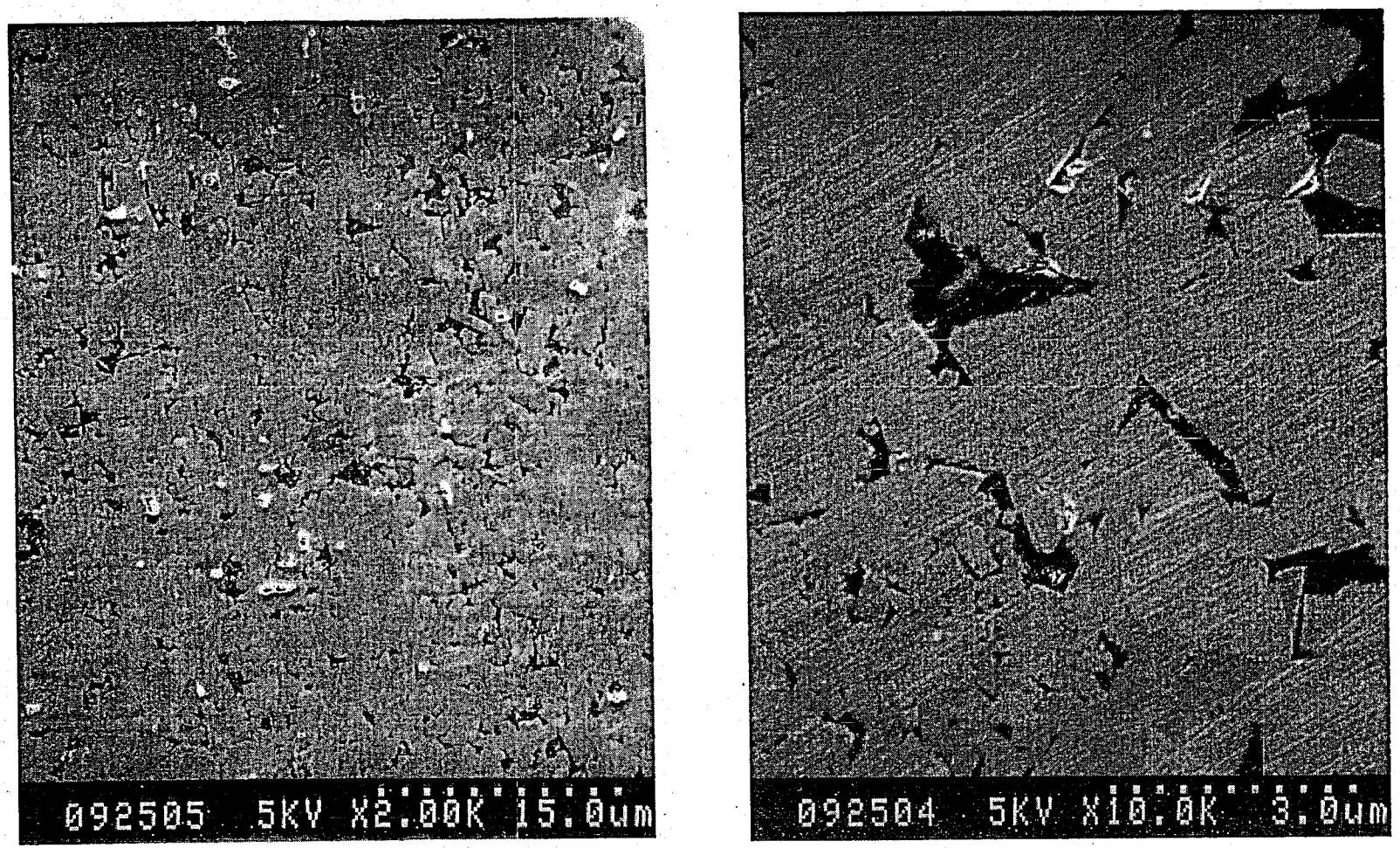

Figure 4. SEM micrographs of the 1290°C hot pressed sample.

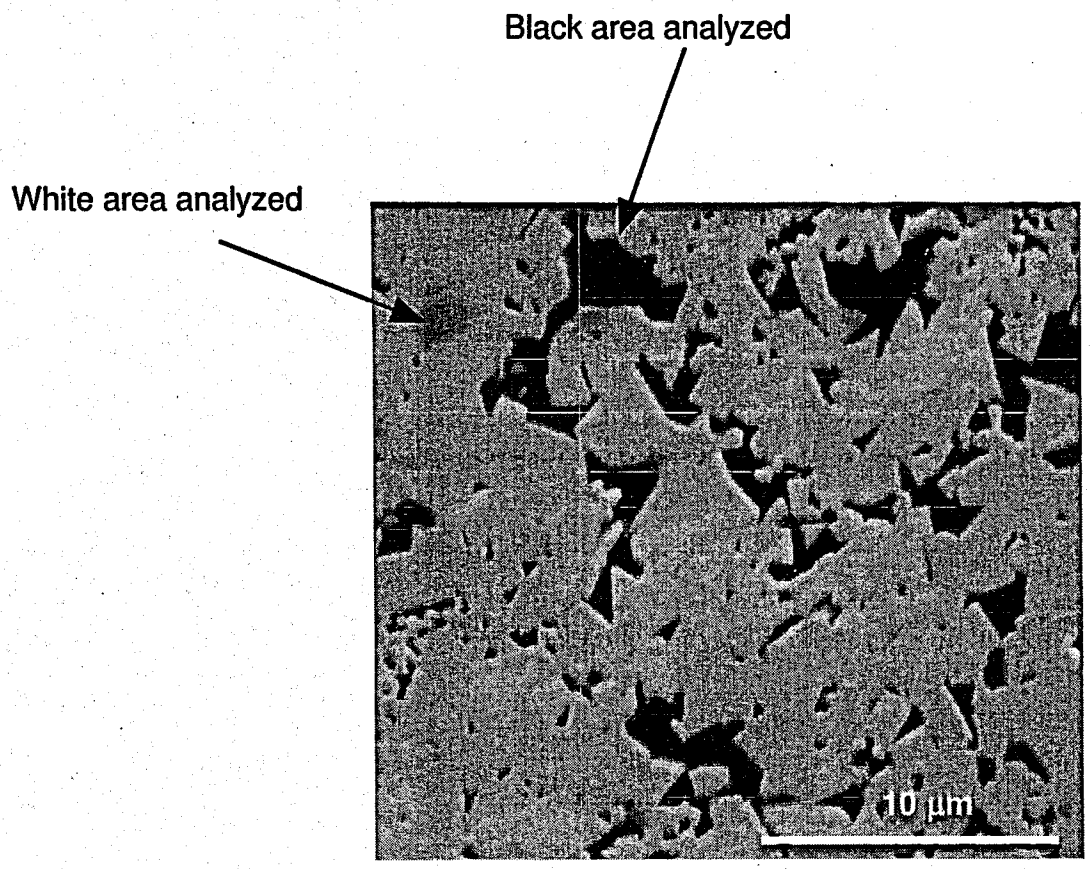

Figure 5. SEM micrograph of the sample hot–pressed at 1290°C. The arrows point to the regions investigated using EDS. This figure is continued on the next page.

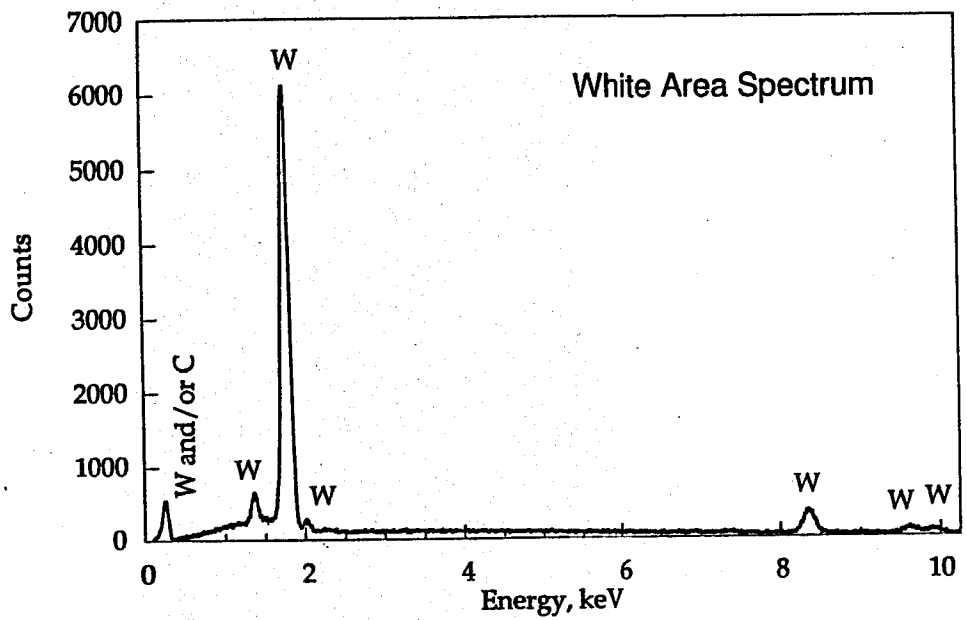

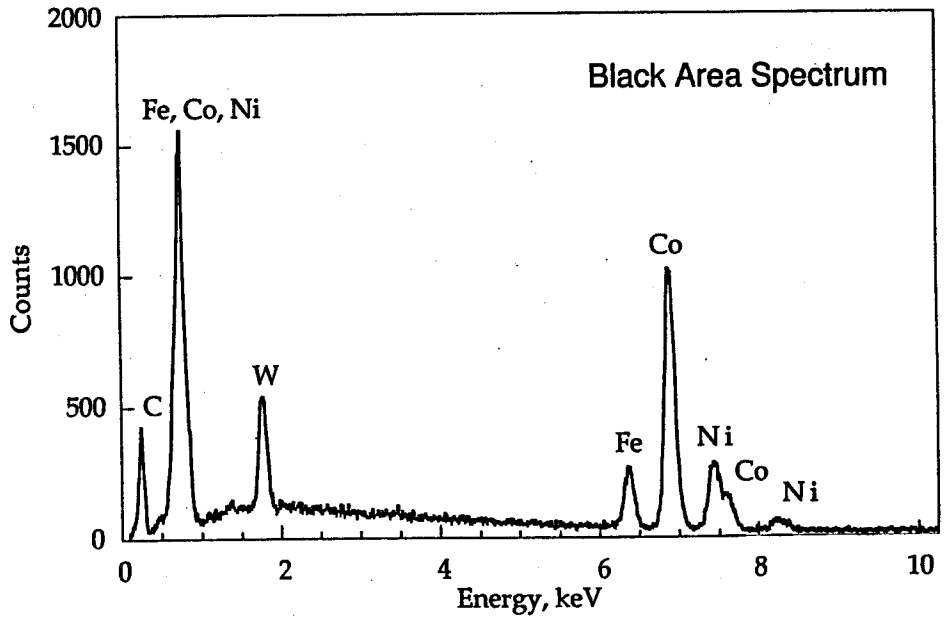

Figure 5 cont. EDS spectrums of the white and black microstructures observed in the sample hot–pressed at 1290°C.

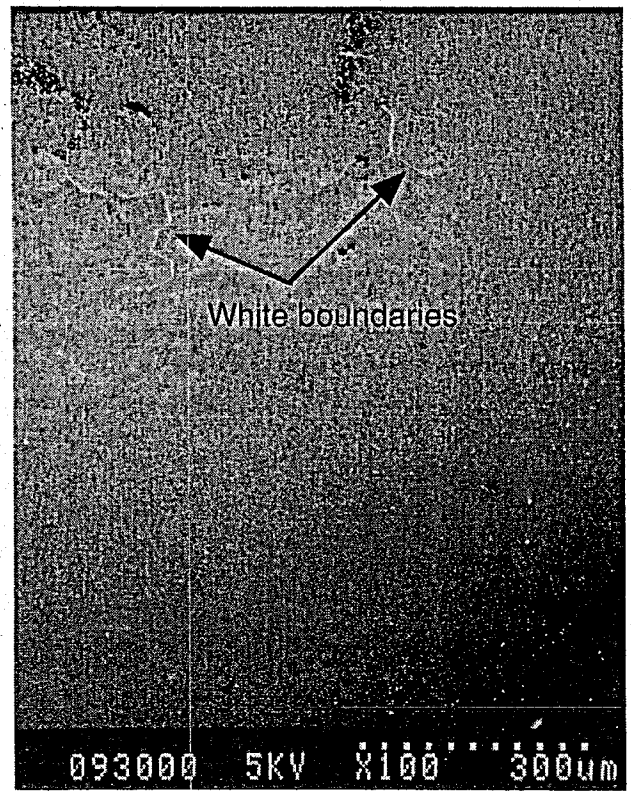

Figure 6. Low magnification image of the sample hot–pressed at 1290°C. A fine network of white boundaries were observed in the upper portion of the micrograph.

Appendix B. Offcuts from the Diamond/WC Fibrous Monolith Feedrods

By

Rodney Trice

THE UNIVERSITY OF MICHIGAN
COLLEGE OF ENGINEERING
MATERIALS SCIENCE AND ENGINEERING

3062 H. H. DOW BUILDING
2300 HAYWARD STREET
ANN ARBOR, MICHIGAN 48109-2136
313 763-4970 FAX 313 763-4788

January 22, 1998

To: Steve Nowell, Greg Hilmas, John Halloran

From: Rodney Trice

RE: Offcuts from WC/Diamond Feedrods

The following report details the microscopy characterization of several offcuts from diamond/WC materials. Eleven samples were received on January 16th or so. The following were varied in each of the samples: (a) the composition of the WC cell boundary material (either 411 or 614); (b) the ratio of the cell boundary (either 10:1, 5:1, or 1:1); (c) and the nominal cell size (200, 100, or 50 μm). The table below lists the particulars of each sample.

Each of the offcuts were polished down to 1 μm and observed in U of M's new Philips XL30 FEG SEM in back–scattered mode. In this mode, the tungsten and cobalt present in the cell boundaries appears as the high contrast phase. All images were taken digitally.

In general, the honeycomb structure was present in all of the samples. The exceptions here include samples C and "Z" (Note: the offcut not included in the original matrix was given the name "Z"). Cell sizes[@] were typically within 30% of the desired size, although the cell size of sample A were 50% larger than desired. In almost all cases, the original bundle was clearly obvious in the images. In samples B, H, I, and J, cells near the bundle boundaries were clearly distorted. In sample F, there was additional cell boundary material at what was believed to be the original bundle boundary. In sample E, there were cracks along some of the original bundle boundary interfaces. If one was to make an overall judgment of the 11 samples, samples A, D, and G appear to be the best. This judgment was based on overall cell size homogeneity (without either cell distortion or bundle boundary cracking).

[@] Cell size is defined as the diameter of the cell plus one cell boundary

Sample	Vol. %	$C:C_b$	Composition	Cell Size	Comments
A	82.5/17.5	10	411 WC	100 μm	Overall "Good"
B	82.5/17.5	10	411 WC	200 μm	Cell distortion near bundle boundaries
C	82.5/17.5	10	614 WC	100 μm	Difficult to observe the structure
D	82.5/17.5	10	614 WC	200 μm	Overall "Good"
E	70/30	5	411 WC	100 μm	Cracking along bundle boundaries
F	70/30	5	411 WC	200 μm	Additional cell boundary material
G	70/30	5	614 WC	100 μm	Overall "Good"
H	70/30	5	614 WC	200 μm	Cell distortion near bundle boundaries
I	50/50	1	411 WC	50 μm	Cell distortion near bundle boundaries
J	50/50	1	614 WC	50 μm	Cell distortion near bundle boundaries
Z*	90/10		411 WC		Difficult to observe structure

* 2 mm to 1 mm spaghetti, not included in original matrix.

Sample A
82.5/17.5 Vol.%
$C:C_b = 10$

411 WC
Nominal Cell Size = 100 μm

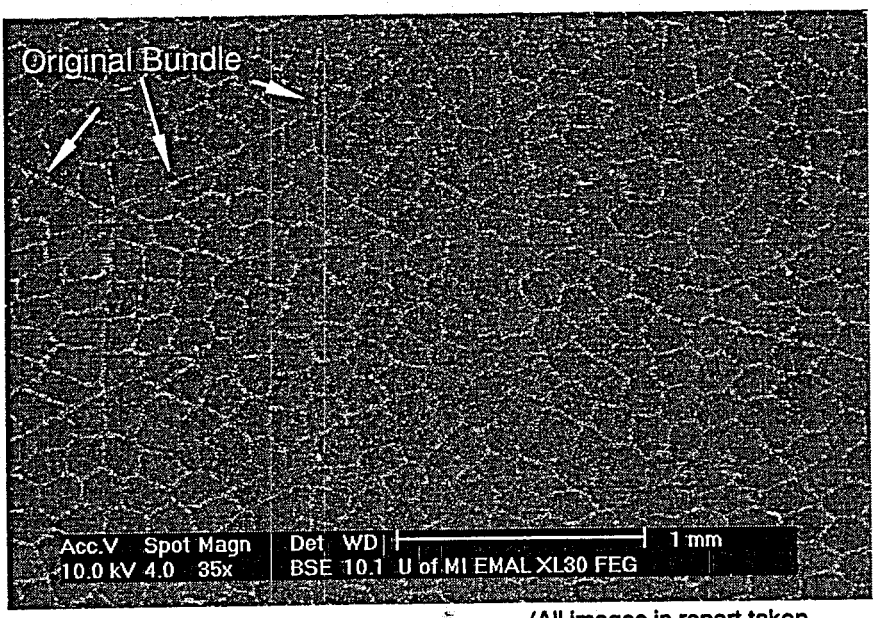

(All images in report taken
in back–scattered imaging mode.)

Sample A
82.5/17.5 Vol.%
$C:C_b = 10$

411 WC
Nominal Cell Size = 100 μm

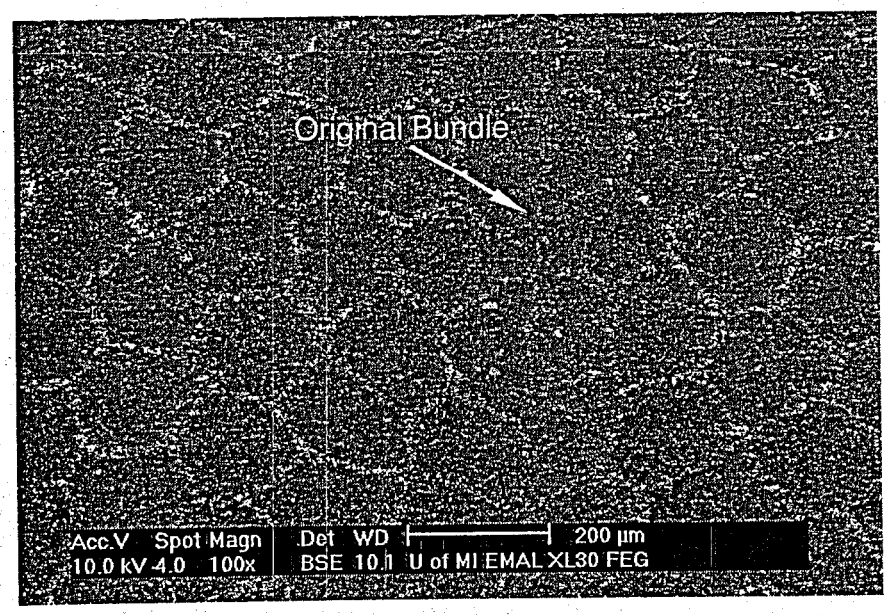

Measured Cell Size = 150 μm (includes cell and one cell boundary)
Measured Thickness of Cell Boundaries = 10–15 μm

Sample A
82.5/17.5 Vol.%
$C:C_b = 10$

411 WC
Nominal Cell Size = 100 μm

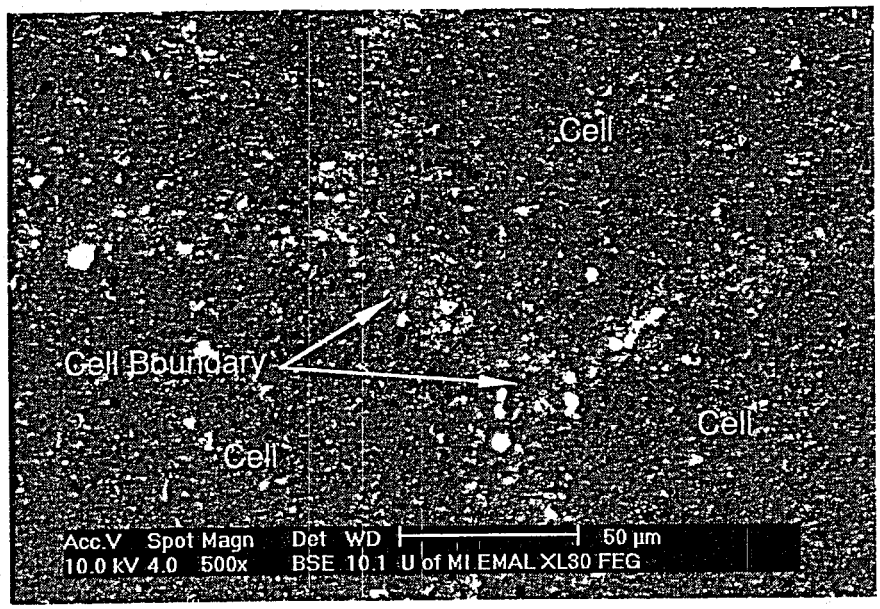

Sample B
82.5/17.5 Vol.%
$C:C_b = 10$

411 WC
Nominal Cell Size = 200 μm

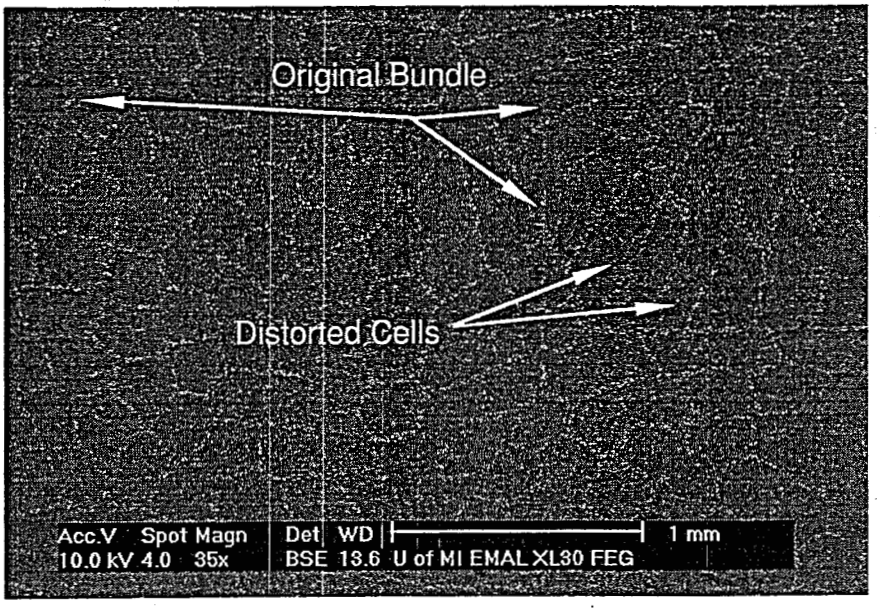

Sample B
82.5/17.5 Vol.%
$C:C_b = 10$

411 WC
Nominal Cell Size = 200 μm

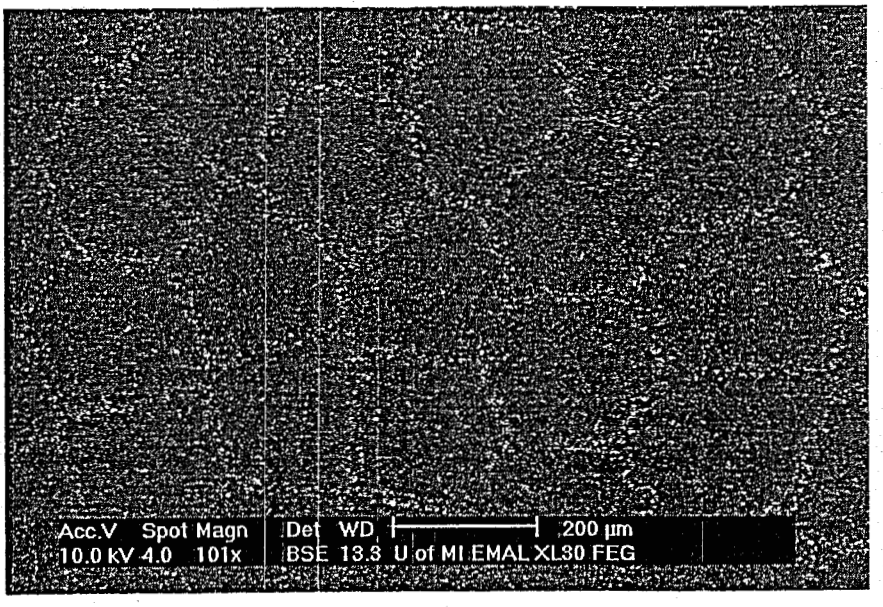

Measured Cell Size = 240 μm
Measured Thickness of Cell Boundaries = 20 μm

Sample C
82.5/17.5 Vol.%
$C:C_b = 10$

614 WC
Nominal Cell Size = 100 μm

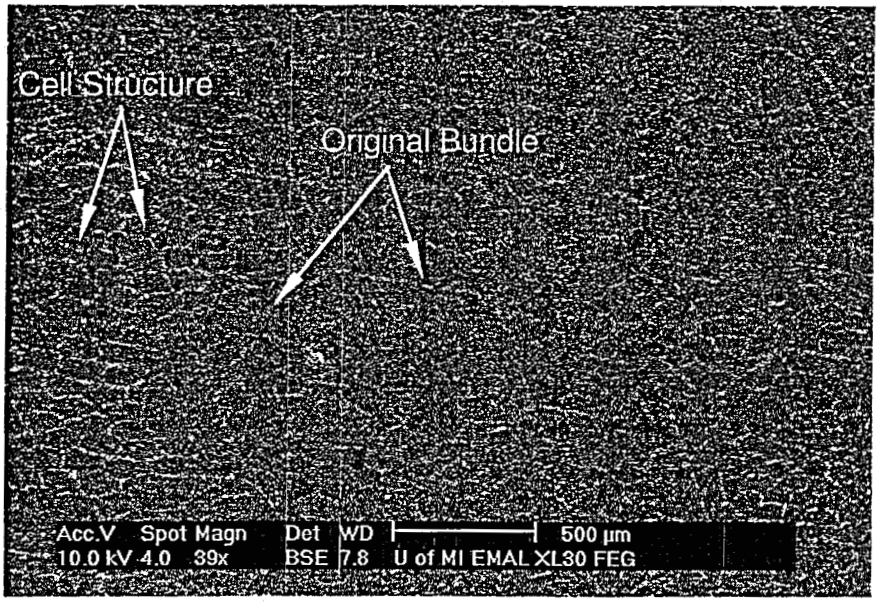

Sample C
82.5/17.5 Vol.%
$C:C_b = 10$

614 WC
Nominal Cell Size = 100 μm

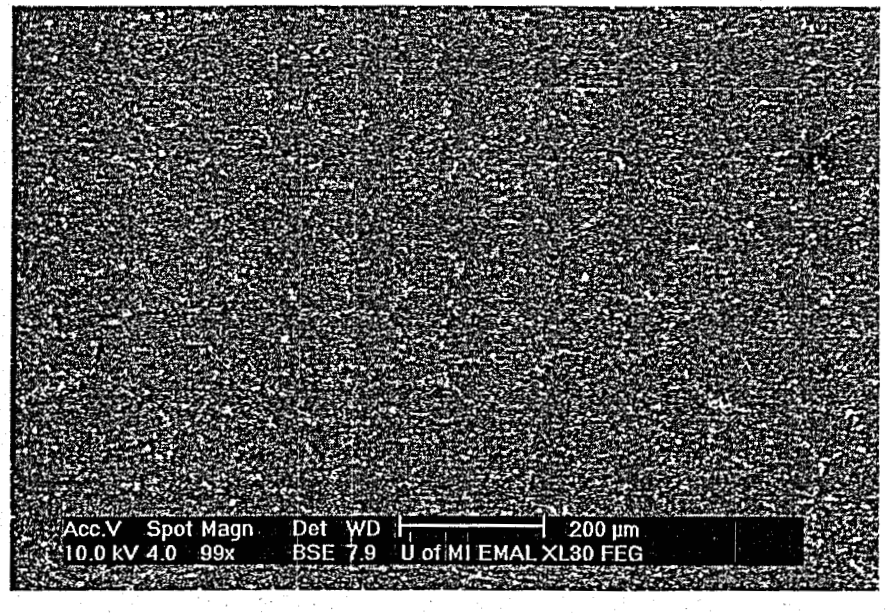

Estimated Average Cell Size = 100 μm
Measured Thickness of Cell Boundaries = 20 μm

Sample D 614 WC
82.5/17.5 Vol.% Nominal Cell Size = 200 μm
$C:C_b = 10$

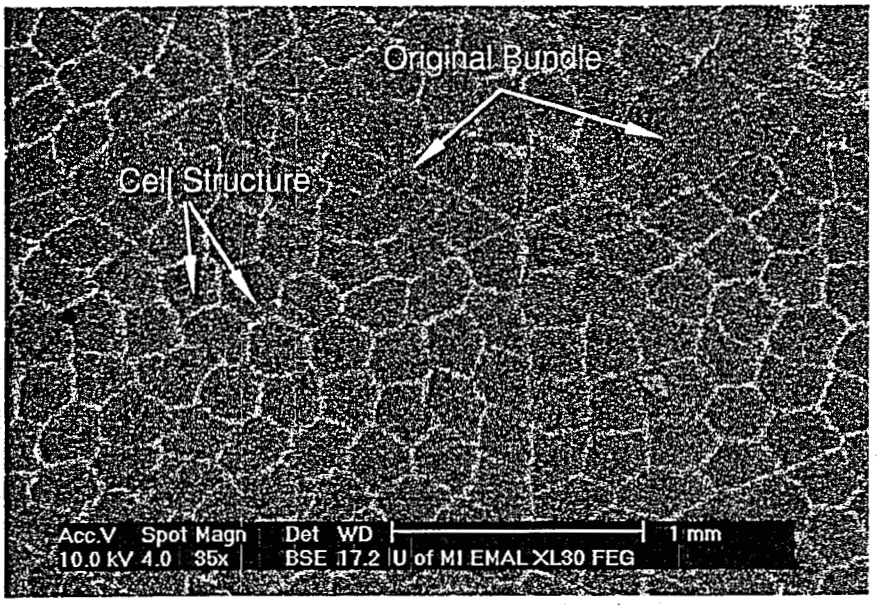

Sample D 614 WC
82.5/17.5 Vol.% Nominal Cell Size = 200 μm
$C:C_b = 10$

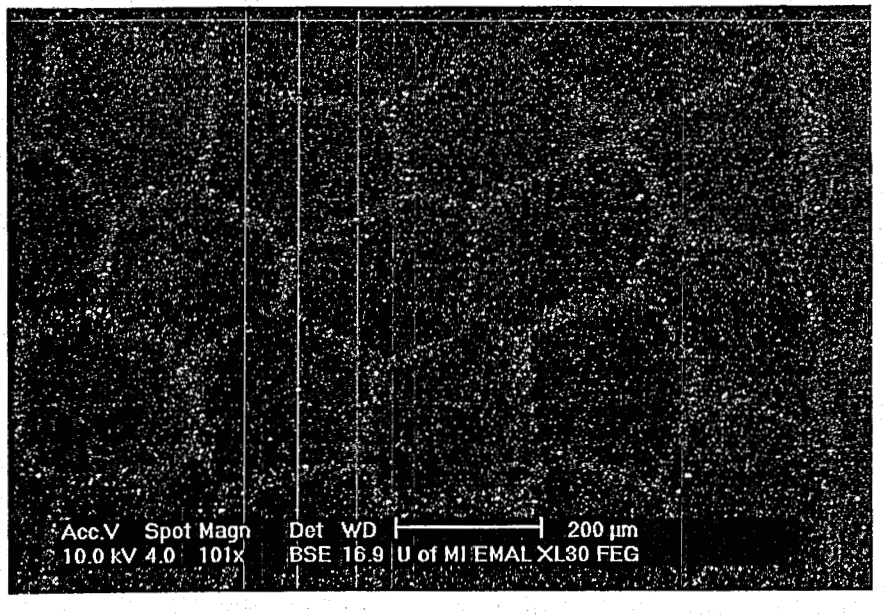

Average Cell Size = 250 μm
Measured Thickness of Cell Boundaries = 20 μm

Sample E
70/30 Vol.%
$C:C_b = 5$

411 WC
Nominal Cell Size = 100 μm

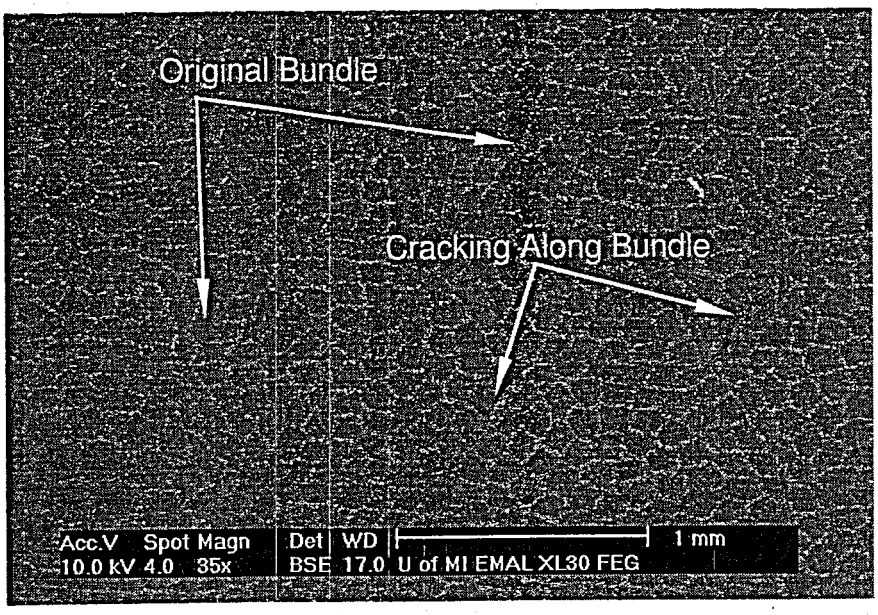

Sample E
70/30 Vol.%
$C:C_b = 5$

411 WC
Nominal Cell Size = 100 μm

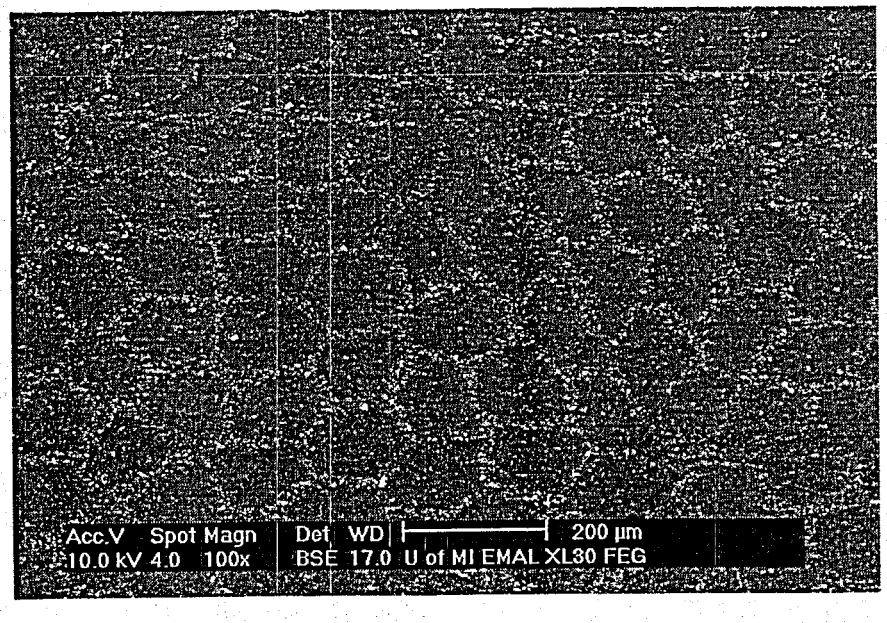

Average Cell Size = 135 μm
Measured Thickness of Cell Boundaries = 12–16 μm

Sample E
70/30 Vol.%
$C:C_b = 5$

411 WC
Nominal Cell Size = 100 μm

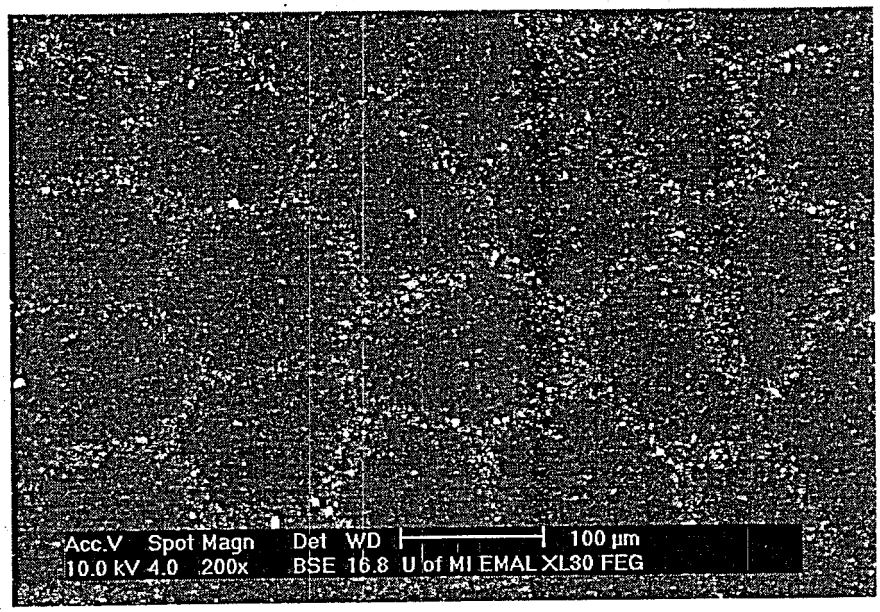

Sample F
70/30 Vol.%
$C:C_b = 5$

411 WC
Nominal Cell Size = 200 μm

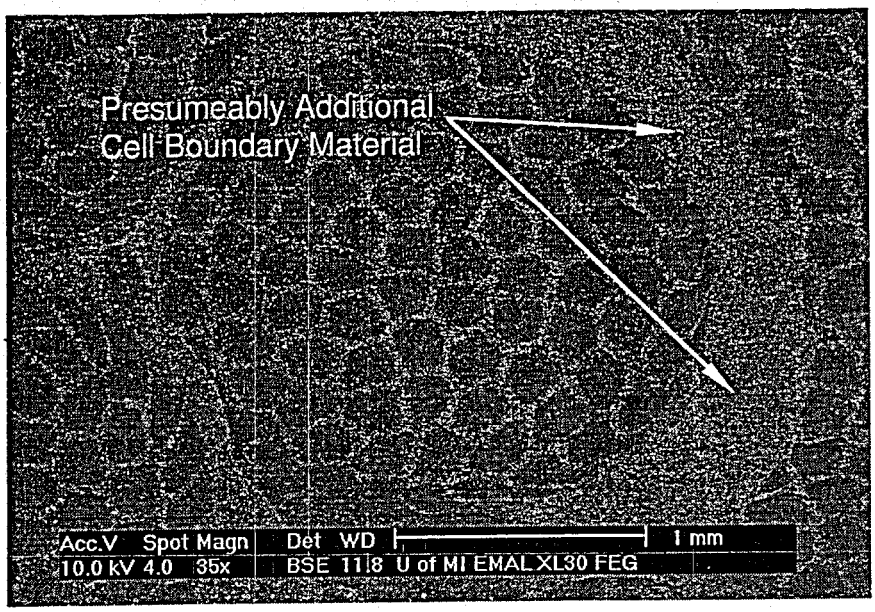

Sample F
70/30 Vol.%
$C:C_b = 5$

411 WC
Nominal Cell Size = 200 μm

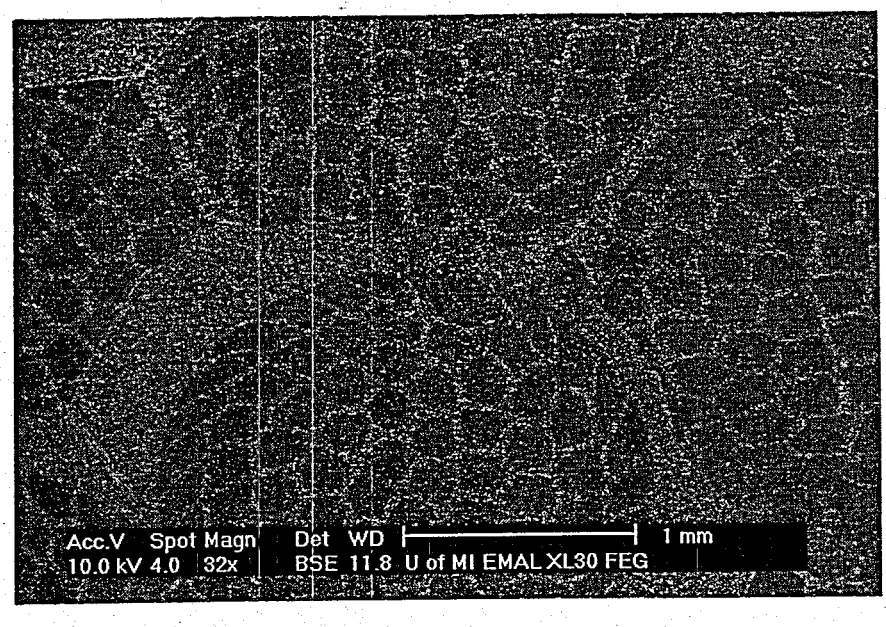

Sample F
70/30 Vol.%
$C:C_b = 5$

411 WC
Nominal Cell Size = 200 μm

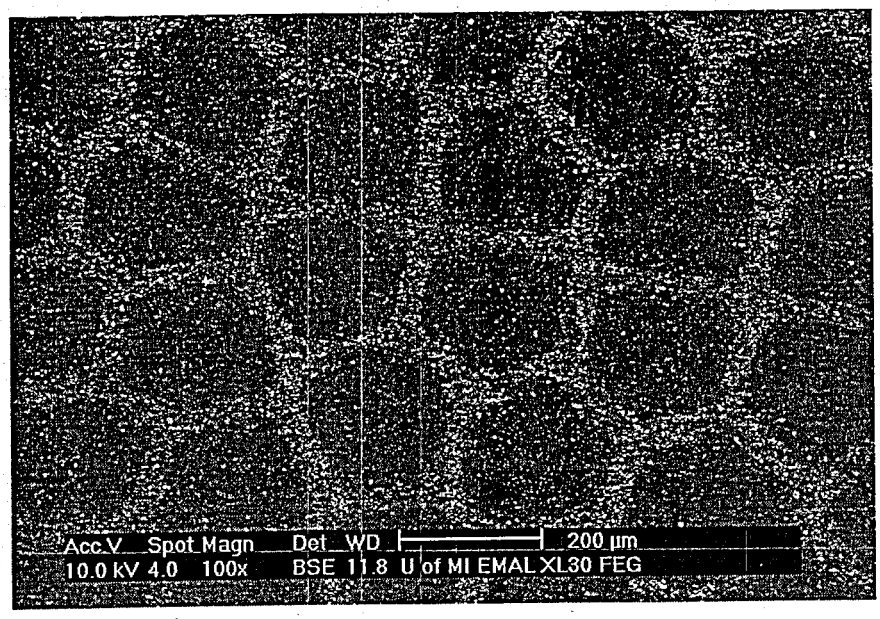

Average Cell Size = 225 μm
Measured Thickness of Cell Boundaries = 35 μm

Sample G
70/30 Vol.%
$C:C_b = 5$

614 WC
Nominal Cell Size = 100 μm

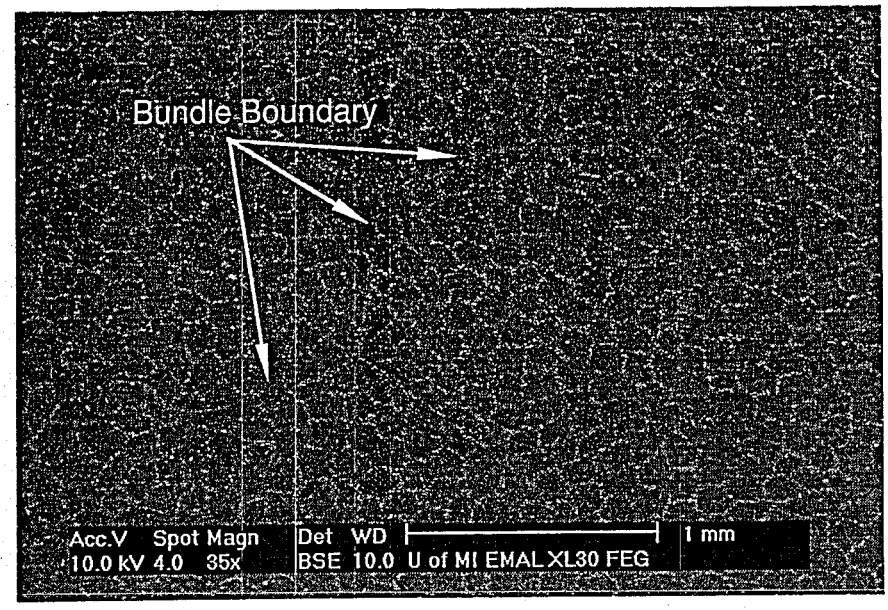

Sample G
70/30 Vol.%
$C:C_b = 5$

614 WC
Nominal Cell Size = 100 μm

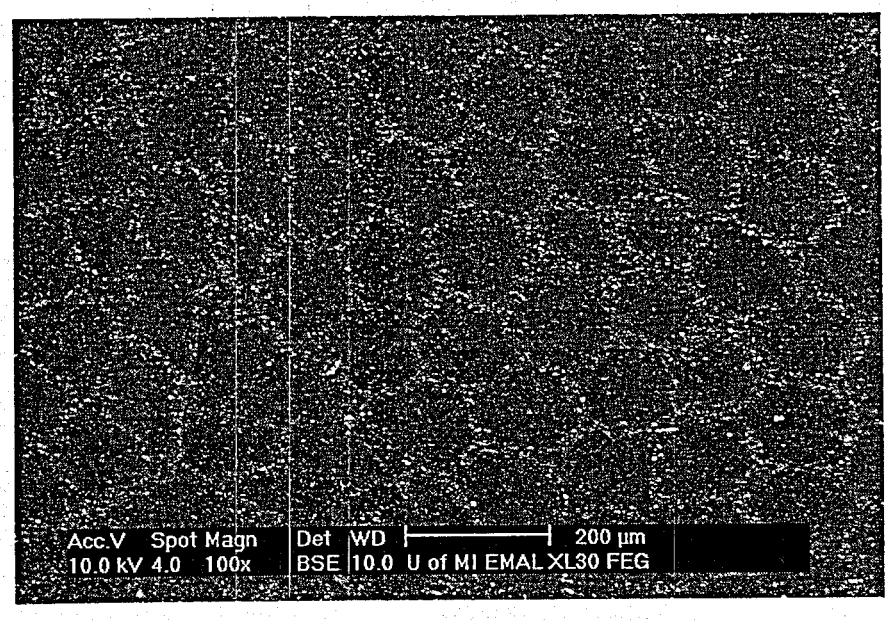

Average Cell Size = 150 μm
Measured Thickness of Cell Boundaries = 20 μm

Sample H
70/30 Vol.%
$C:C_b = 5$

614 WC
Nominal Cell Size = 200 μm

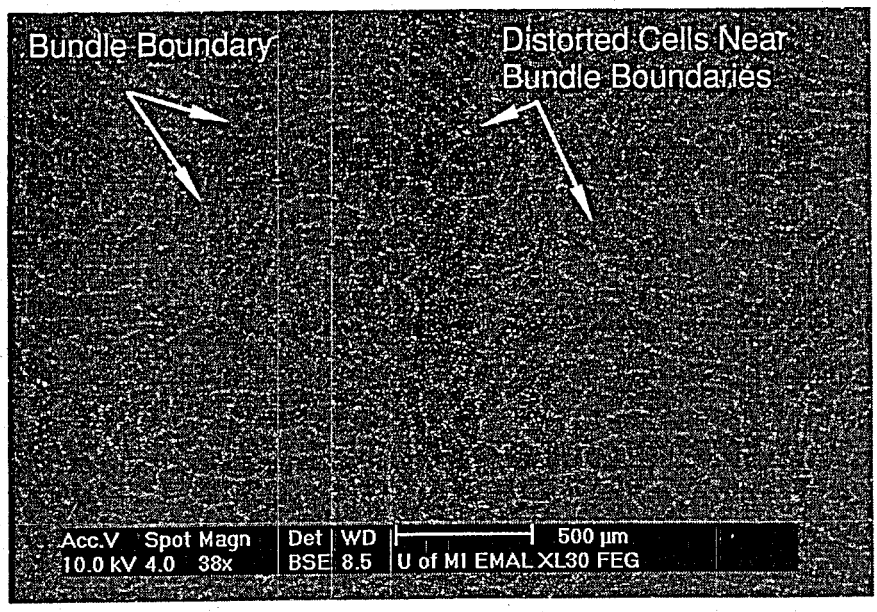

Sample H
70/30 Vol.%
$C:C_b = 5$

614 WC
Nominal Cell Size = 200 μm

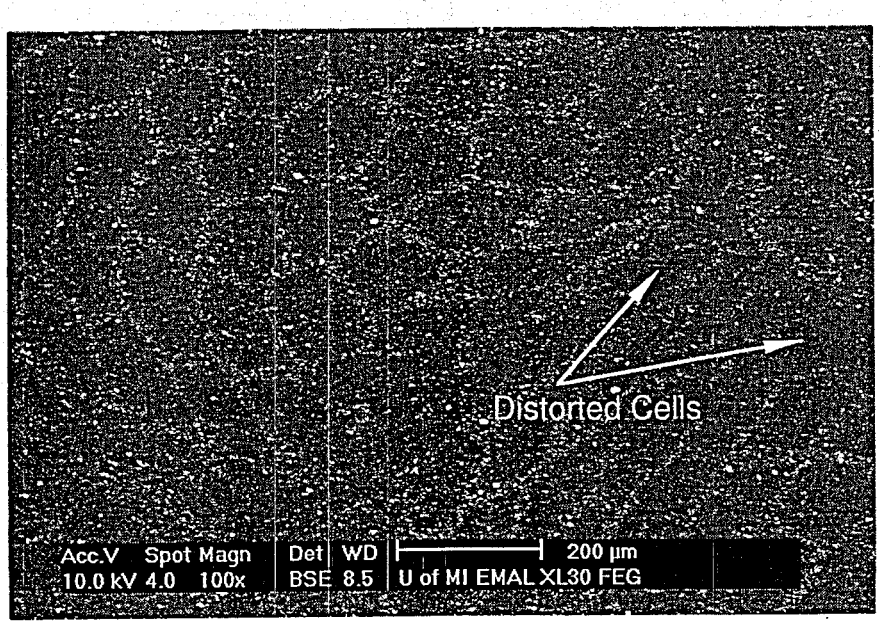

Average Cell Size = 145 μm
Measured Thickness of Cell Boundaries = 25 μm

Sample I
50/50 Vol.%
$C:C_b = 1$

411 WC
Nominal Cell Size = 50 μm

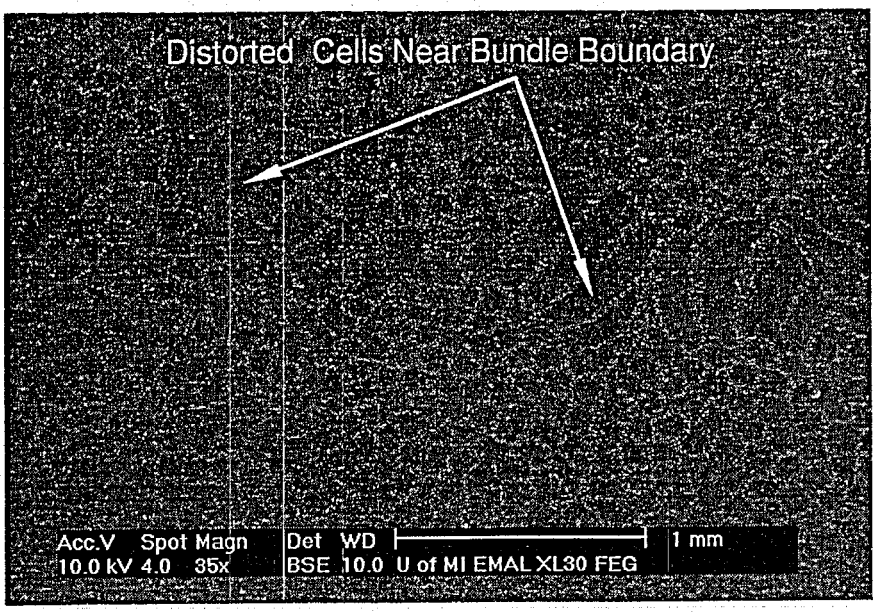

Sample I
50/50 Vol.%
$C:C_b = 1$

411 WC
Nominal Cell Size = 50 μm

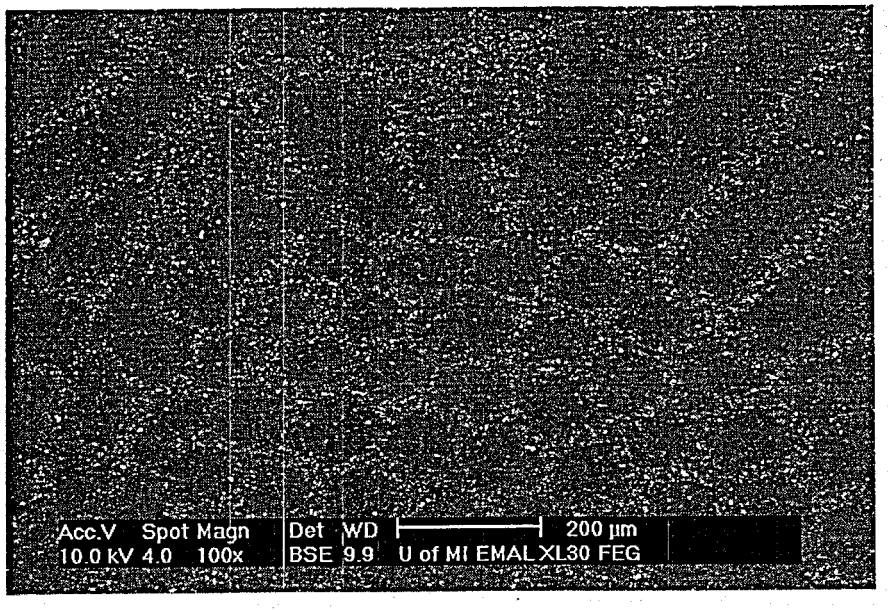

Average Cell Size = 140 μm
Measured Thickness of Cell Boundaries = 25–30 μm

Sample J
50/50 Vol.%
$C:C_b = 1$

614 WC
Nominal Cell Size = 50 μm

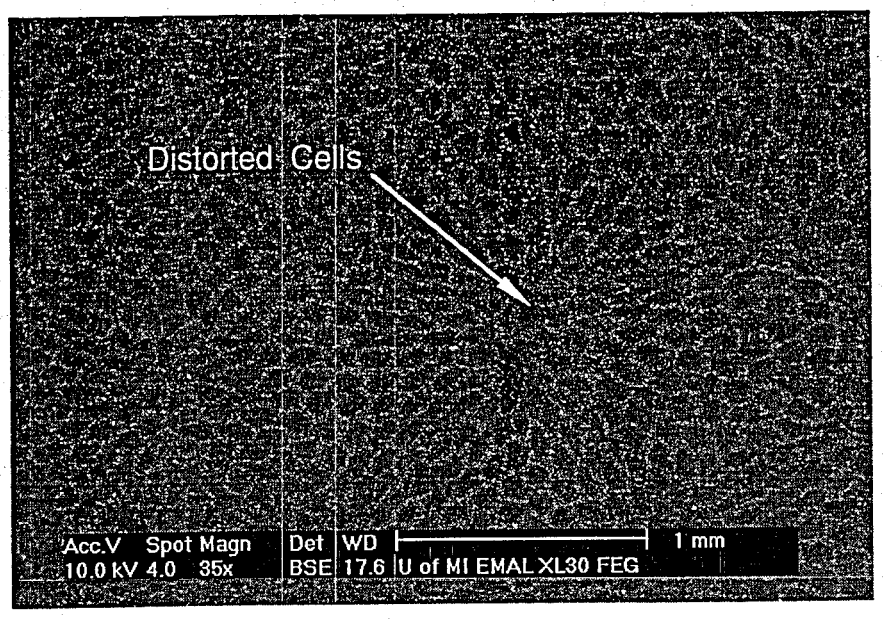

Sample J
50/50 Vol.%
$C:C_b = 1$

614 WC
Nominal Cell Size = 50 μm

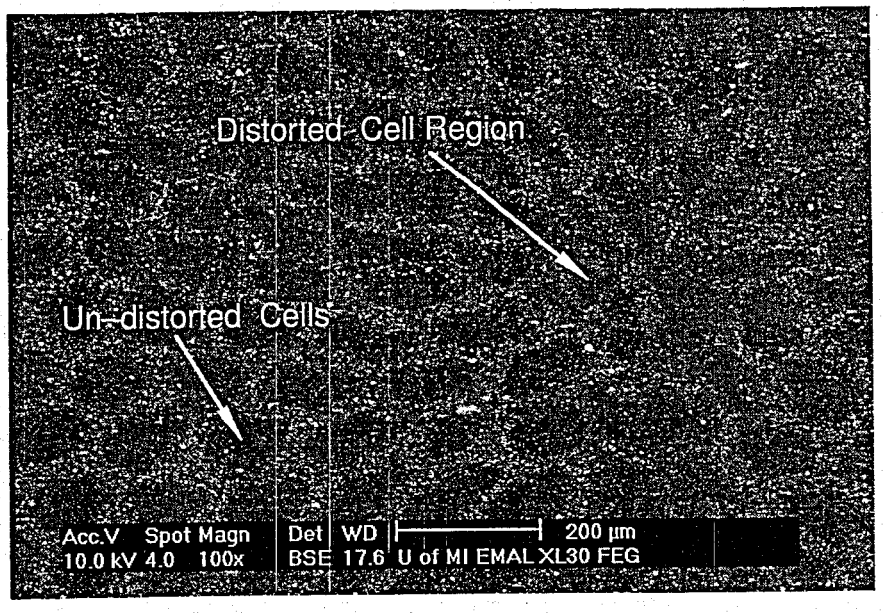

Average Cell Size = 140 μm
Measured Thickness of Cell Boundaries = 35 μm

Sample "Z"
90/10 Vol.%

411 WC
2 mm to 1 mm Spag.

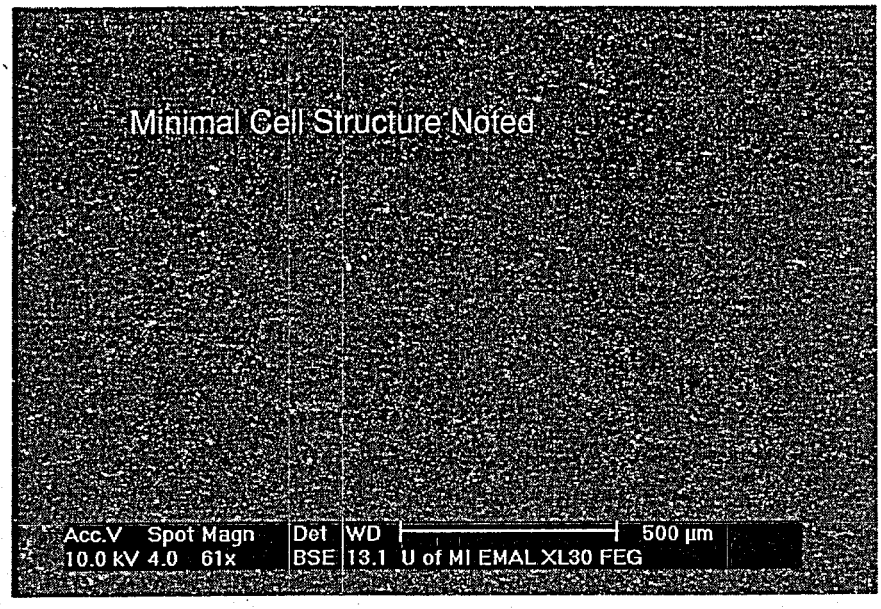

Appendix C. Microscopic Images of the Diamond/WC Drill Bit Insert in an As-Received Condition

By

Rodney Trice

THE UNIVERSITY OF MICHIGAN
COLLEGE OF ENGINEERING
MATERIALS SCIENCE AND ENGINEERING

3062 H. H. DOW BUILDING
2300 HAYWARD STREET
ANN ARBOR, MICHIGAN 48109-2136
313 763-4970 FAX 313 763-4788

February 2, 1998

To: Greg Hilmas, John Halloran

From: Rodney Trice

RE: Microscopy Images of the WC Drill Bit in the As–Received Condition

The following report details the initial microscopy characterization of the WC drill bit with the FM cap. Scanning electron microscopy was performed on the new Philips XL30 FEG SEM in back–scattered and secondary electron mode. In this mode, the tungsten and cobalt present in the cell boundaries appeared as the high contrast phase. All images were taken digitally. EDS was also performed.

The images were taken on the "as–received" insert after cleaning and applying a small layer of Au/Pd coating to the outer surface. Images were taken from two perspectives - looking down from the top and side of the insert. These are clearly shown in the accompanying micrographs.

In general, the cells associated with the fibrous monolith cap were very homogeneous in size over the entire hemisphere. Cell distortion was only noted in the very small region where the cap "ran out" into the original WC drill bit (along the side of the insert). Discontinuities in the cell boundary were numerous over the entire hemisphere represented by the FM cap. Close–ups within the interior of the cells indicated the presence of a high–constrast phase similar in composition to that of the cell boundary.

Location: Near the Top of the Insert

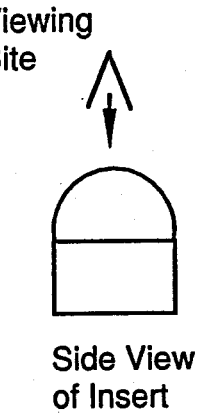

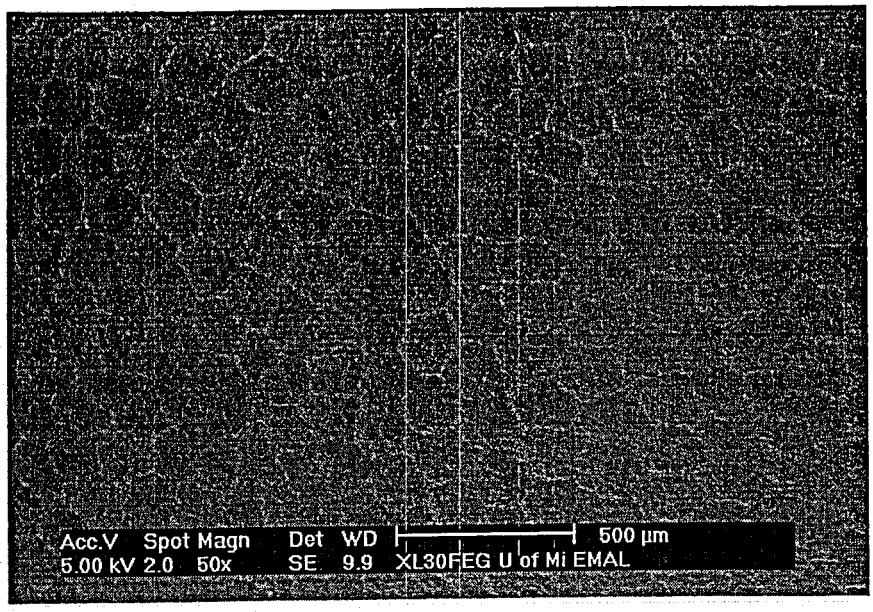

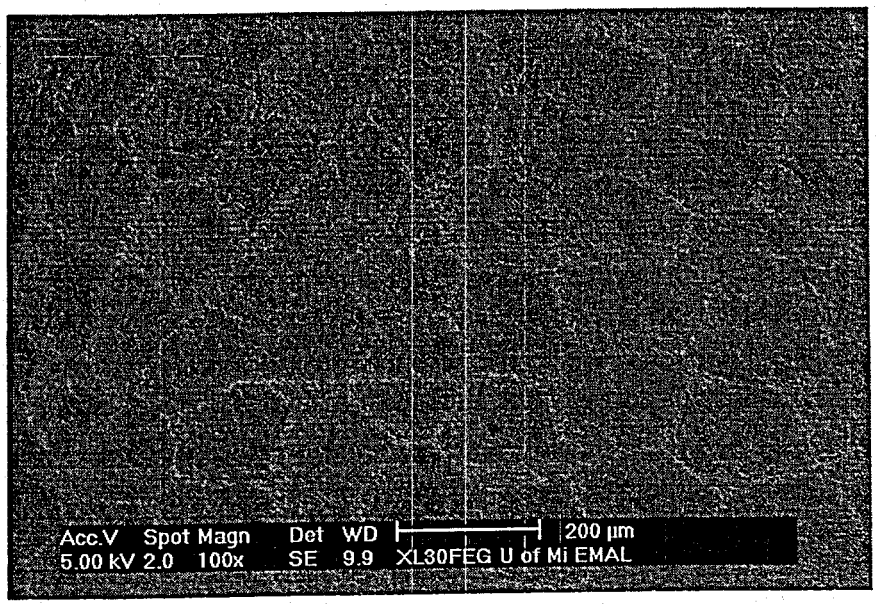

Both images are secondary electron generated near the top of the cap. The original bundle boundaries are still visible. Cells where reasonably homogenous in size. No distorted cells were noted in this region.

Location: Near the Top of the Insert

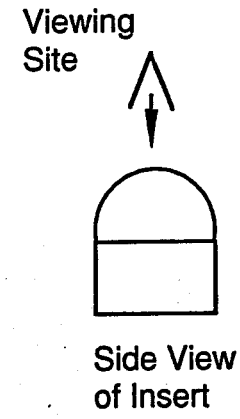

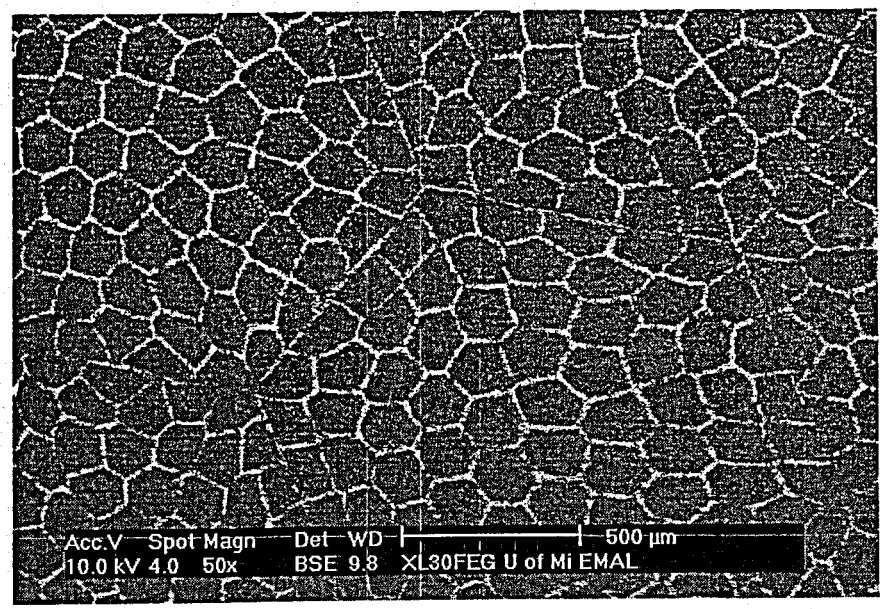

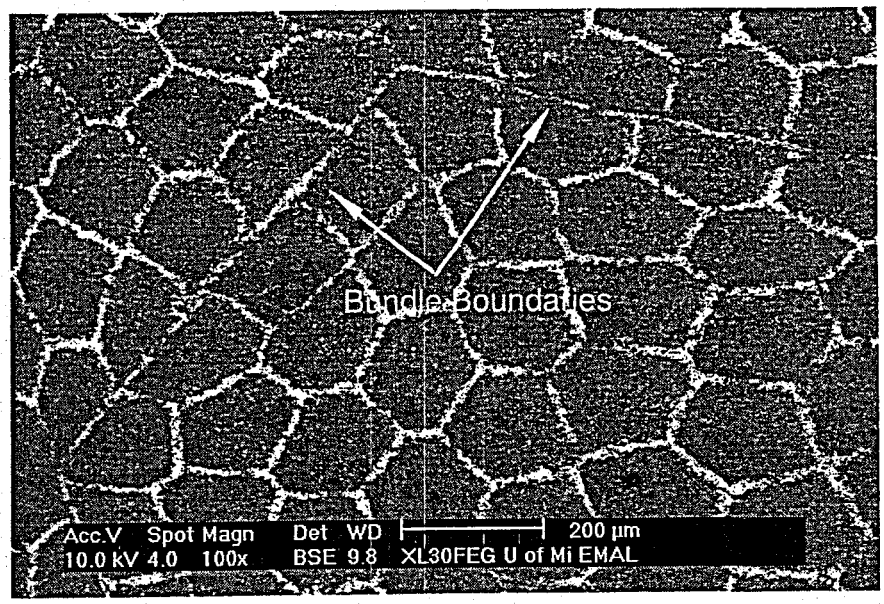

Both images are back–scattered electron generated near the top of the cap. The cell boundaries are more clearly defined in these images than the secondary electron generated images. The original bundle boundaries are still visible. Cells where reasonably homogenous in size. No distorted cells were noted in this region.

Location: Near the Top of the Insert

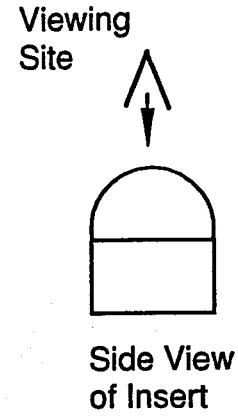

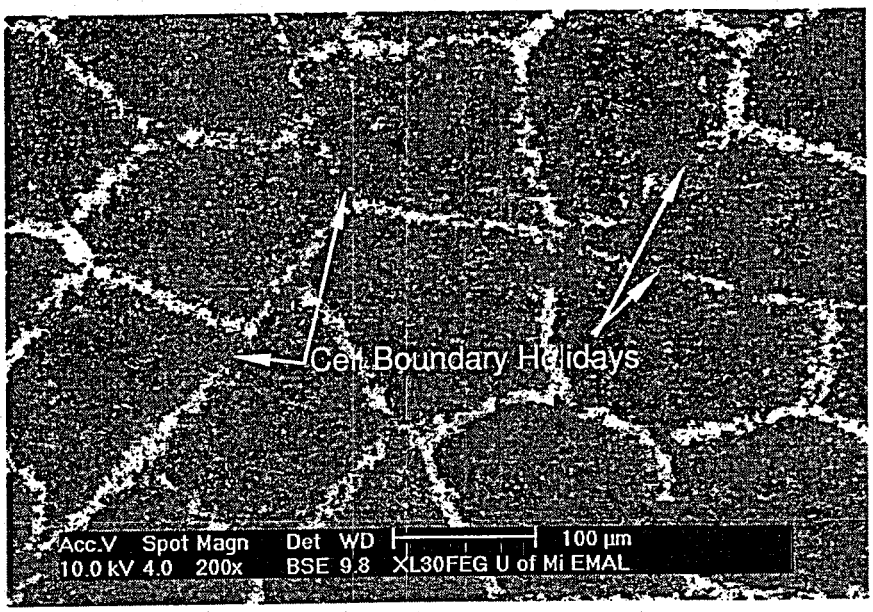

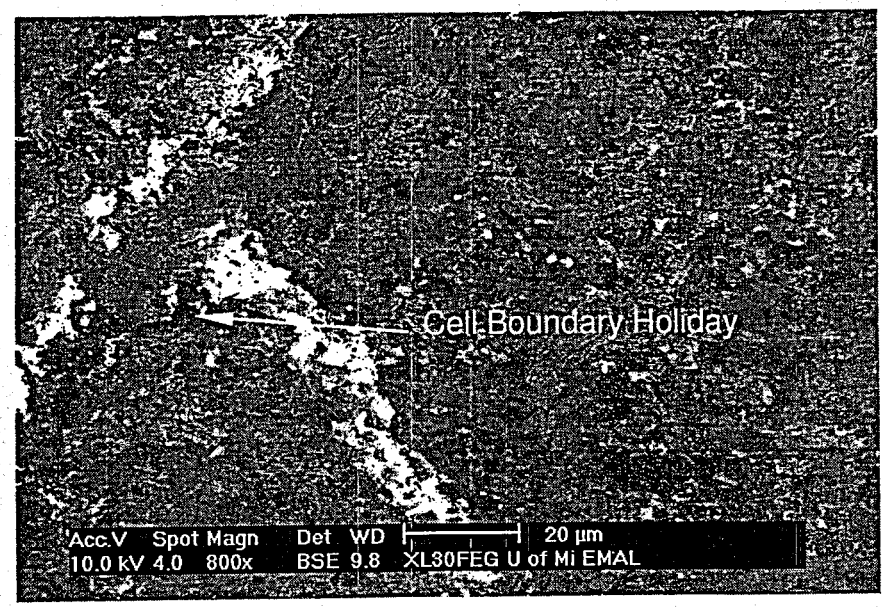

Both images are back–scattered electron generated near the top of the cap. The cell boundaries were discontinous in regions, forming "holidays." These defects in the cell boundary seem to be numerous.

Location: Near the Top of the Insert

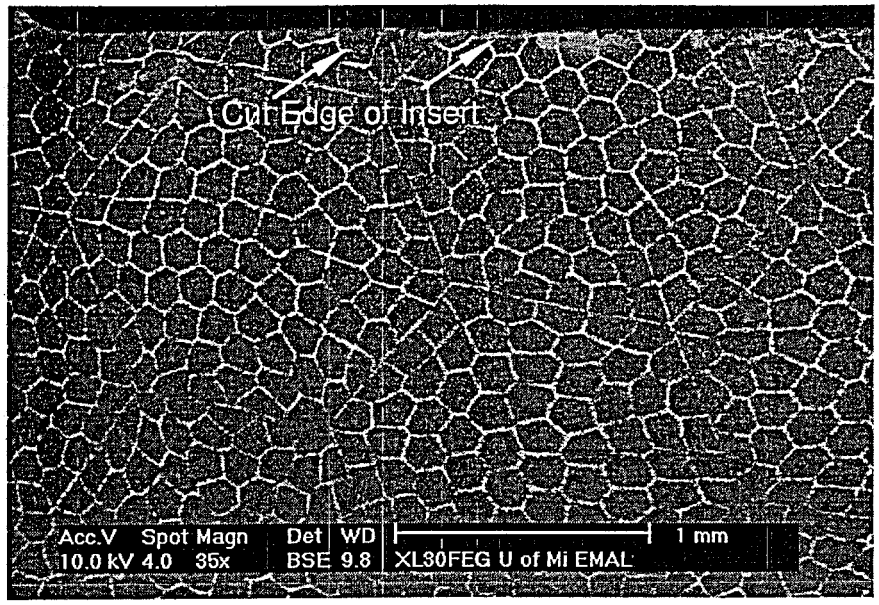

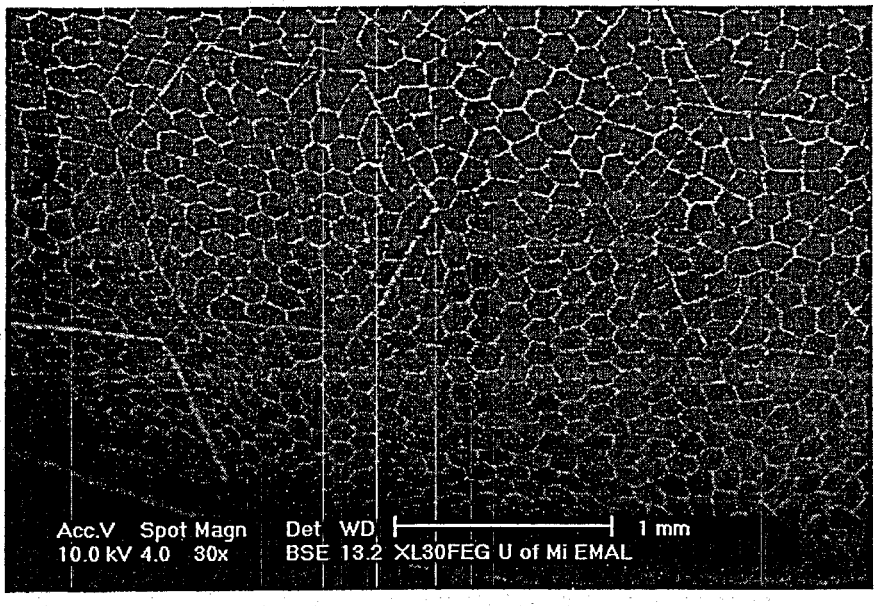

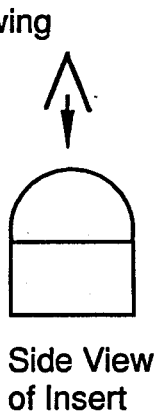

Several low magnification views of the insert, looking down from the top. In the top image, the cut edge is apparent (as a reminder, the insert was cut in half before sending it to U of M). In the bottom image we are looking down the side of the insert. Clearly shown in both images are homogenous and undistorted cells.

Location: Near the Top of the Insert

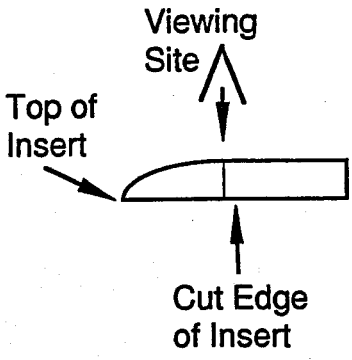

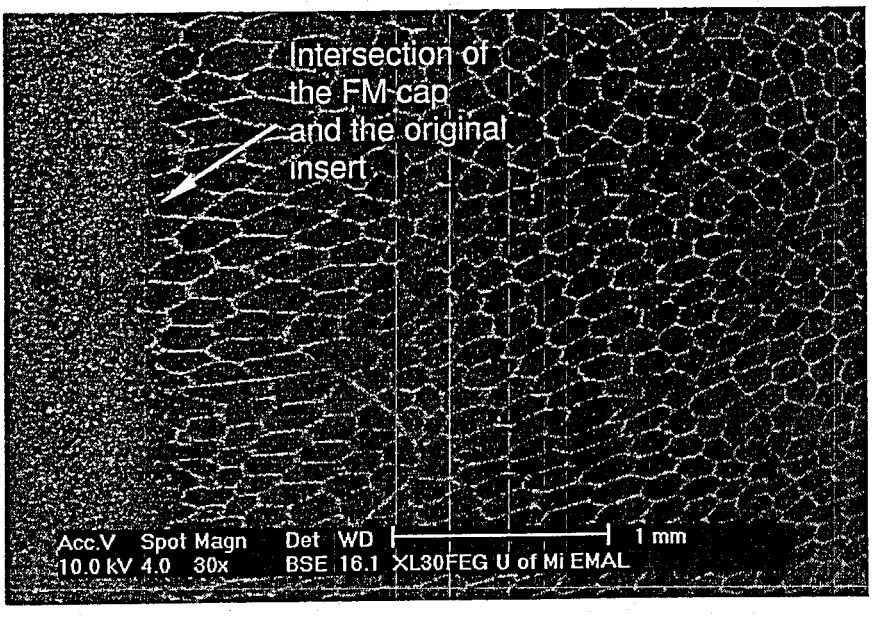

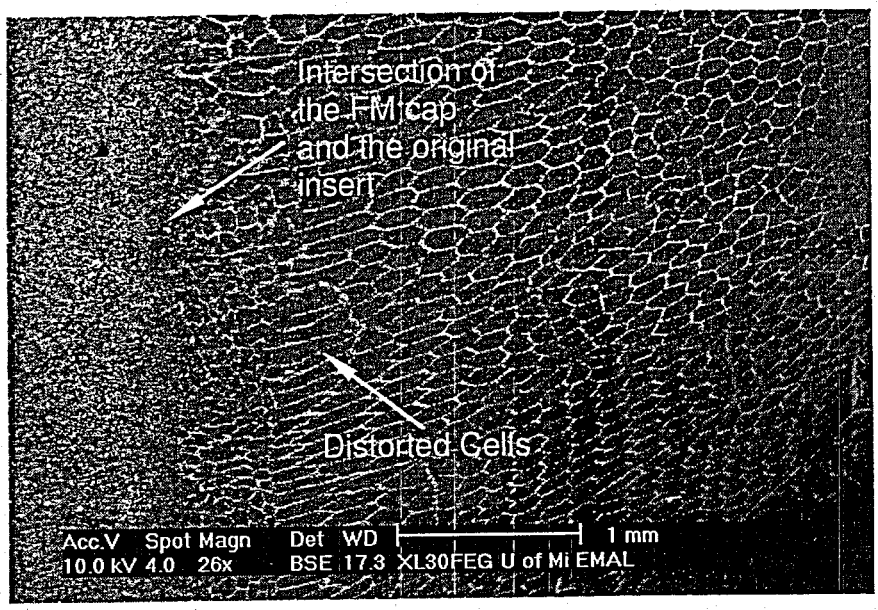

Several low magnification views of the insert, looking down from the side. Both images show where the fibrous monolith cap intersected the original insert. This was the only location where any cell distortion was noted.

Location: Near the Top of the Insert

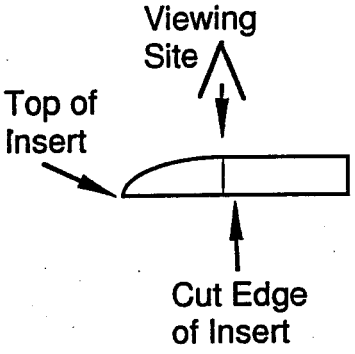

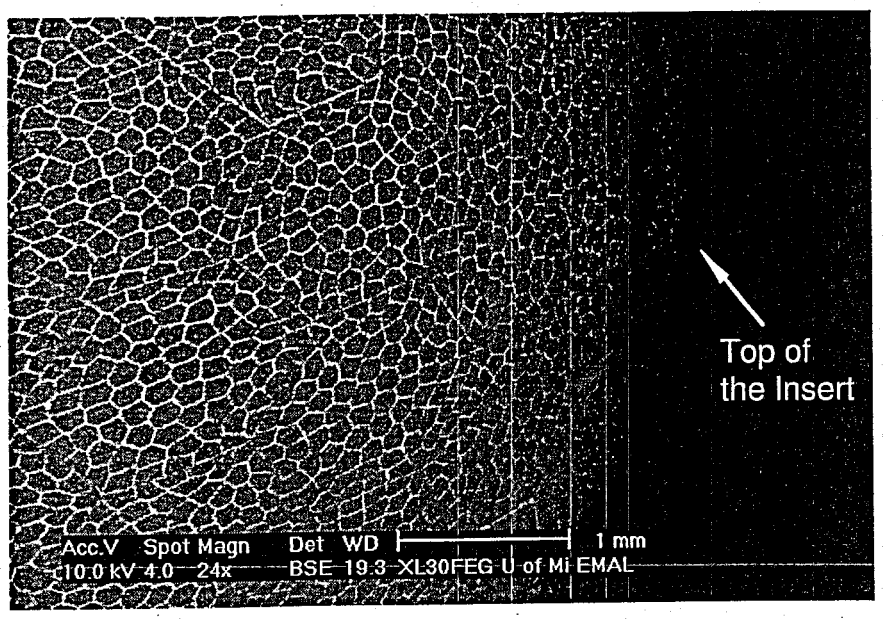

Low magnification view of the insert, looking down from the side.

EDS Results

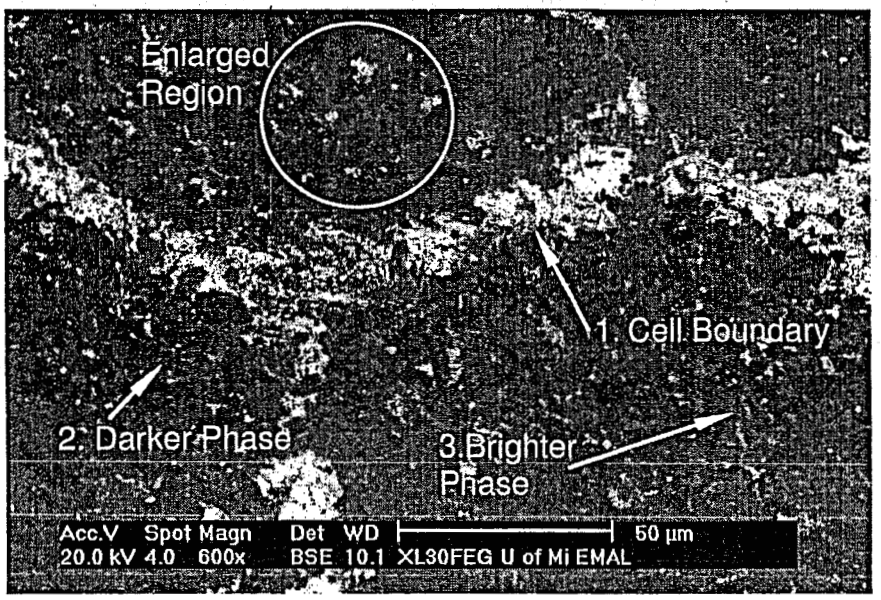

Several regions were investigated with an EDS detector. These areas included:

1. Cell boundary (highest contrast phase)
2. Darker phase in the cell region
3. Brighter phase in the cell region
4. High constrast phases in the cell region

Enlarged region in the cell

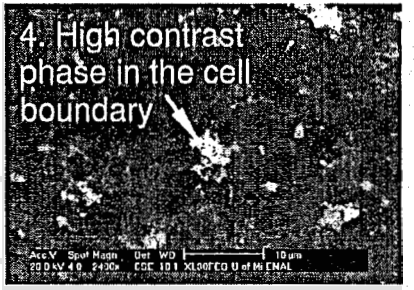

Enlarged region in the cell

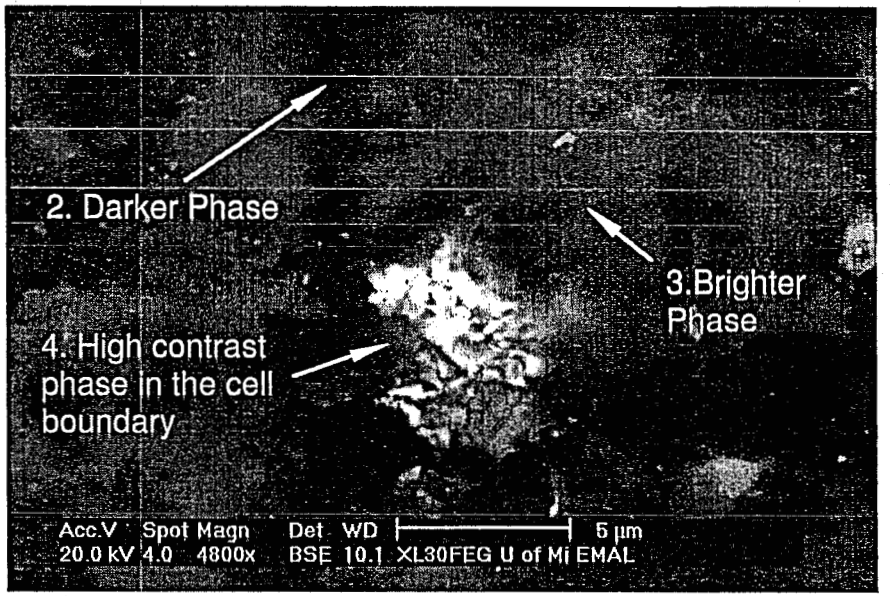

The EDS results indicated the following elements were in the described regions:

1. Cell boundary (highest contrast phase) - predominantly W, also Co and some C.
2. Darker phase in the cell region - predominantly C, also Co.
3. **Brighter phase in the cell region - predominantly Si, also C and Co.**
4. High constrast phases in the cell region - predominantly W, also Co and some C.

Appendix D. Cross Section Microscopy Images of the Diamond/WC FM Drill Bit

By

Rodney Trice

February 4, 1998

To: Greg Hilmas, John Halloran

From: Rodney Trice

RE: Cross–Section Microscopy Images of the WC Drill Bit

The following report details the cross–sectional microscopy performed on the WC drill bit with the FM cap. Scanning electron microscopy was performed on the Philips XL30 FEG SEM in predominantly the secondary electron imaging mode. All images were taken digitally. EDS was also performed.

The drill bit was surface ground with a 600 grit diamond wheel. Polishing of the sample was attempted with diamond polishing wheels with little success. A thin layer of Au/Pd was applied before viewing in the SEM. All images are taken from a cross–sectional perspective.

Low magnification images reveal 3 distinct layers (Layers 1, 2 and the FM cap) and the original insert. The FM cap is approximately 300 μm thick near the top of the drill. Higher magnification images reveal no cracking at any of the interfaces.

EDS results are consistent with earlier reports (Feb. 2, 1998). There are three phases apparent in the cells. The dark or low contrast regions are predominantly C. A medium contrast phase is also apparent that is rich in Co. The high contrast phase in the cells has an identical composition to the cell boundary phase – predominantly W with some Co.

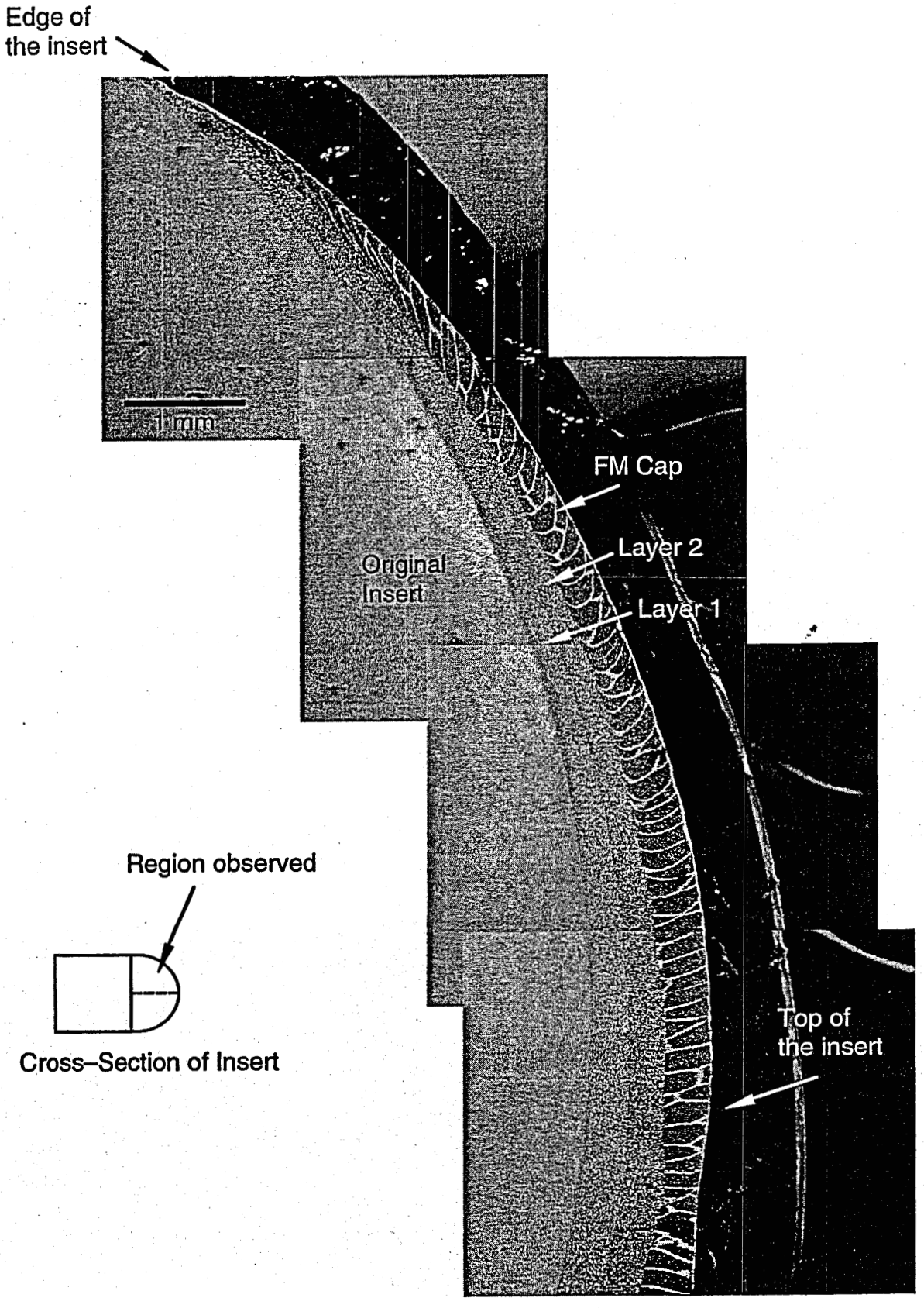

Composite image showing one–half of the FM cap. The thickness of the cap is greatest at the top of the insert.

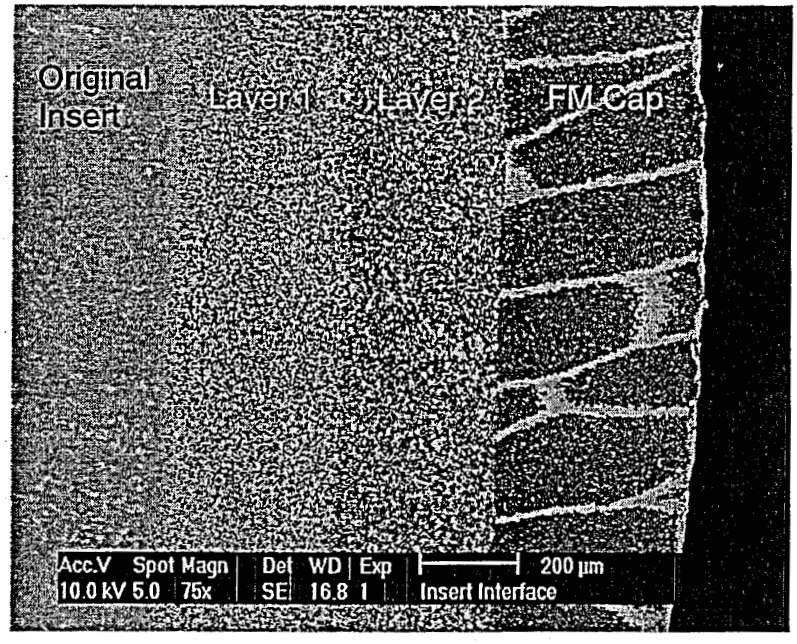

(a). Secondary electron image

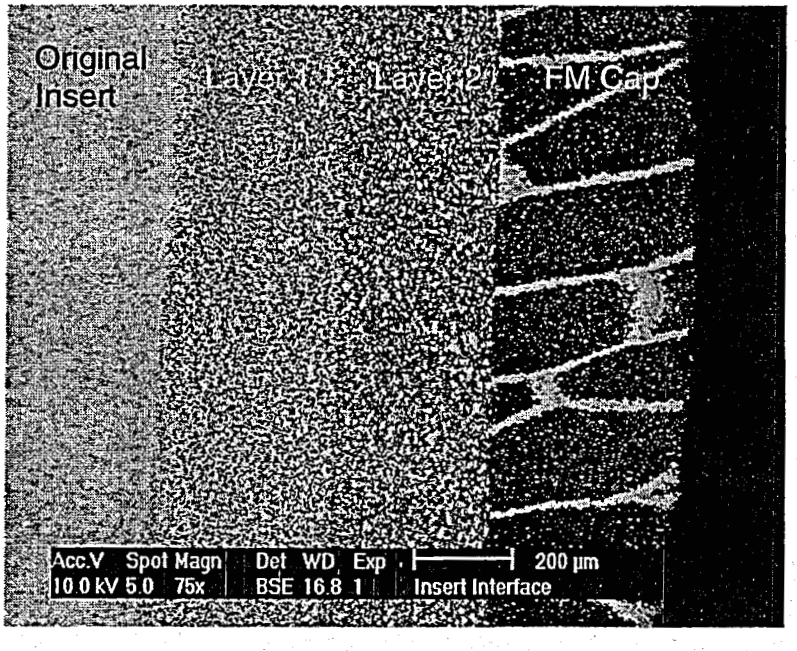

(b). Back–scattered electron image

Cross–sectional overview of the interfaces in the insert. The top image was taken in a secondary electron imaging mode while the bottom micrograph was taken in a back–scattered electon imaging mode. Four distinct regions were noted. The fibrous monolithic cap was approximately 300 µm. Its thickness depended upon position on the insert (see composite image).

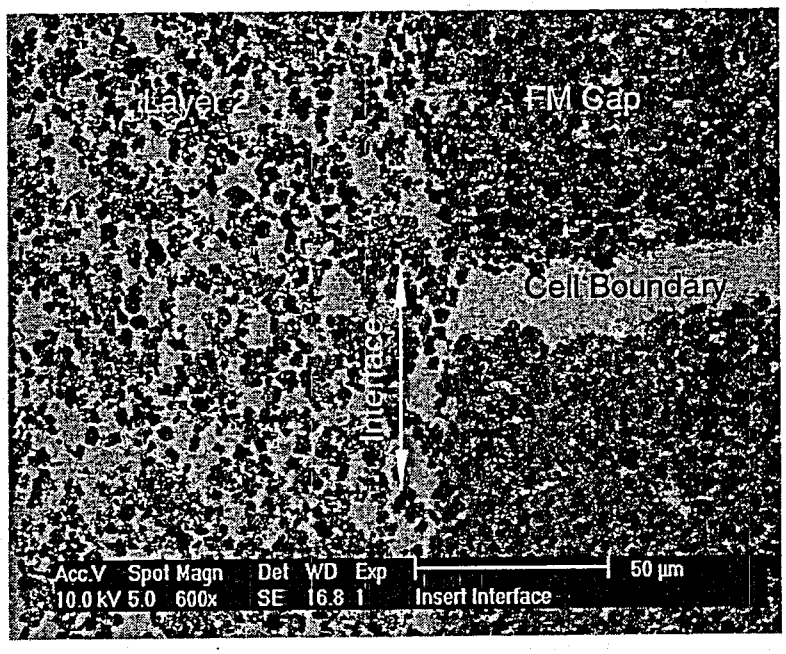

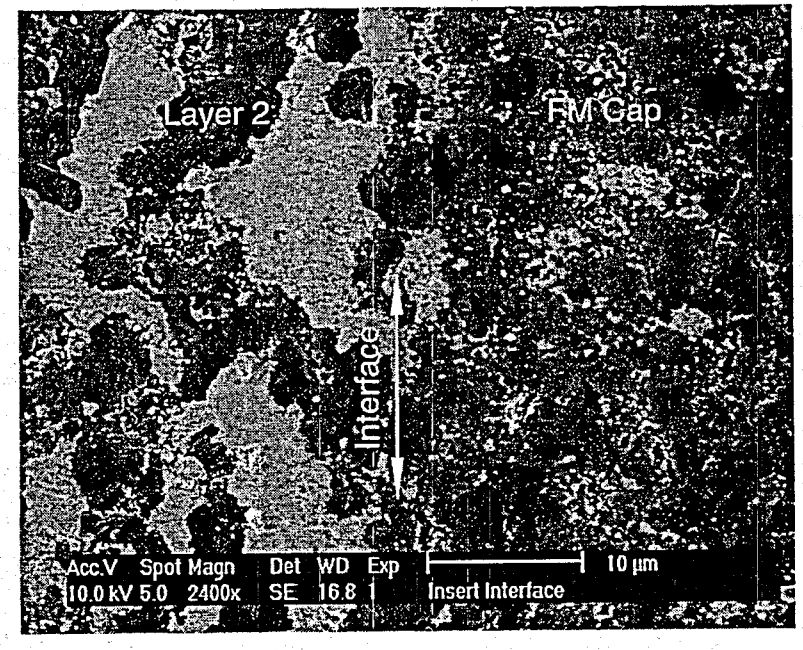

Close–up of the interface between Layer 2 and the fibrous monolithic cap. No cracking along the interface was observed.

EDS Results at the Layer 2–FM Cap Interface

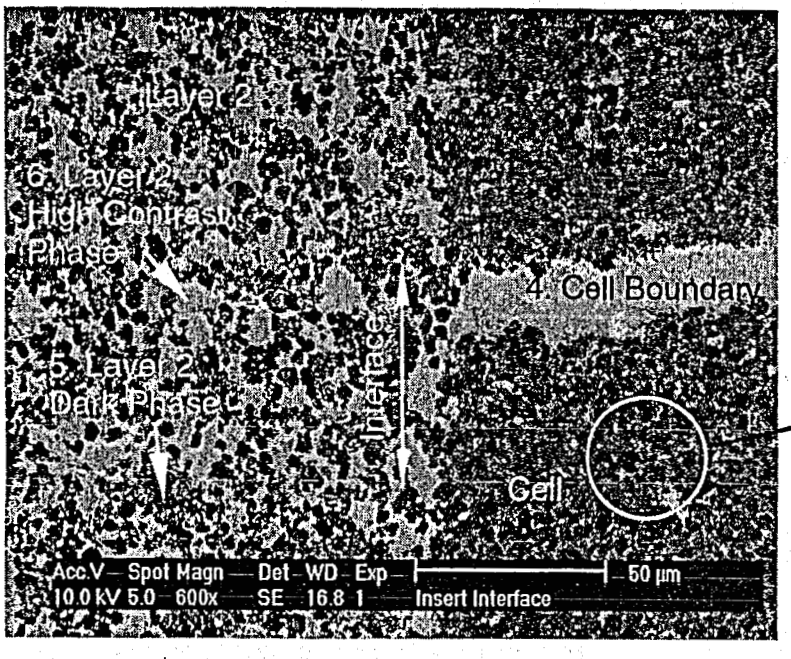

Typical Area in a cell

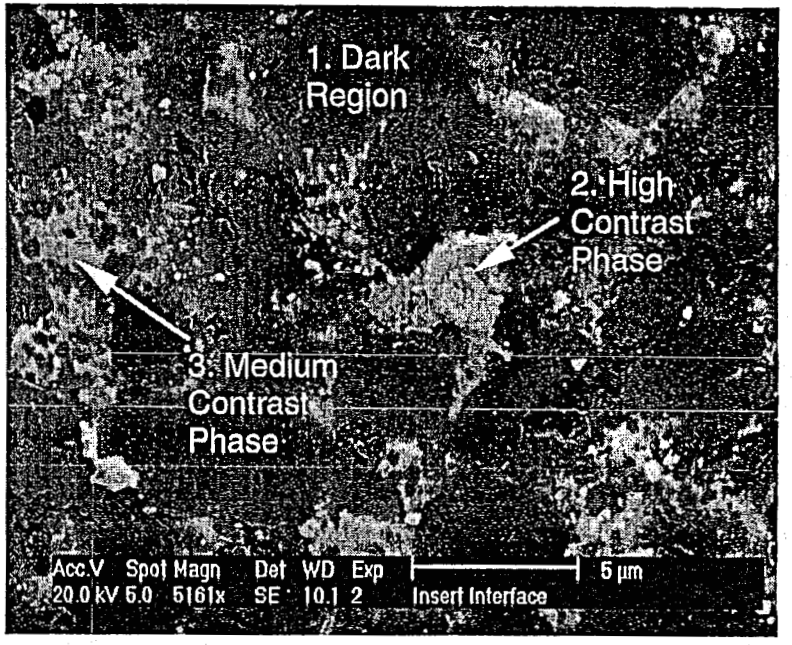

1. Dark Region in Cell – predominantly C, small amounts of O, Co, and Au (artifact of preparation)
2. High Contrast Phase in Cell – predominantly W, small amounts of C, Co
3. Medium Contrast Phase in Cell – predominantly Co, some W, C, O and Au
4. Cell Boundary – predominantly W, small amounts of C, Co
5. Layer 2 Dark Phase – predominantly C, some O
6. Layer 2 High Contrast Phase – predominantly W, some Co and C

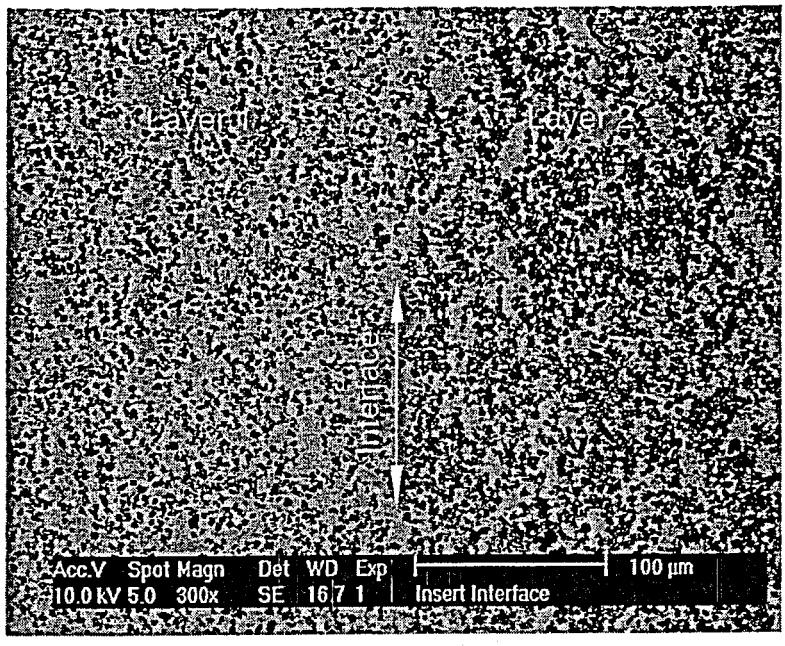

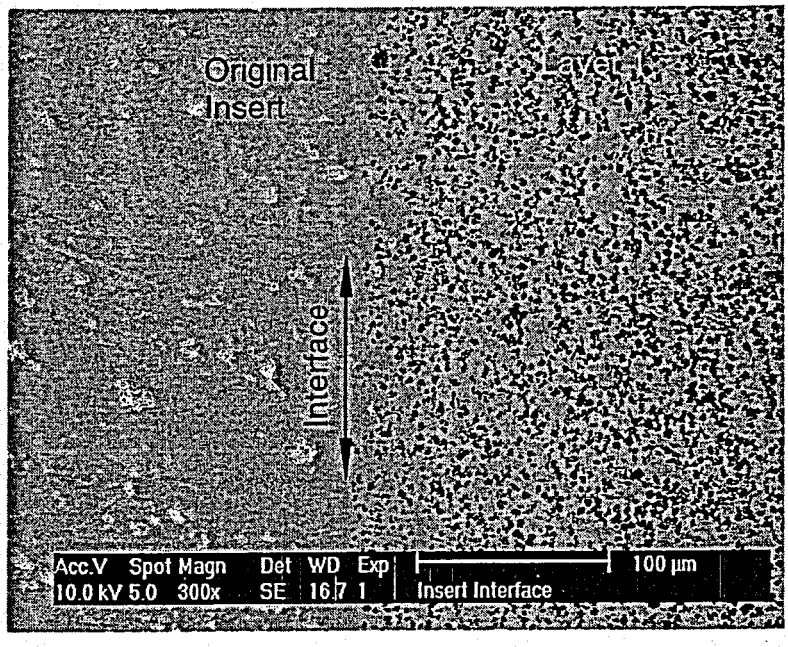

Images show the interfaces between Layers 1 and 2 (top micrograph) and the orginal insert and Layer 1 (bottom micrograph). As in the interface between the FM cap and Layer 2, no cracking was observed at either interface.